

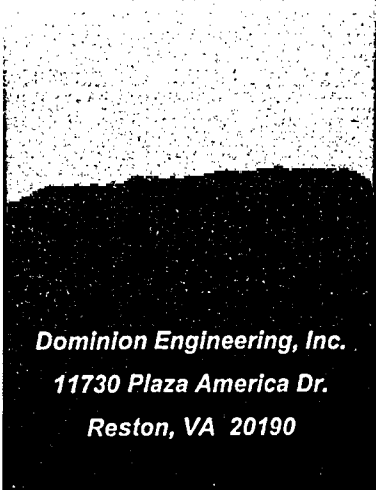
Welding Residual and Operating Stress Analysis RPV Top and Bottom Head Nozzles

Vessel Head Penetration Inspection,
Cracking and Repair Conference

September 29 – October 2, 2003
Gaithersburg, MD

By:

John Broussard, Dominion Engineering, Inc.
David Gross, Dominion Engineering, Inc.

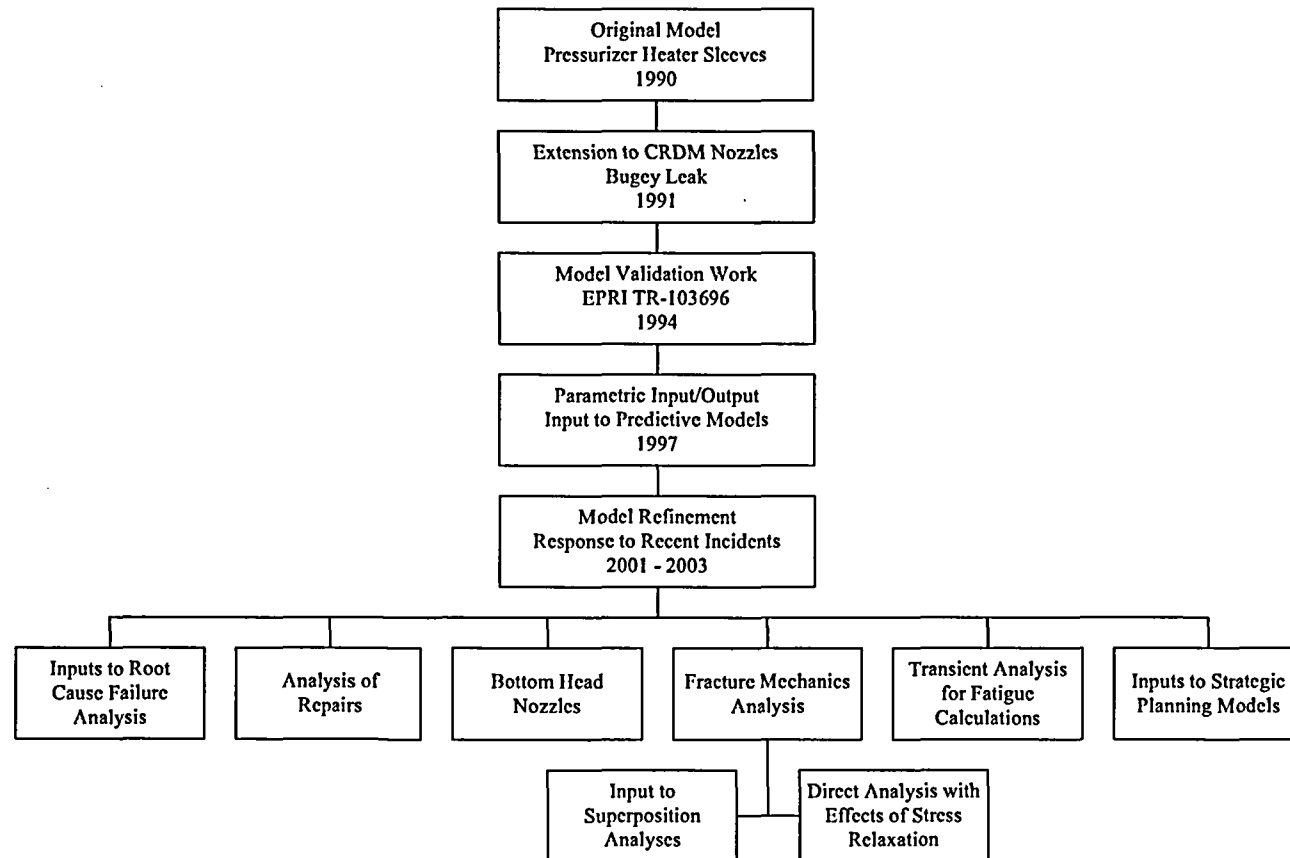


*Dominion Engineering, Inc.
11730 Plaza America Dr.
Reston, VA 20190*

Overview

- Development of RPV Head Stress Analysis Model
- Model Description and Validation
- Results for RPV Top Head Nozzles
- Results for RPV Bottom Head Nozzles
- Transient Analyses for Fatigue Analysis
- Additional Weld Residual Stress Modeling
- Fracture Mechanics Modeling with Stress Relaxation

Development of RPV Head Nozzle Stress Analysis Model

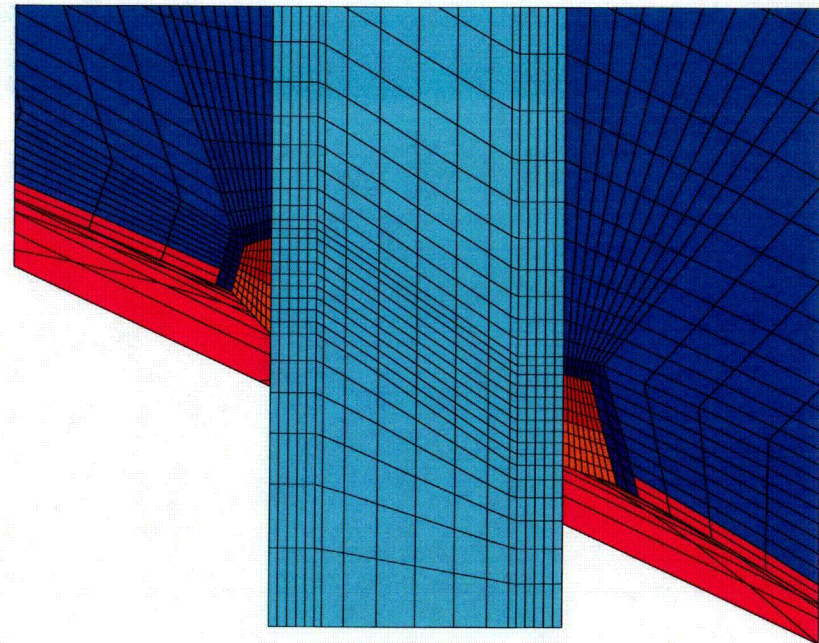


Welding Residual and Operating Stress Analysis - RPV Top and Bottom Head Nozzles 3

Model Description and Validation

Description

- 3D FEA modeling
 - ANSYS FEA software
 - Parametric input/output modeling
- Multi-pass welding
 - Thermal analysis of each weld pass
 - Structural analysis during weld cooling
 - Alloy 600 tubes have strain hardening properties
 - Welds assumed elastic-perfectly plastic
- Analysis includes
 - Deposition and stress relief of buttering prior to making J-weld
 - Interference fit between nozzle and bore in vessel head
 - Counterbores at top and bottom of head
 - Hydrostatic test pressure
 - Operating pressure and temperature



Model Description and Validation

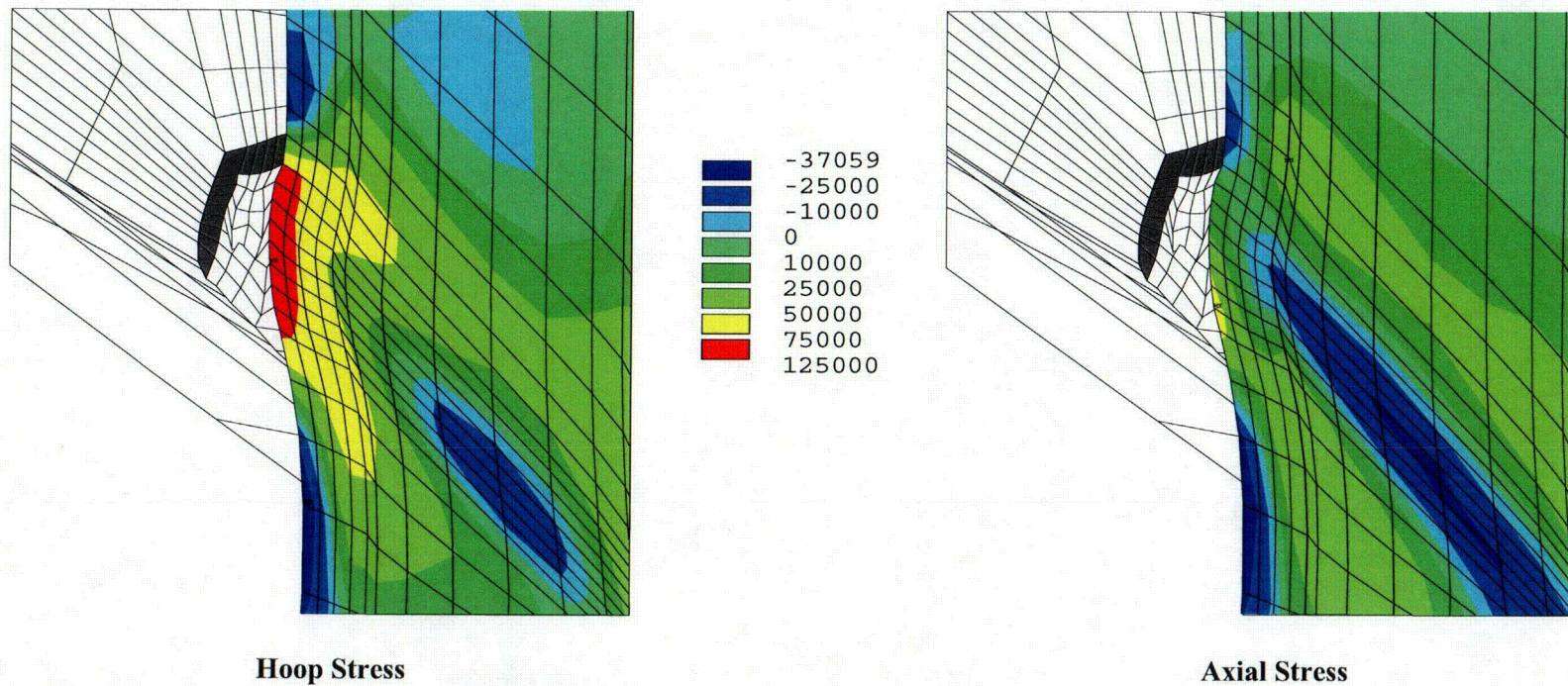
Validation

- Nozzle lateral deflection and ovality
 - Pressurizer heater sleeves
 - CRDM nozzles
 - Bottom head nozzles
- Correlation with reported crack locations and orientations
 - Pressurizer heater sleeves
 - CRDM nozzles
 - Bottom head nozzles
- Correlation with x-ray and strain gauge hole drilling residual stress measurements
 - CRDM nozzle mockups
 - Pressurizer heater sleeve mockups
- Comparison to EMC² results
 - Material properties
 - Stresses
- Early validation work reported in EPRI TR-103696

Results for RPV Top Head Nozzles

Typical Hoop and Axial Stresses

- Typical hoop and axial stresses at uphill location



Welding Residual and Operating Stress Analysis - RPV Top and Bottom Head Nozzles 6

Results for RPV Top Head Nozzles

Correlation of Crack Orientation with Predictions

- Field experience consistent with typical analysis results
 - Over 90% of cracks have been axial
 - More cracks on the OD surface than on the ID surface
 - Circumferential cracks are more likely to initiate on the OD surface below the J-weld than on the ID surface

		No. of Indications on the Nozzle ID	No. of Indications on the Nozzle OD	Total
No. of Axial Tube Indications		112	224	336
No. of Circumferential Tube Indications	Above Weld	0	7	7
	Weld Elevation	0	12	12
	Below Weld	6	10	16
Total		118	253	371

Notes

1. 498 Indications in the Database (as of 09/2003).
2. Craze Cracking/Shallow Cracks are not Included.

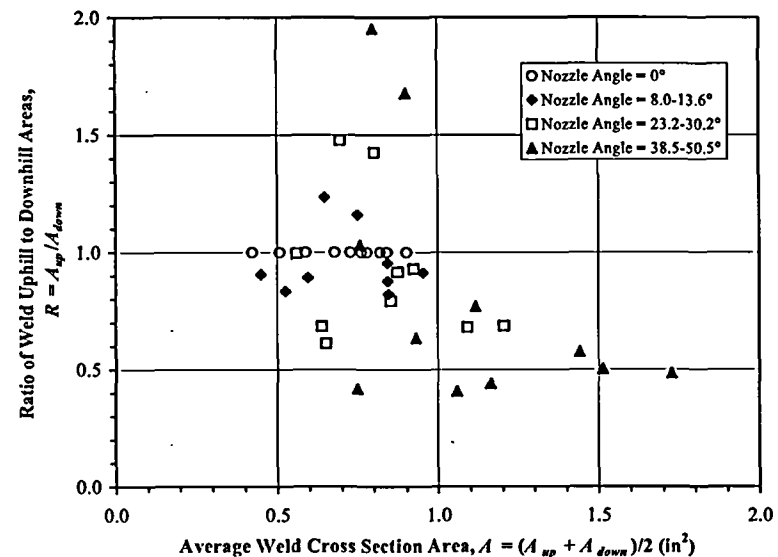
		% Indications on the Nozzle ID	% Indications on the Nozzle OD	Total
% Axial Tube Indications		30%	60%	91%
% Circumferential Tube Indications	Above Weld	0%	2%	2%
	Weld Elevation	0%	3%	3%
	Below Weld	2%	3%	4%
Total		32%	68%	100%

Notes

1. 498 Indications in the Database (as of 09/2003).
2. Craze Cracking/Shallow Cracks are not Included.

Results for RPV Top Head Nozzles *Range of J-Weld Geometries*

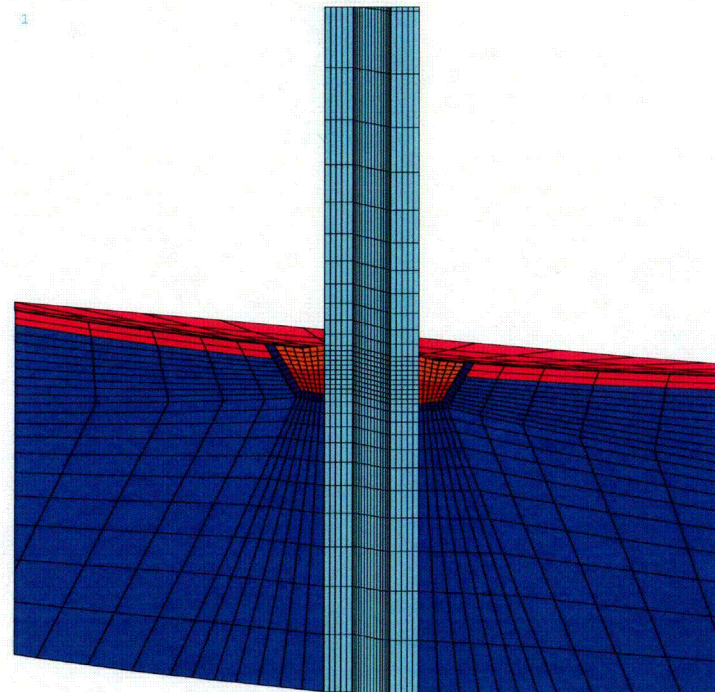
- All J-welds are not the same design
 - Weld cross section areas vary
 - Ratio of uphill-to-downhill areas vary
- Analyses show differences in stress and stress distribution with J-weld geometry
- As-built weld sizes determined by UT inspections differ from design dimensions
 - Oversize downhill welds can reduce maximum OD stresses at weld toe due to lower restraint



Results for RPV Bottom Head Nozzles

Typical Westinghouse BMI Nozzle

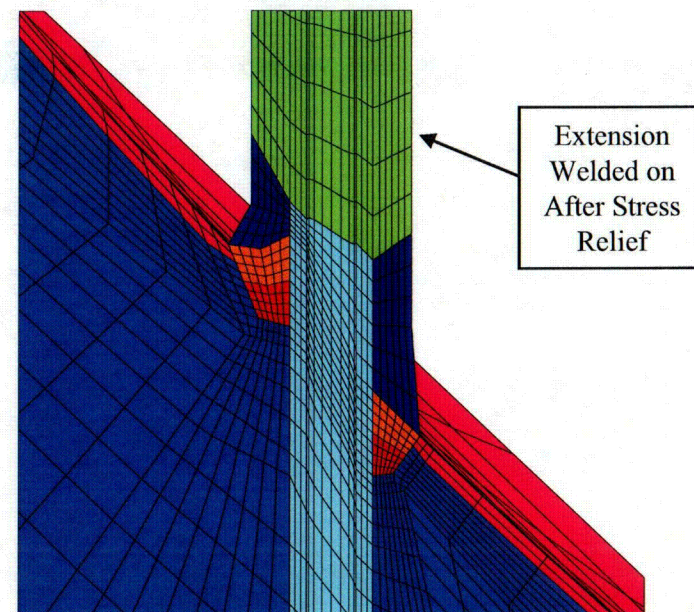
- Nozzles typically have lower D/T ratio than CRDM nozzles
- Typical results show
 - Ovalization is lower than in CRDM nozzles which have higher D/T ratio
 - Stresses are higher than in CRDM nozzles due to larger relative weld size
 - Hoop stresses in nozzle exceed axial stresses at high stress locations
 - Straightening the nozzle by plastic deformation does not increase total operating condition stresses



Results for RPV Bottom Head Nozzles

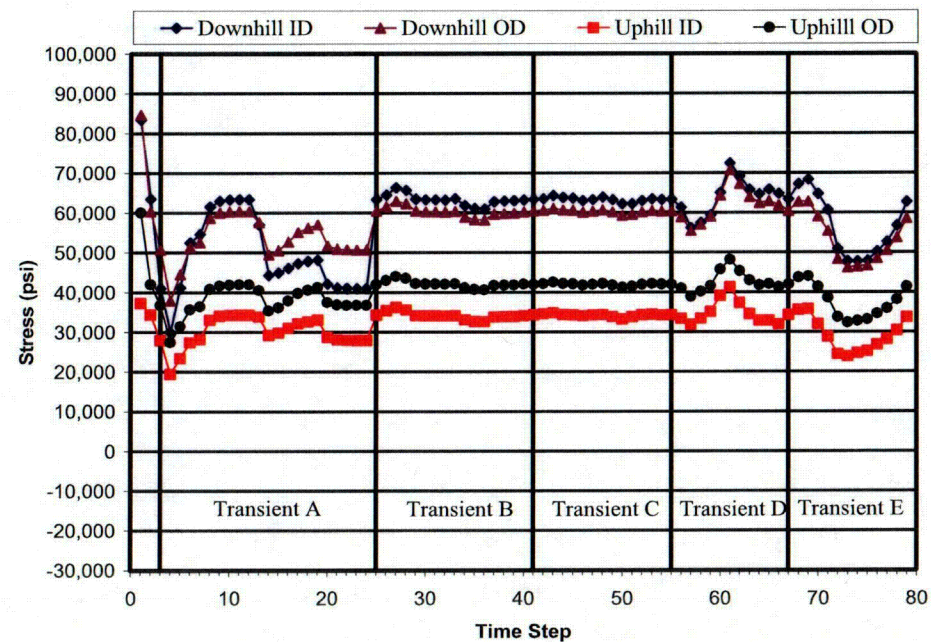
Typical B&W IMI Nozzle

- B&W IMI nozzles repaired
 - Original nozzles and J-welds stress relieved with vessel
 - Prior to plant operation the part of the nozzle inside the vessel was removed and replaced by larger diameter nozzle
- Typical results show
 - Peak stresses in nozzle are higher than in CRDM nozzles due to larger relative weld size
 - Hoop stresses in nozzle exceed axial stresses at high stress locations
 - Stresses in repaired part of nozzle trend to be lower due to less restraint during welding



Transient Analyses for Fatigue Evaluation

- Representative transients selected for analysis
- Thermal transient analysis followed by structural analysis with temps and pressures
- Typical results show:
 - Stress trends consistent throughout model
 - Crack growth rates dominated by PWSCC



Additional Weld Residual Stress Modeling

- Various nozzle repair techniques simulated with stress results used as inputs to fracture mechanics models
 - Nozzle removal repair
 - Embedded flaw repair
- Other penetrations being analyzed
 - Pressurizer side shall penetrations
 - Hot leg nozzle penetrations
 - Pressurizer top and bottom head penetrations

Fracture Mechanics Analyses with Stress Relaxation

Background

- Stress intensity factors are often calculated using superposition method
- For cases with high residual stresses, superposition
 - Conservatively applies residual stresses as primary loads
 - Does not allow for stress relaxation and redistribution with crack growth
- Development work was performed to modify the existing stress analysis model to calculate stress intensities for circumferential flaws above the J-weld including the effects of stress relaxation with crack growth

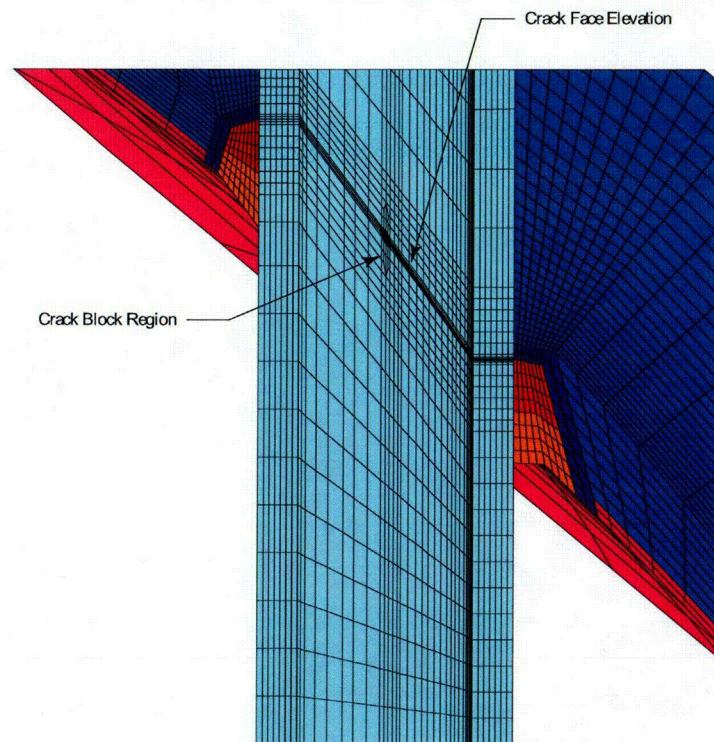
Fracture Mechanics Analyses with Stress Relaxation *Calculation Methodology*

- Initial application is for through-wall crack in outer row CRDM nozzle parallel to weld contour with variable distance above top of weld
- Custom fracture mechanics code added to DEI welding residual finite-element stress model for J-groove nozzles
- Stress redistribution from intact to cracked conditions modeled
 - Redistribution modeled as an elastic unloading problem amenable to LEFM
- Equivalent stress intensity factor (K) calculated from J-integral
 - J-integral calculated using numerical volume integration
 - J-integral averaged across nozzle wall
 - J-integral approach captures effect of Mode II and III contributions

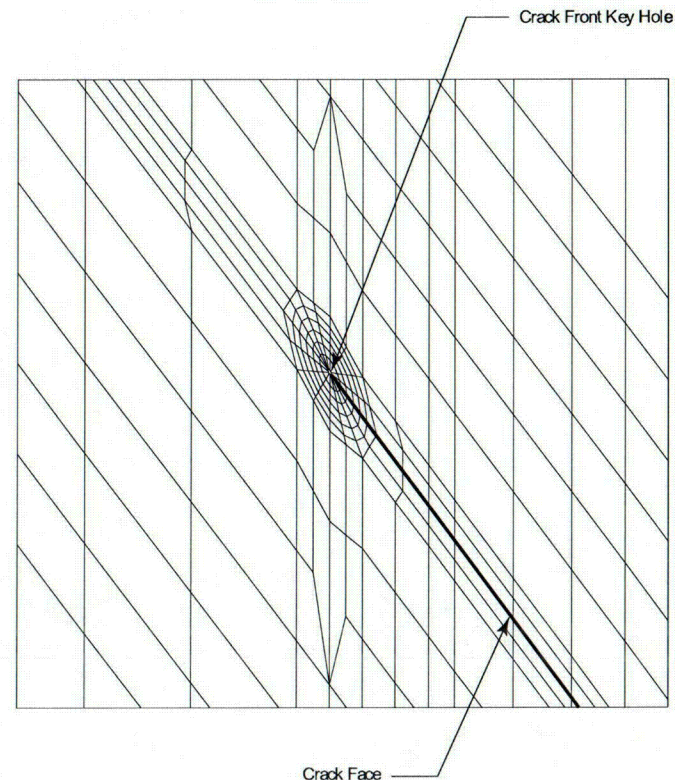
$$K_{eq} = \sqrt{\frac{J_{avg} E}{1 - \nu^2}}$$

Fracture Mechanics Analyses with Stress Relaxation

Fracture Mechanics Model



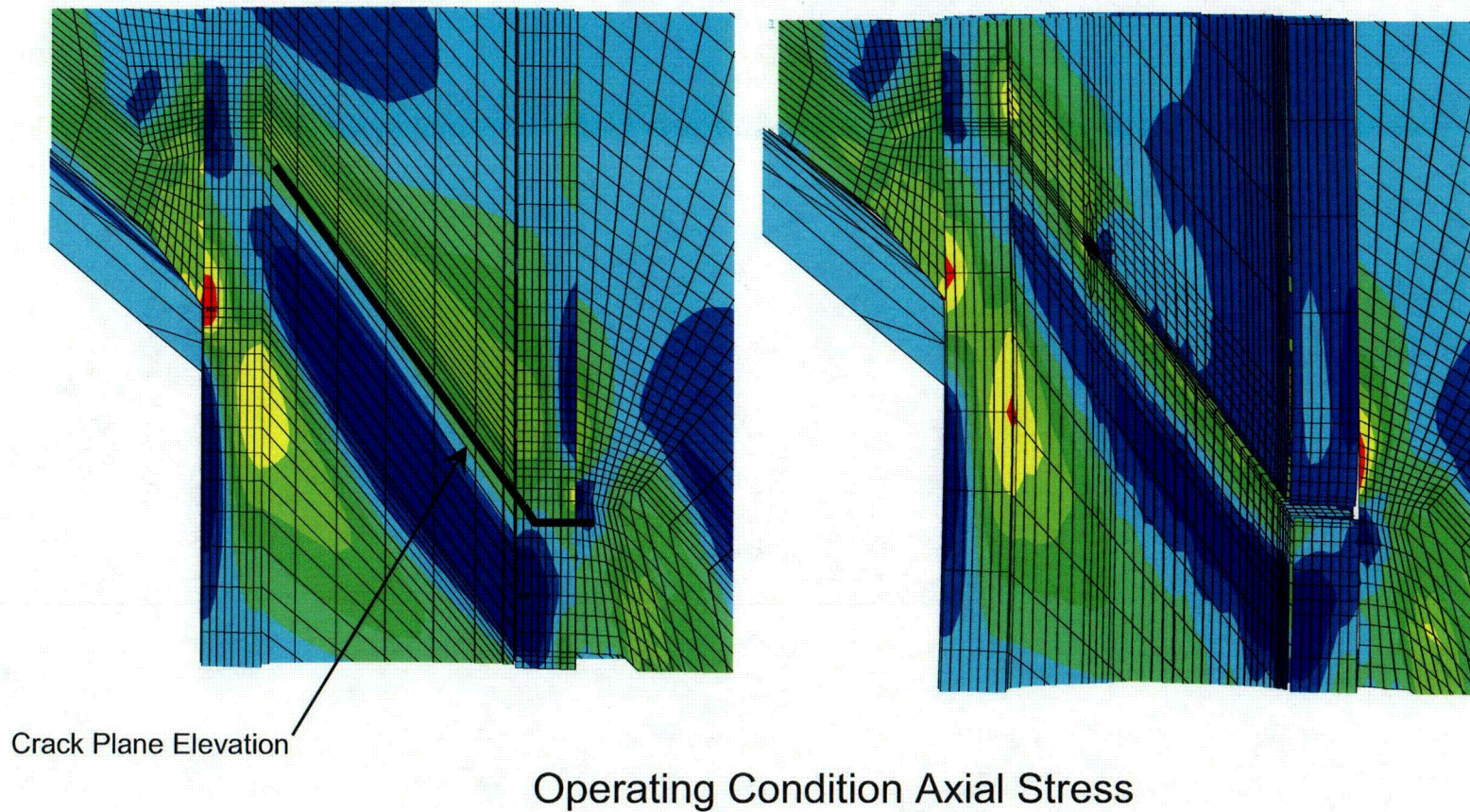
180° Downhill-Centered Crack



Crack Mesh Detail

Fracture Mechanics Analyses with Stress Relaxation

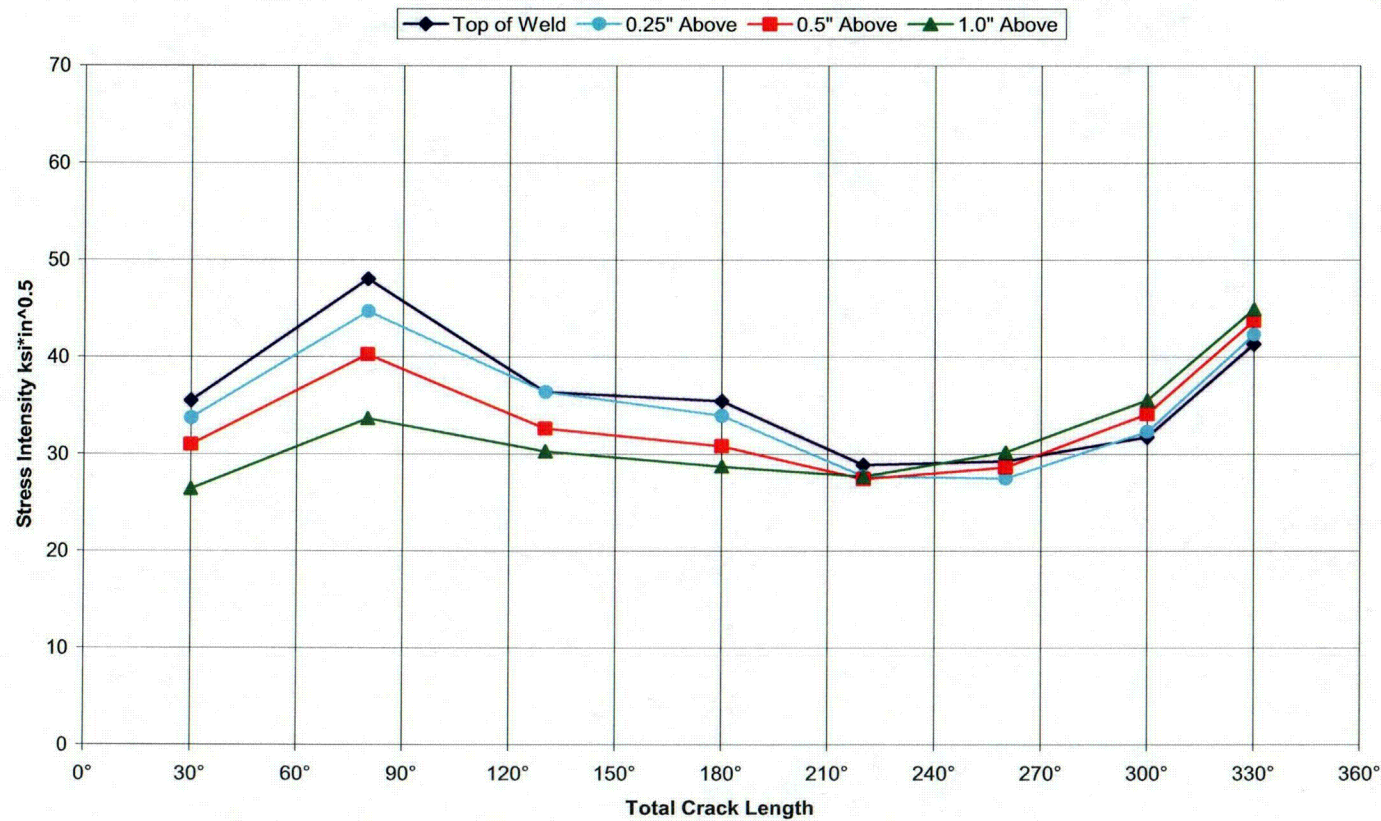
Relief of Axial Stress With Crack Growth



Welding Residual and Operating Stress Analysis - RPV Top and Bottom Head Nozzles 16

Fracture Mechanics Analyses with Stress Relaxation

Stress Intensity: Downhill-Centered Cracks

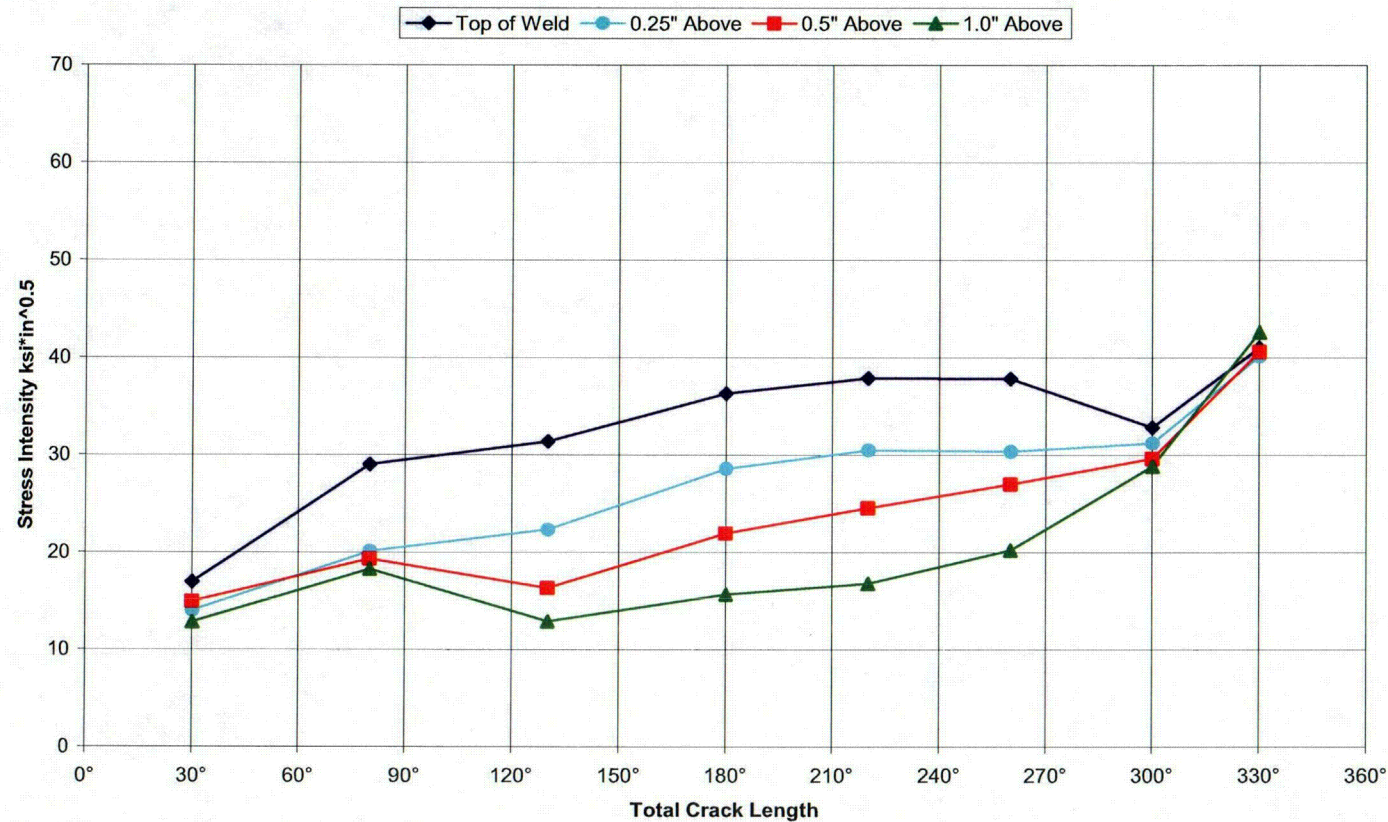


Welding Residual and Operating Stress Analysis - RPV Top and Bottom Head Nozzles 17

C134

Fracture Mechanics Analyses with Stress Relaxation

Stress Intensity: Uphill-Centered Cracks

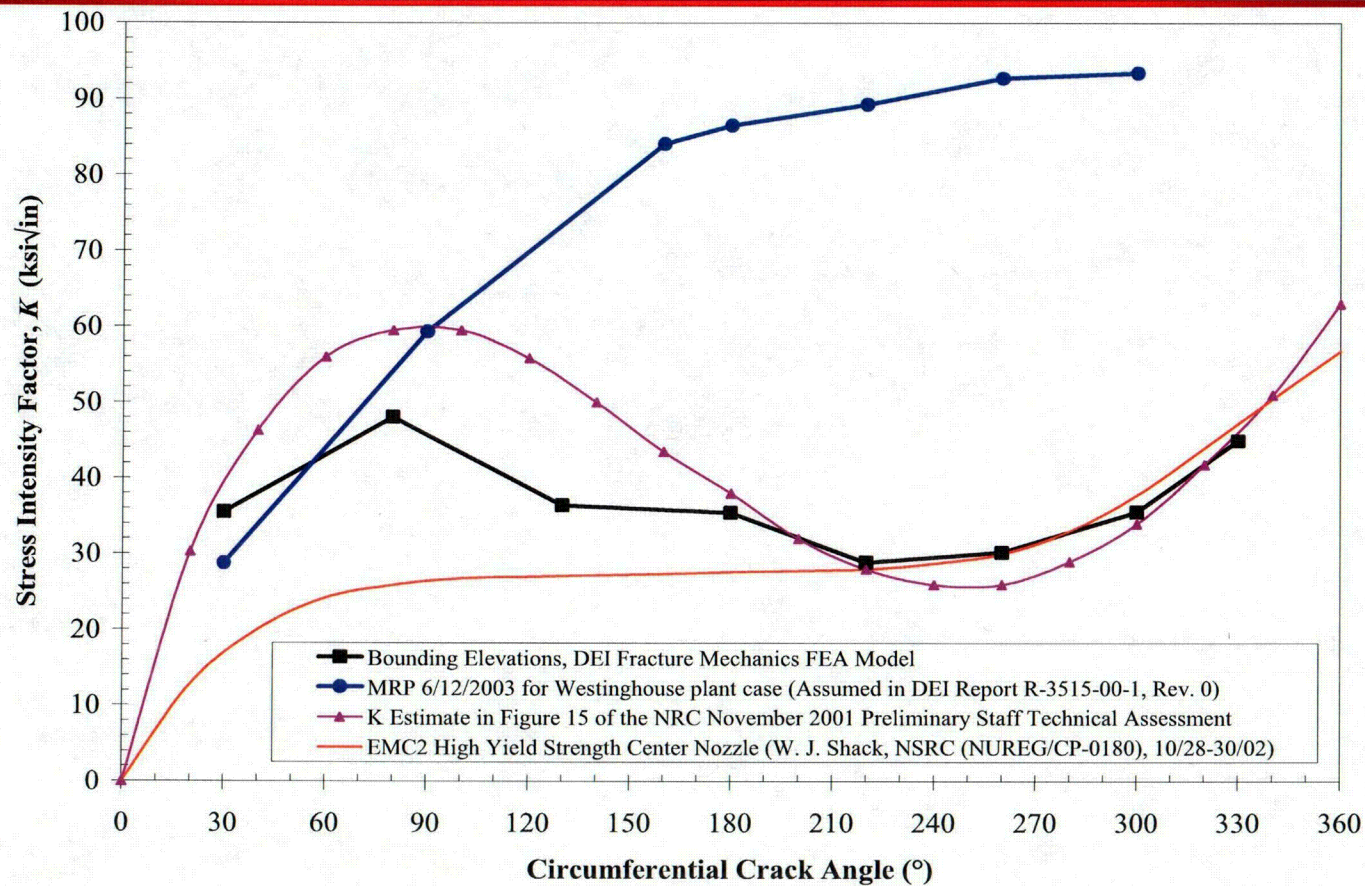


Welding Residual and Operating Stress Analysis - RPV Top and Bottom Head Nozzles 18

C135

Fracture Mechanics Analyses with Stress Relaxation

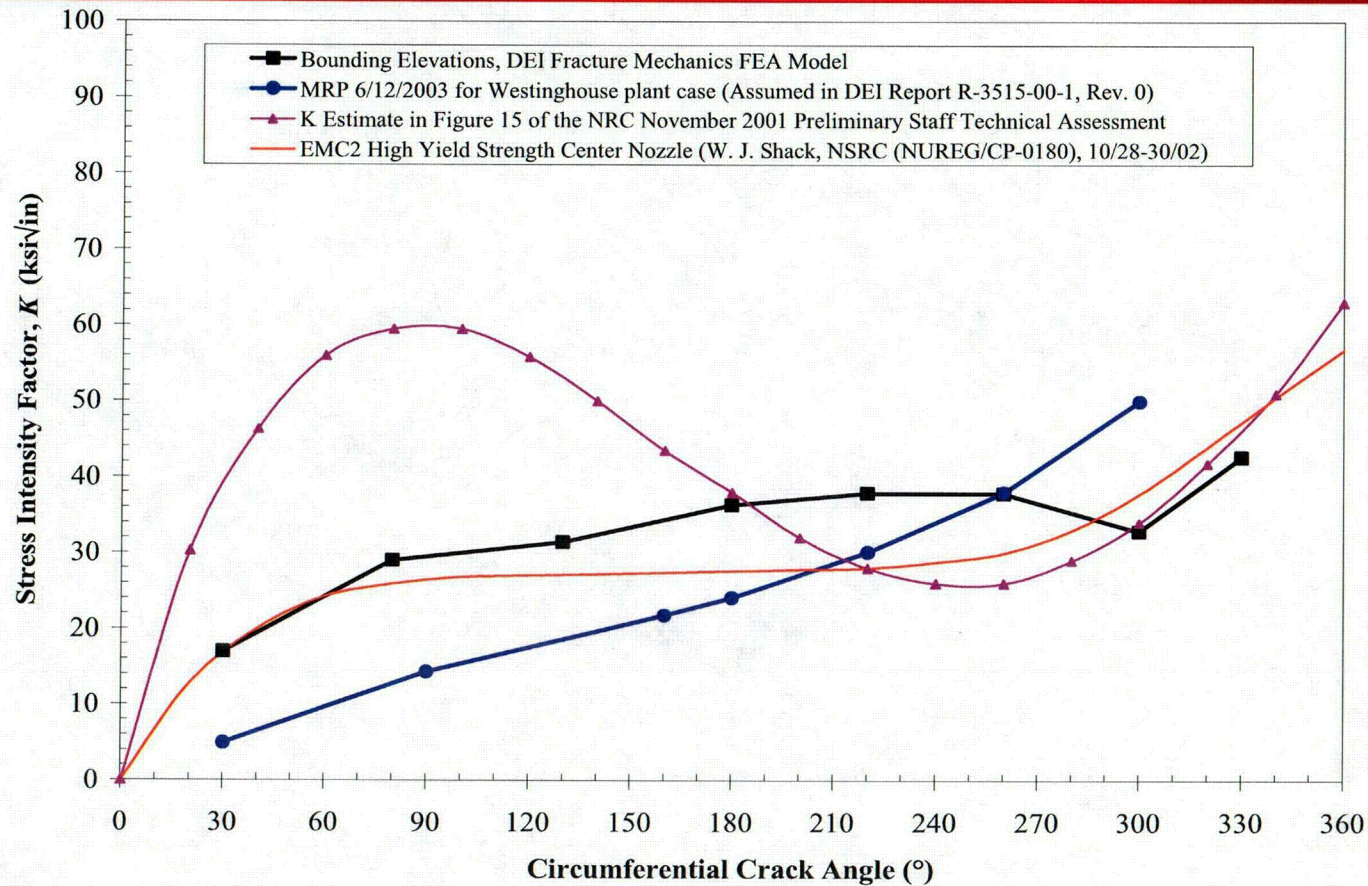
Comparison to Other Data: Downhill-Centered Cracks



Welding Residual and Operating Stress Analysis - RPV Top and Bottom Head Nozzles 19

Fracture Mechanics Analyses with Stress Relaxation

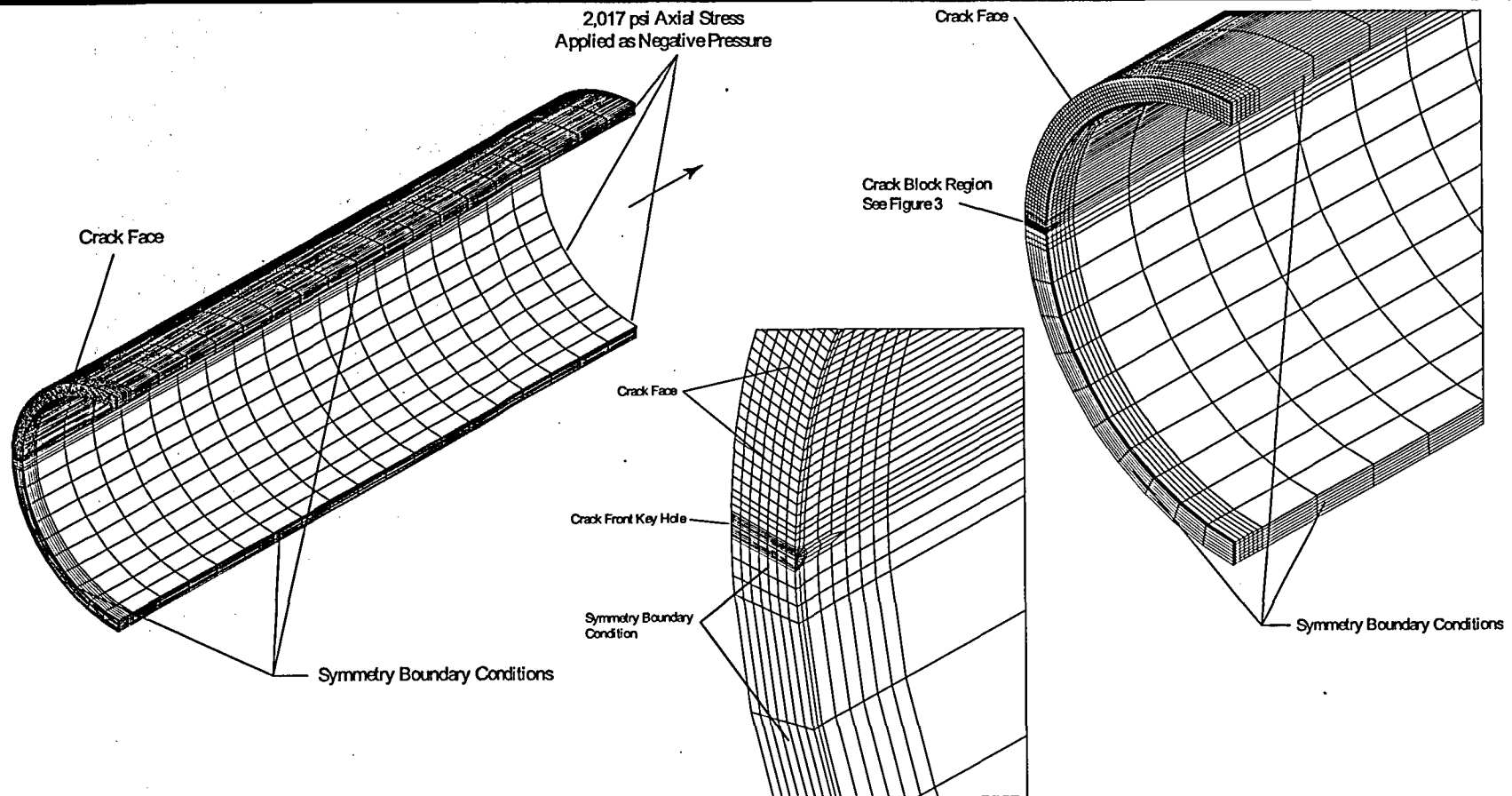
Comparison to Other Data: Uphill-Centered Cracks



Welding Residual and Operating Stress Analysis - RPV Top and Bottom Head Nozzles 20

Fracture Mechanics Analyses with Stress Relaxation

Model Validation Case 1: Pipe with Axial Tension



Fracture Mechanics Analyses with Stress Relaxation

Validation Case 1: Pipe with Axial Tension

- The stress intensity factor calculated for this model was compared to the results published by Zahoor¹ for a mean radius to wall thickness ratio of 10 and a maximum total crack arc of 180°:
 - Results agree within about 10%

Crack Length	K_I Calculated Using Zahoor ¹	K Calculated per FEA Model Test Case
30°	2.9 ksi√in	2.9 ksi√in
80°	6.6 ksi√in	7.1 ksi√in
130°	12.7 ksi√in	13.6 ksi√in
180°	24.0 ksi√in	26.5 ksi√in

¹A. Zahoor, *Ductile Fracture Handbook, Volume 1*, EPRI, Palo Alto, CA: 1989. NP-6301-D.

Fracture Mechanics Analyses with Stress Relaxation Model

Validation Case 2: Through-Wall Center Crack in Plate

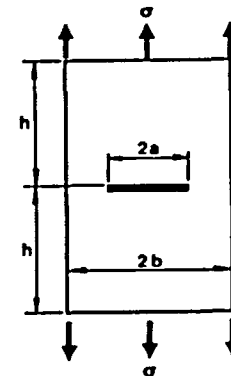
- For large crack sizes, the residual stresses are mostly relieved and the pressure stress determines the stress intensity factor
- A published solution² for a through-wall crack in a finite plate for all a/b and large h/b was compared to the results for large circumferential cracks

- The remote axial stress σ was based on the axial pressure loading including pressure on the crack face

$$K_0 = \sigma \sqrt{\pi a}; \quad \frac{K_I}{K_0} = \frac{1 - 0.5 \frac{a}{b} + 0.326 \left(\frac{a}{b}\right)^2}{\sqrt{1 - \frac{a}{b}}}$$

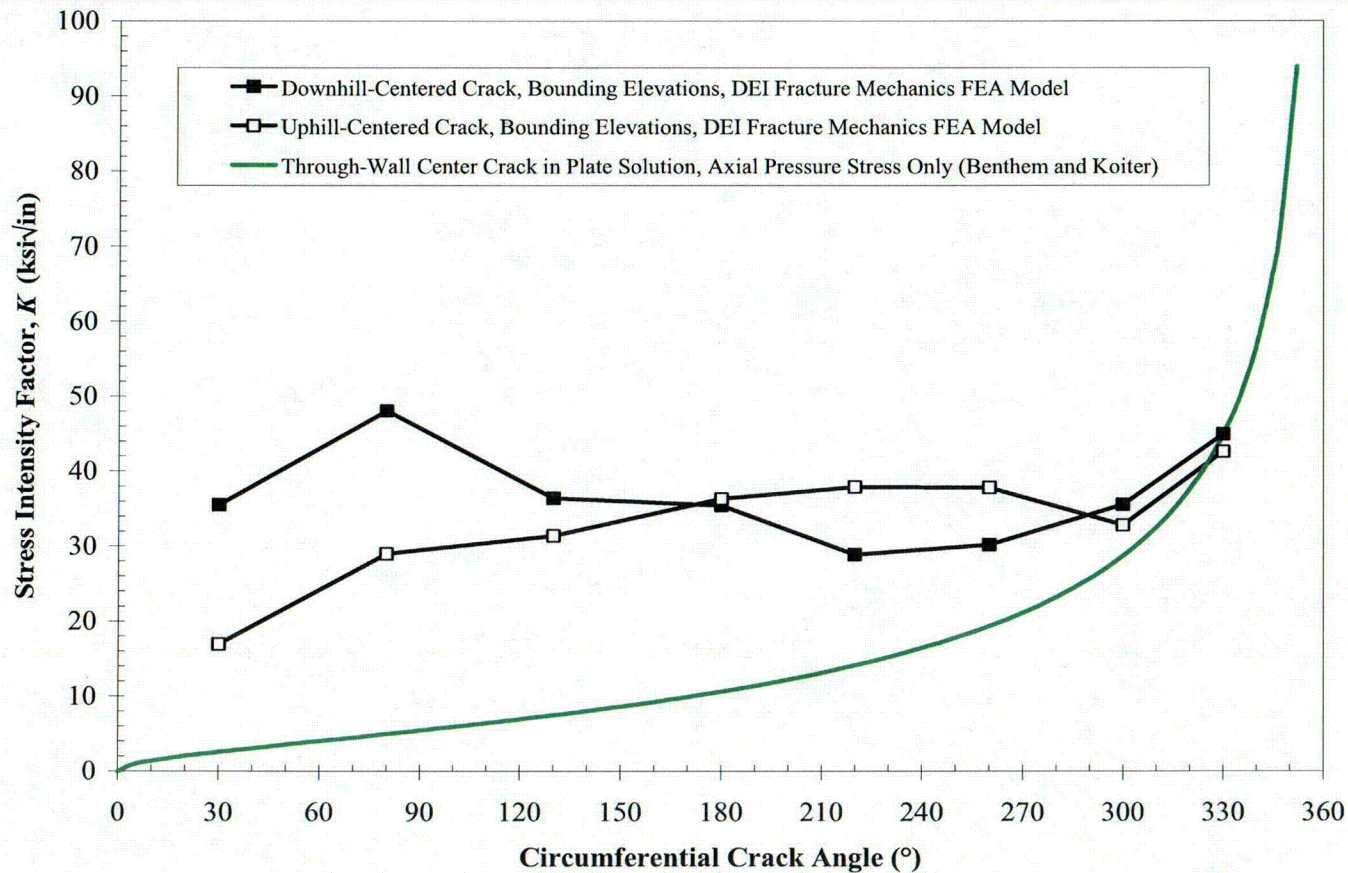
Note: a is taken as the projection of the crack midwall half-length on a horizontal plane.

²D. P. Rooke and D. J. Cartwright, *Compendium of Stress Intensity Factors*, Her Majesty's Stationery Office, London, 1976, p. 10.



Fracture Mechanics Analyses with Stress Relaxation Model

Validation Case 2: Through-Wall Center Crack in Plate



Welding Residual and Operating Stress Analysis - RPV Top and Bottom Head Nozzles 24

Fracture Mechanics Analyses with Stress Relaxation

Conclusions

- Analysis work shows that stress intensities calculated by superposition without the effect of stress relaxation can be conservative

RPV Penetration Stress Analysis and Fracture Mechanics

Future Efforts

- Continued comparisons of welding residual stress and fracture mechanics model results with others
- New opportunity for comparison between model and as-built results in North Anna RPV head
- Additional fracture mechanics applications:
 - Through-wall axial cracks for wastage analyses
 - J-groove weld cracks for time to grow to leak as well as leak rate calculations

Predicting the First Failure

Roger W. Staehle

Adjunct Professor, University of Minnesota

Vessel Penetration Conference

September 29-October 2, 2003

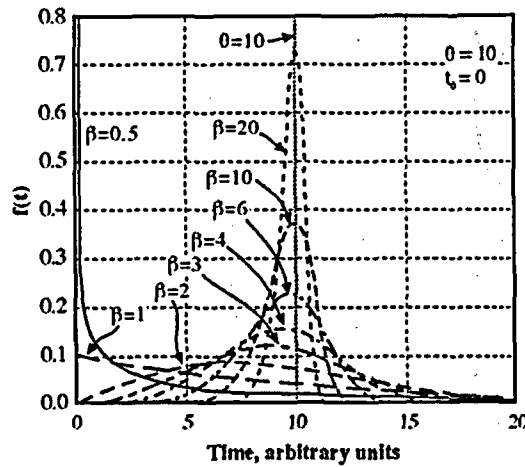
Washington, D. C.

Objectives and Scope

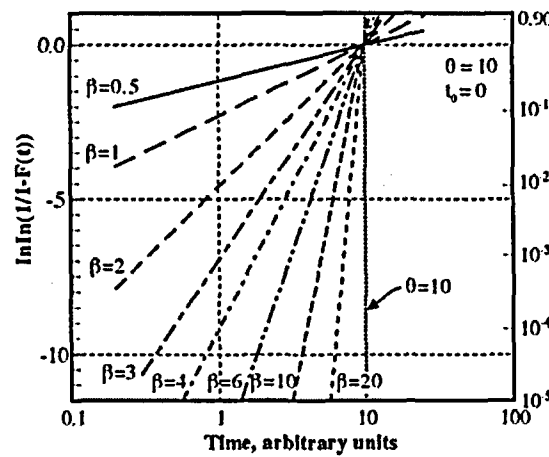
- Predict the first failure as it occurs in a statistical distribution. The first failure is usually the most important and often cannot be readily obtained
- Predict statistical distribution of SCC *a priori* based on physical variables from prior experience.
- Combine statistical distribution with physical variables of pH, potential, species, alloy composition, alloy structure, temperature, stress.
- Integrate multiple environments and submodes using product of reliabilities.
- Can apply to initiation and propagation.
- Evaluate in environments.

Weibull Distribution (Constant θ , Variable β)

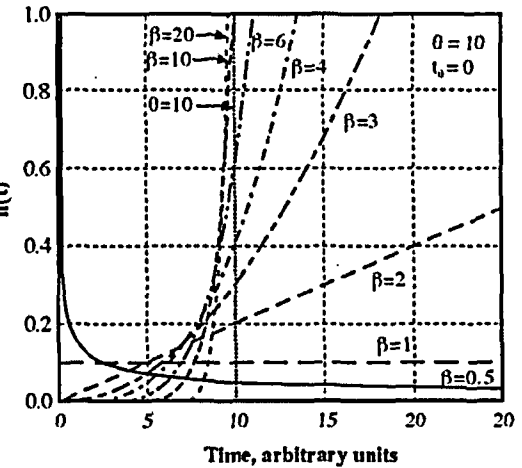
Probability density
function



Cumulative
distribution function



Hazard function



$$f(t) = \left[\frac{\beta}{(\theta - t_0)^\beta} \right] (t - t_0)^{\beta-1} \exp \left[- \left(\frac{t - t_0}{\theta - t_0} \right)^\beta \right], t > t_0 \quad (1)$$

$$F(t) = P\{t \leq t\} = \int_0^t f(t) dt \quad (2)$$

$$h(t) = \frac{f(t)}{1 - F(t)} \quad (5)$$

θ = Scale parameter

β = Shape parameter

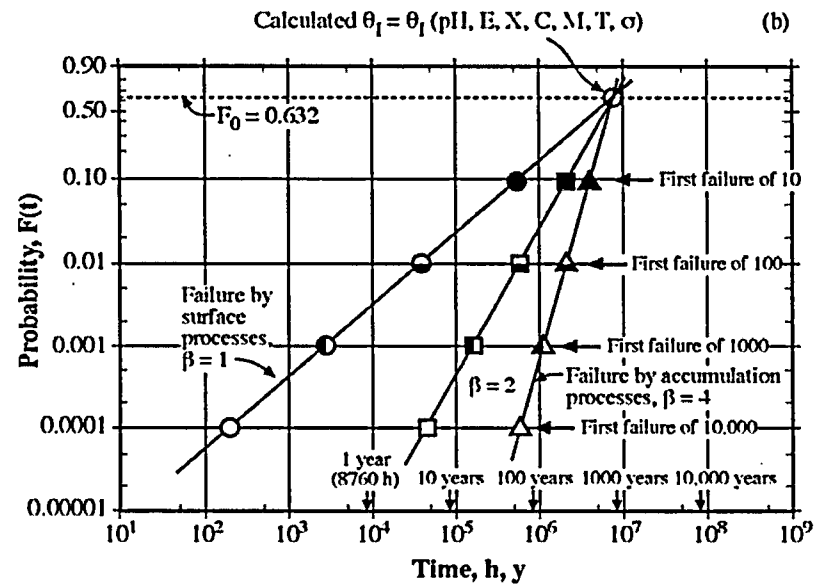
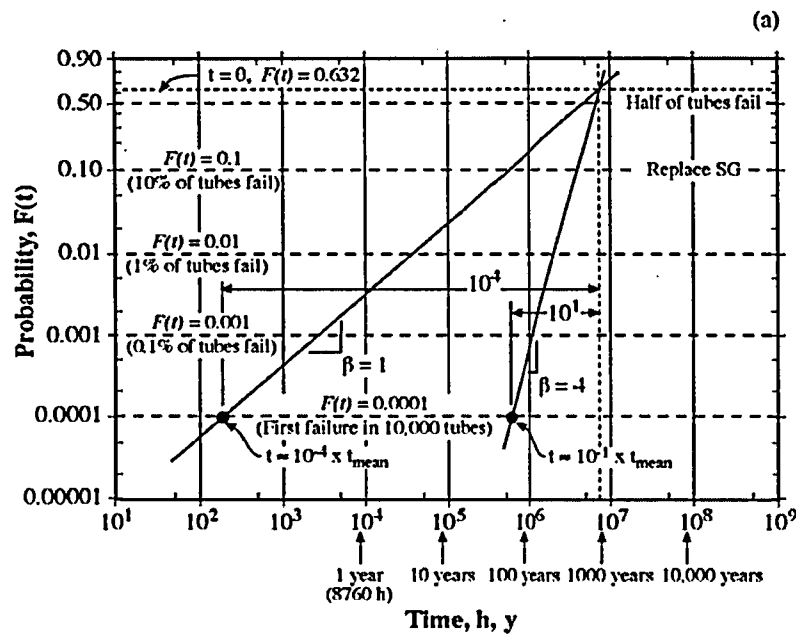
t_0 = Location parameter

$$F(t) = 1 - \exp \left[- \left(\frac{t - t_0}{\theta - t_0} \right)^\beta \right] \quad (3)$$

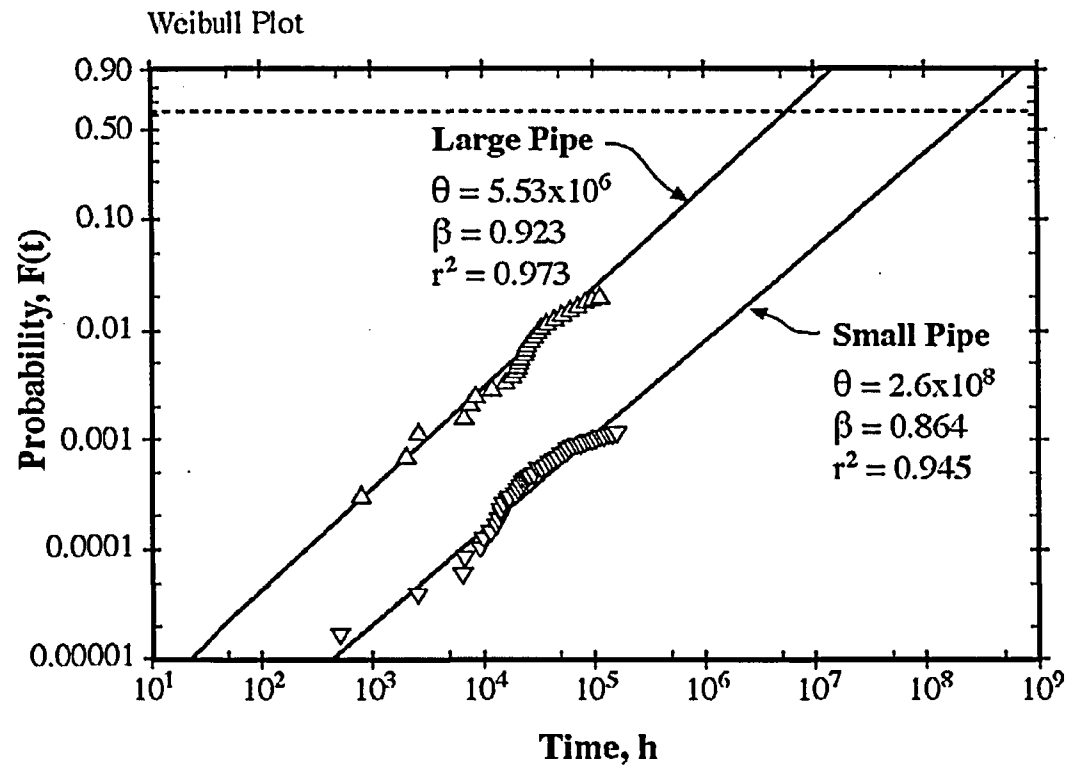
$$h(t) = \left(\frac{\beta}{\theta - t_0} \right) \left(\frac{t - t_0}{\theta - t_0} \right)^{\beta-1} = \frac{\beta}{(\theta - t_0)^\beta} (t - t_0)^{\beta-1} \quad (6)$$

$$\ln \left[\ln \left(\frac{1}{1 - F(t)} \right) \right] = \beta [\ln(t - t_0) - \ln(\theta - t_0)] \quad (4)$$

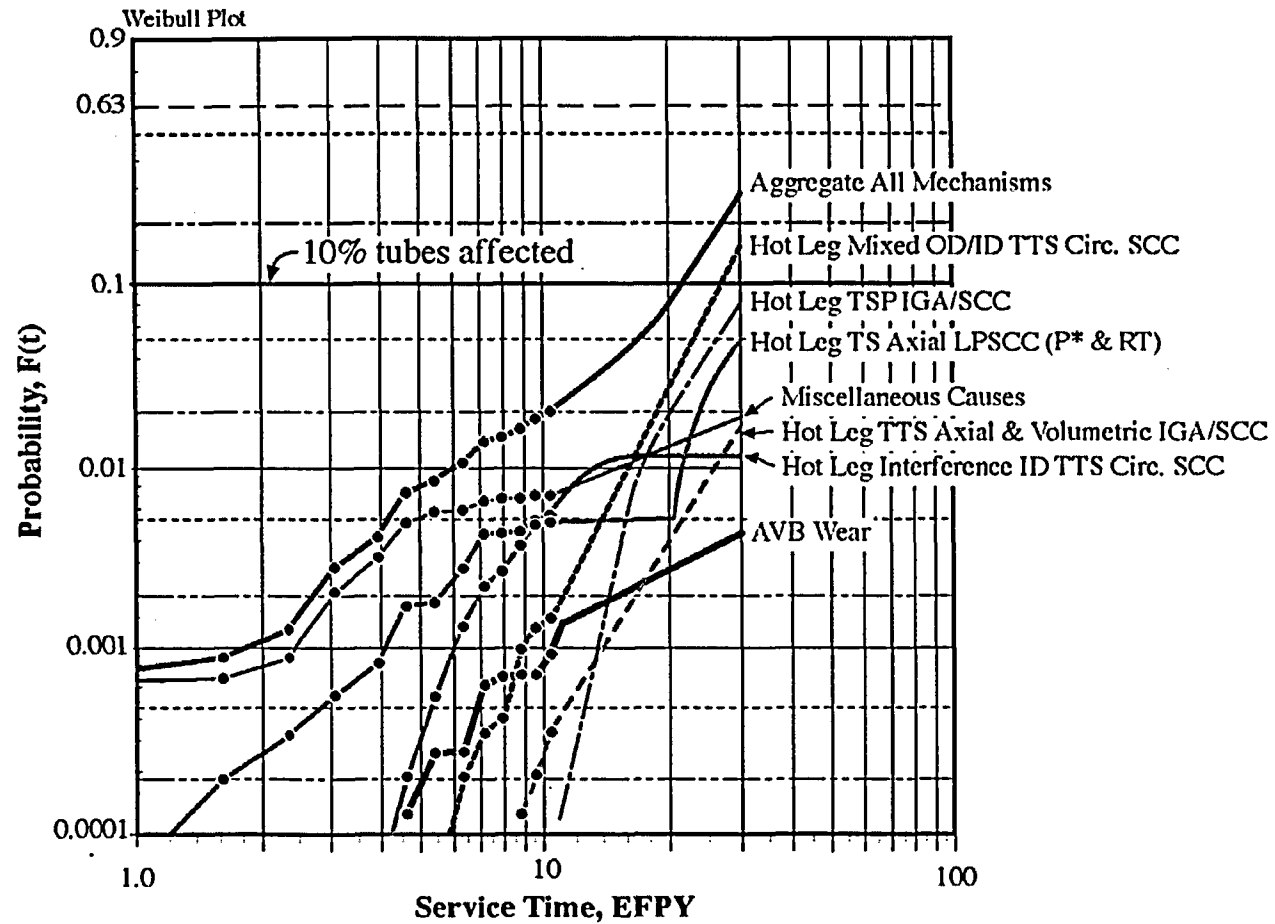
Magnitudes of cdf Depending on Shape Parameter And Number in Sample



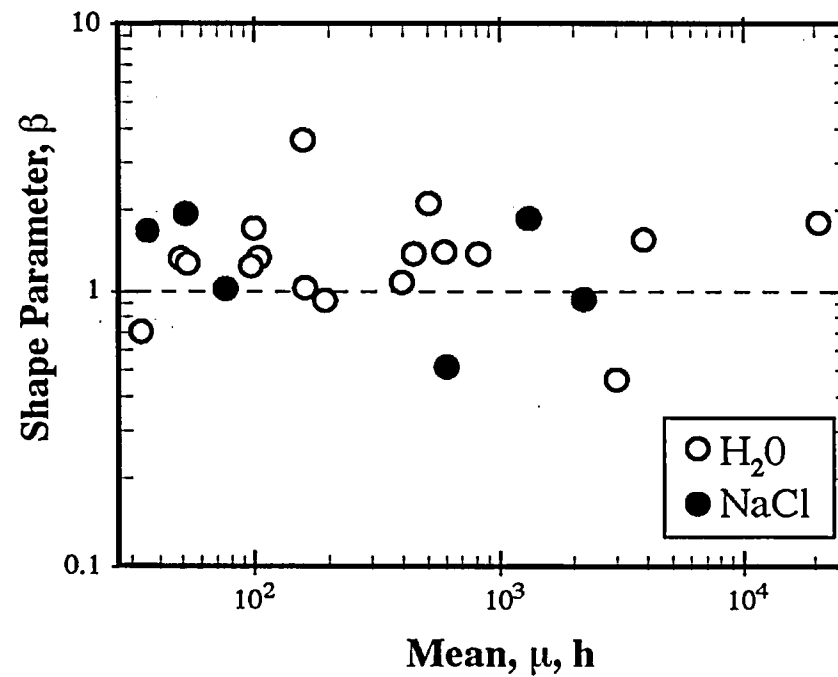
Probability of SCC vs. Time in Large (4 inch diameter)
and Small (2 inch diameter) of Welded Stainless Steel Piping
in BWR Water (Easton and Shusto)



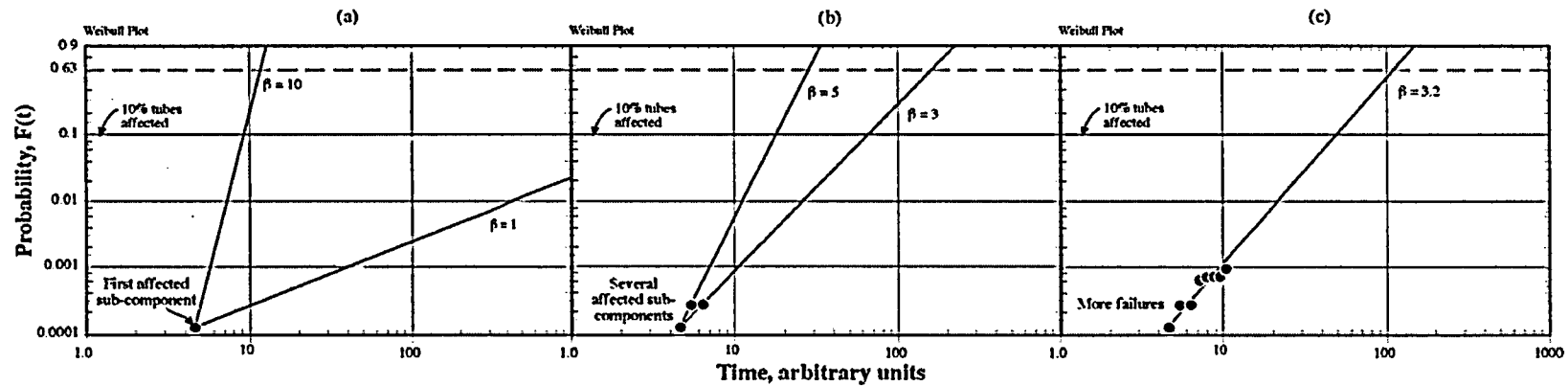
Probability vs. EFPY for Alloy 600 Tubing in Ringhalls-4 PWR Steam Generator (Gorman and Bjornquist)

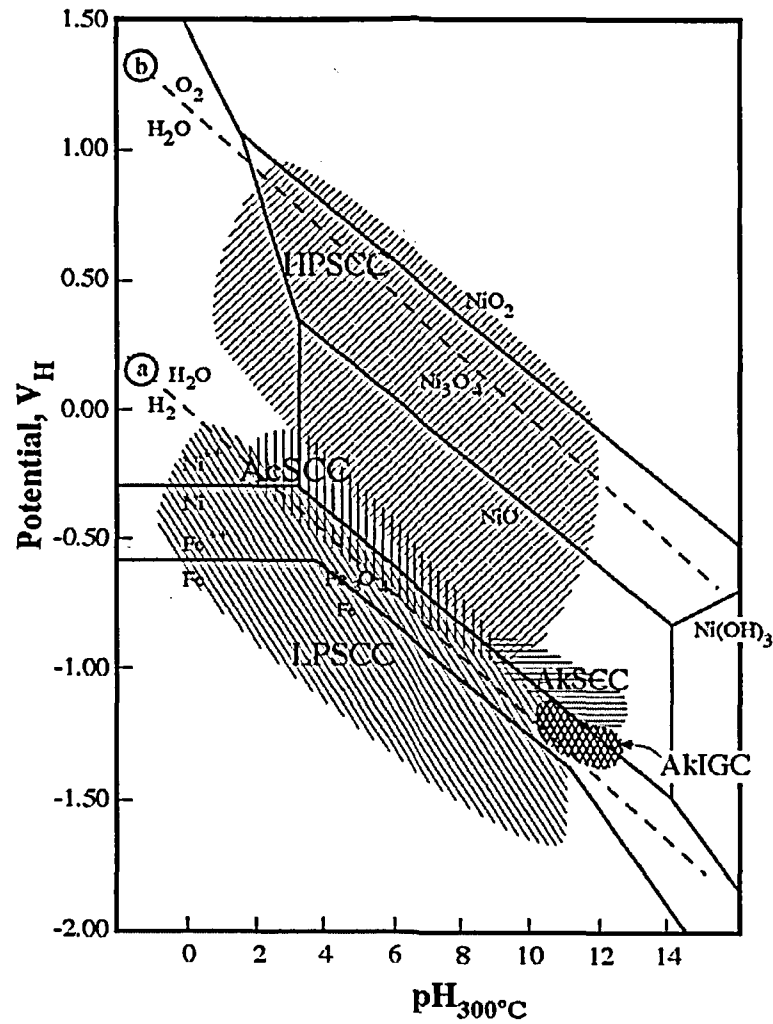


Shape Parameter, β , vs Mean Failure Time in NaCl solutions
Using Sensitized Stainless Steel and No Crevices 30-80°C
(Akashi and Nakayama)

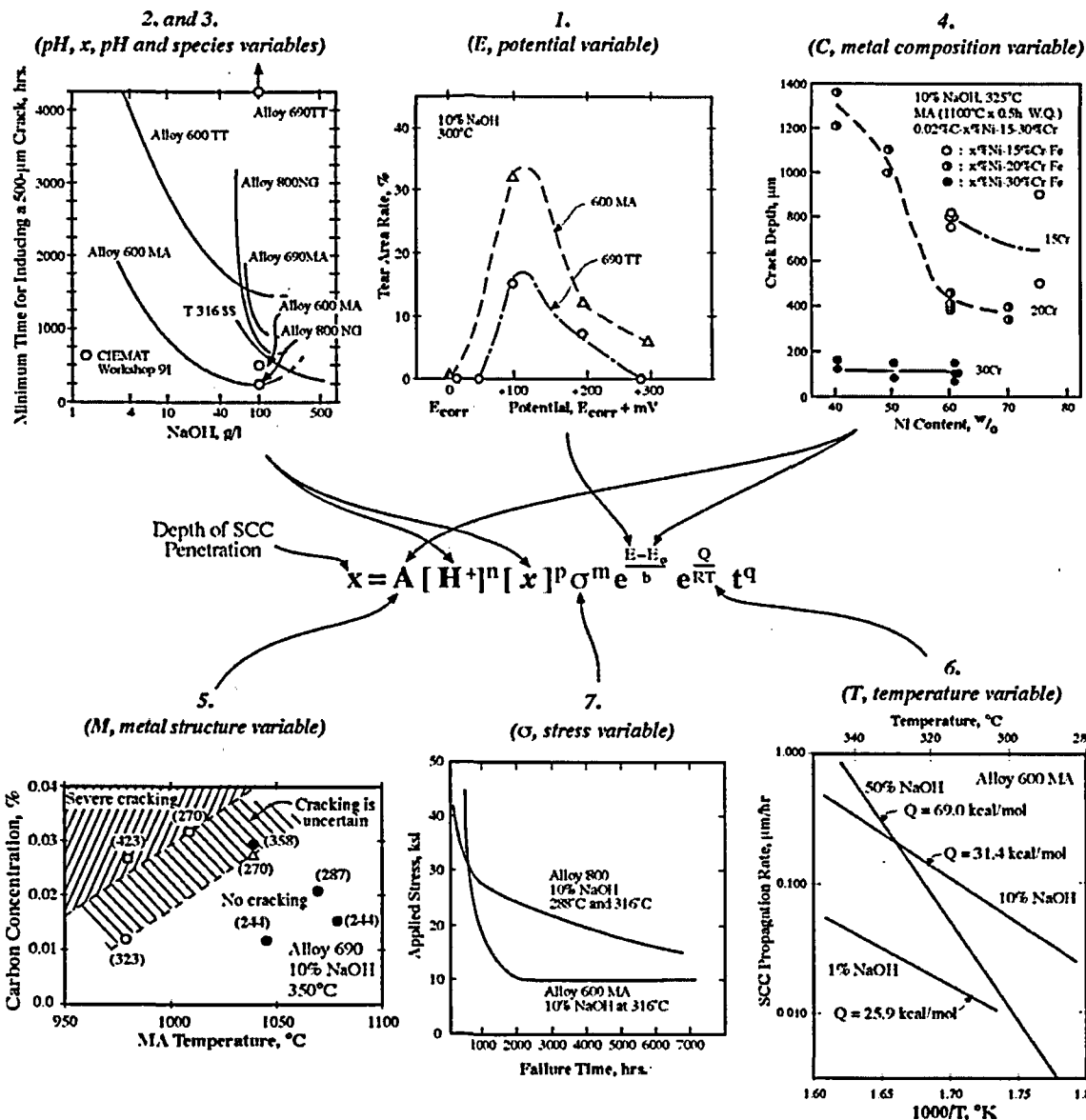


Progressive Development of Prediction from Early Data Using Weibull cdf

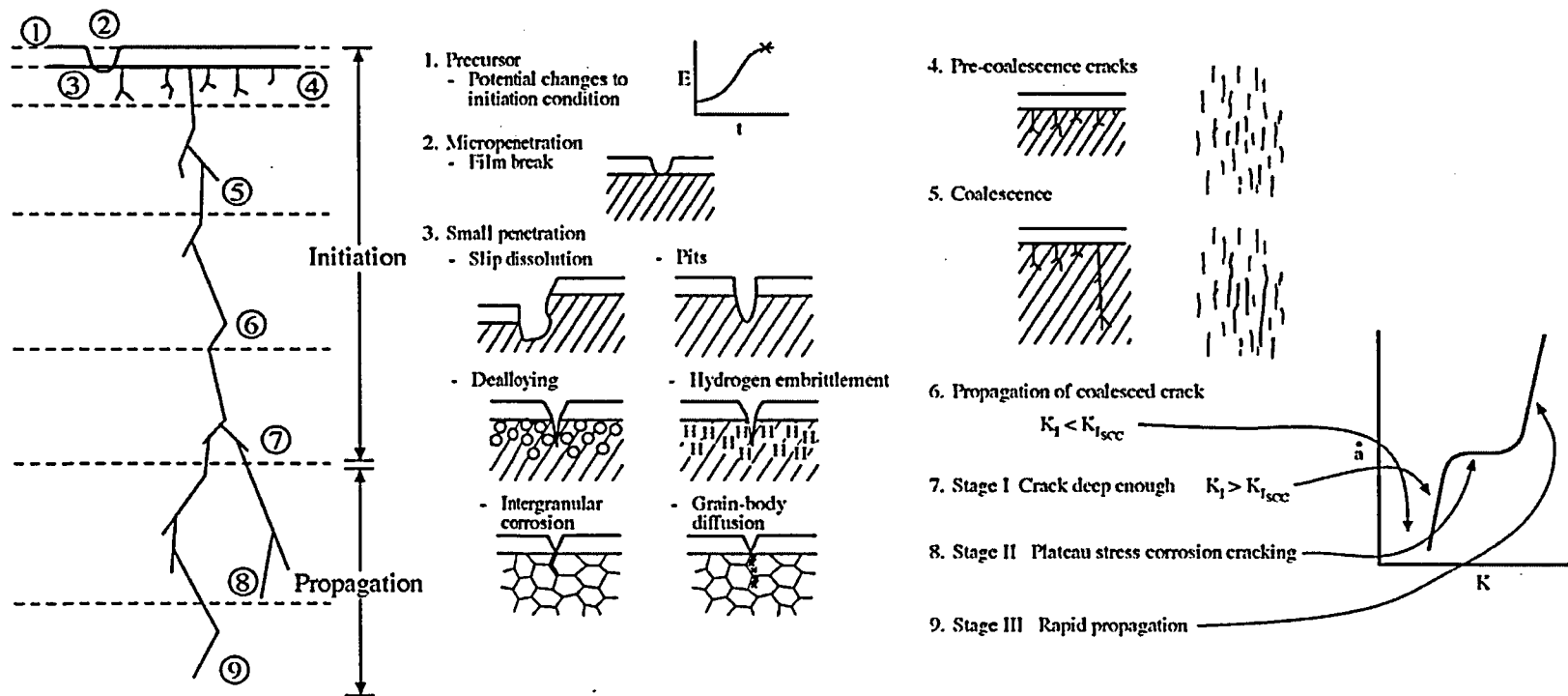




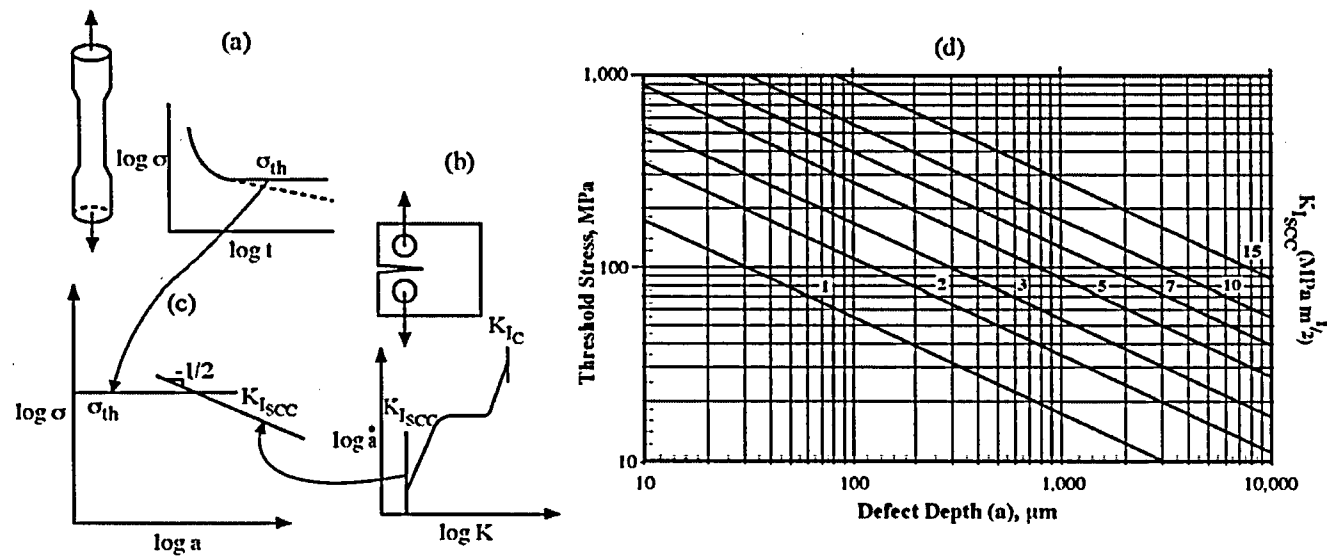
Mode Diagram for SCC of
Alloy 600 in 300-350°C
Range in Pure Water Applied to
PWR Steam Generators

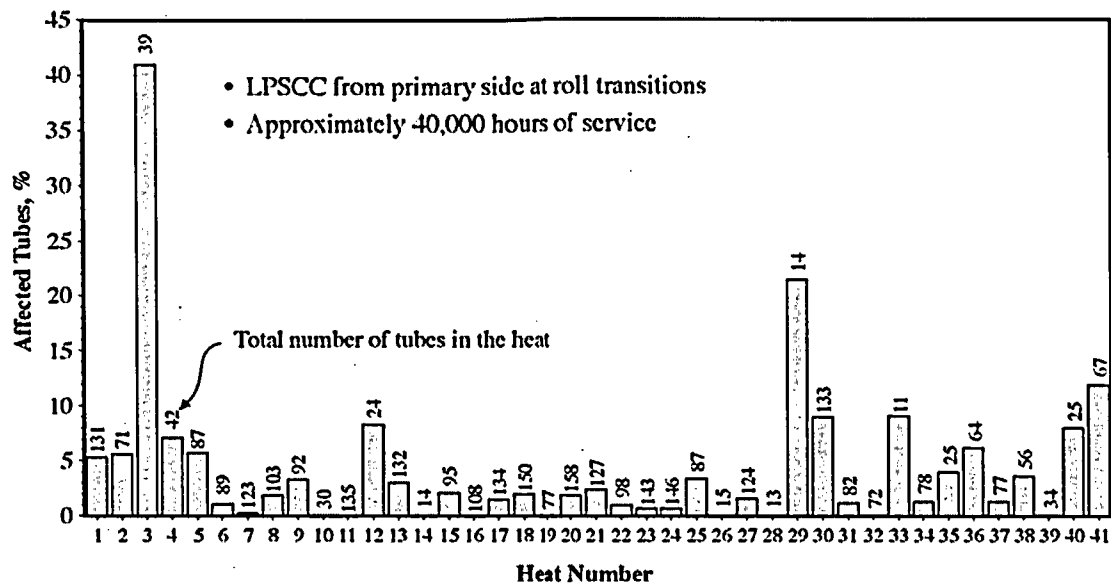


Nine Stages of SCC



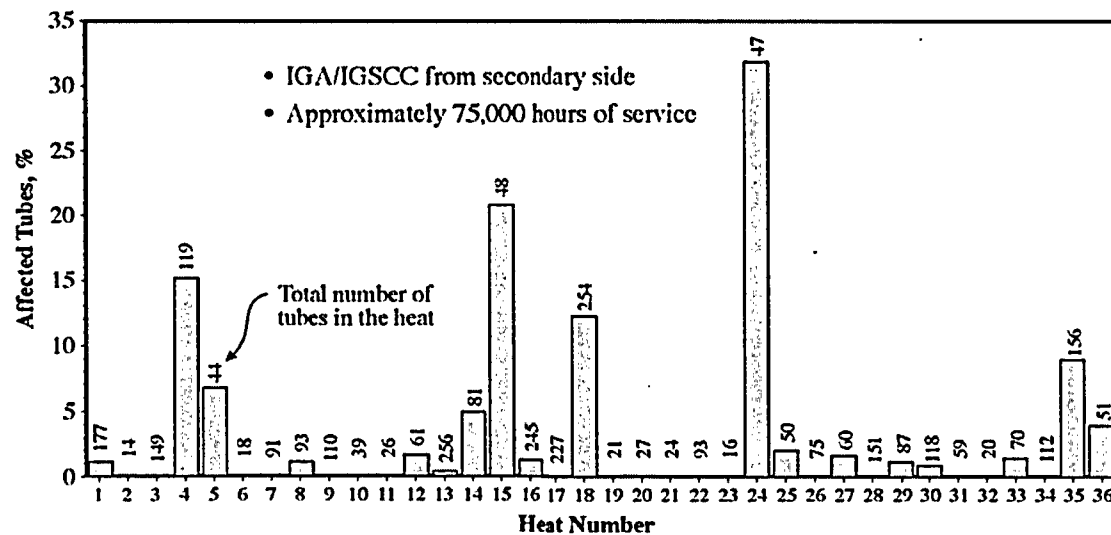
Estimation of Depth of Transition from Initiation to Propagation





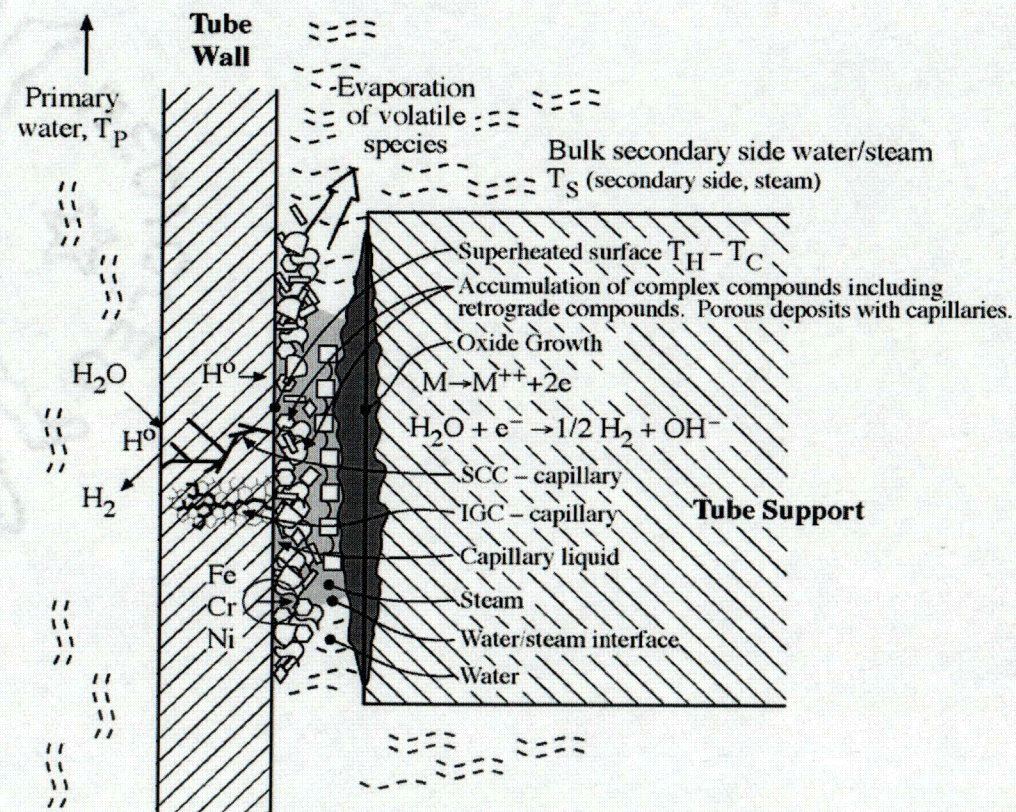
(a)

Percent Failure of SG Tubes per Heat for Primary (Upper) and Secondary (Lower) Sides vs.. Heats Produced by Single Manufacturer in Chronological Sequence. (Number of tubes from each heat used shown)

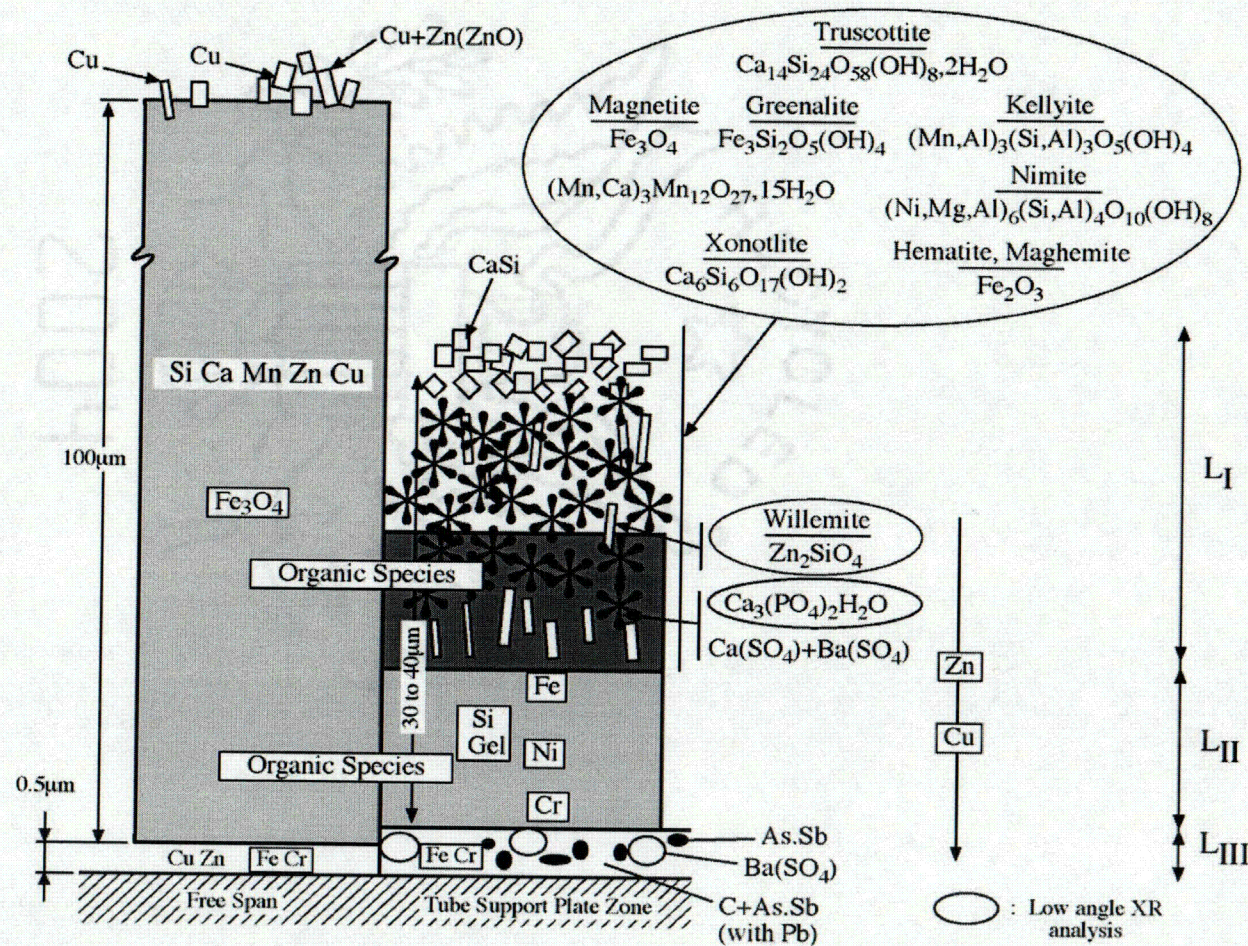


(b)

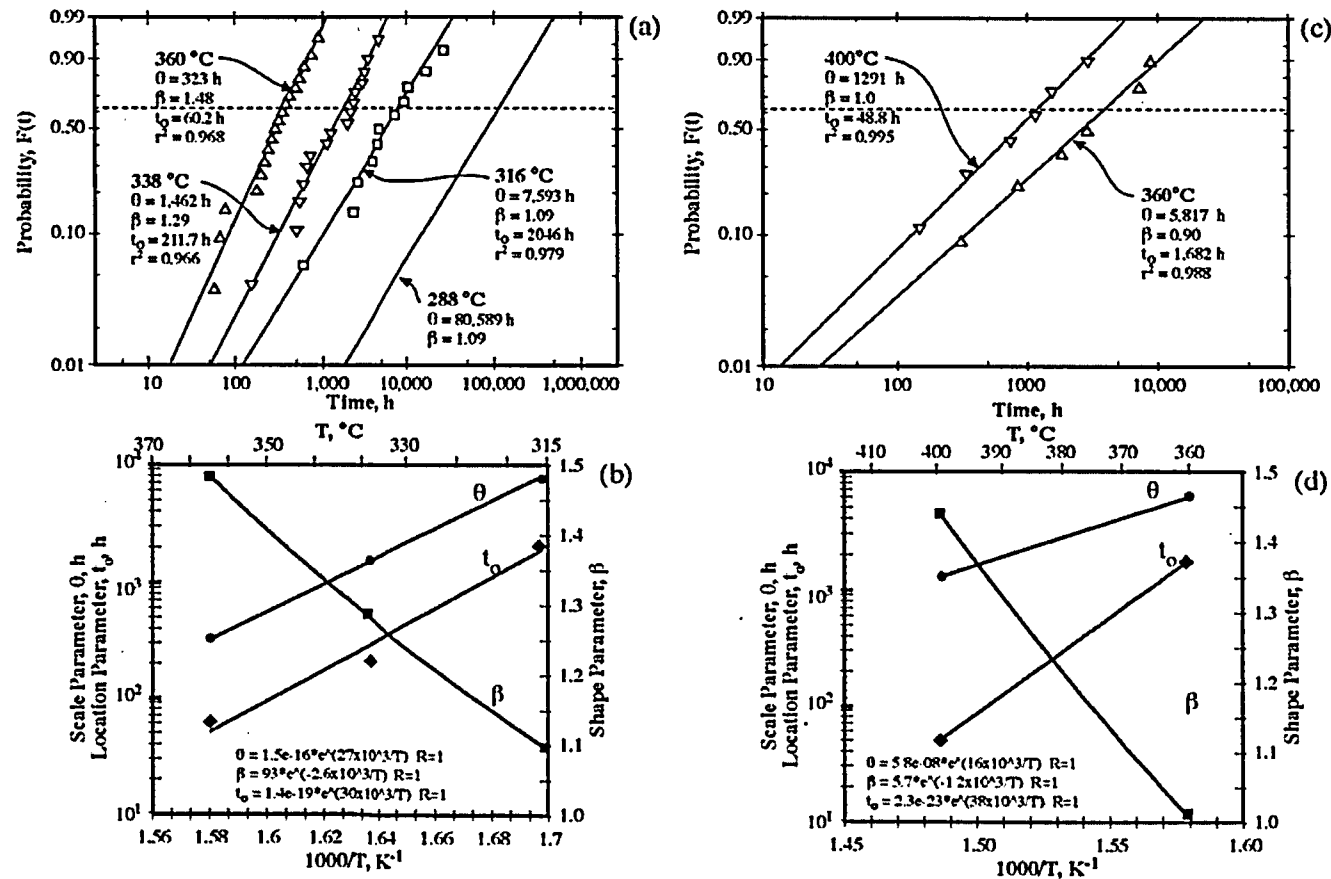
Complexity of Environments in Heat Transfer Crevices



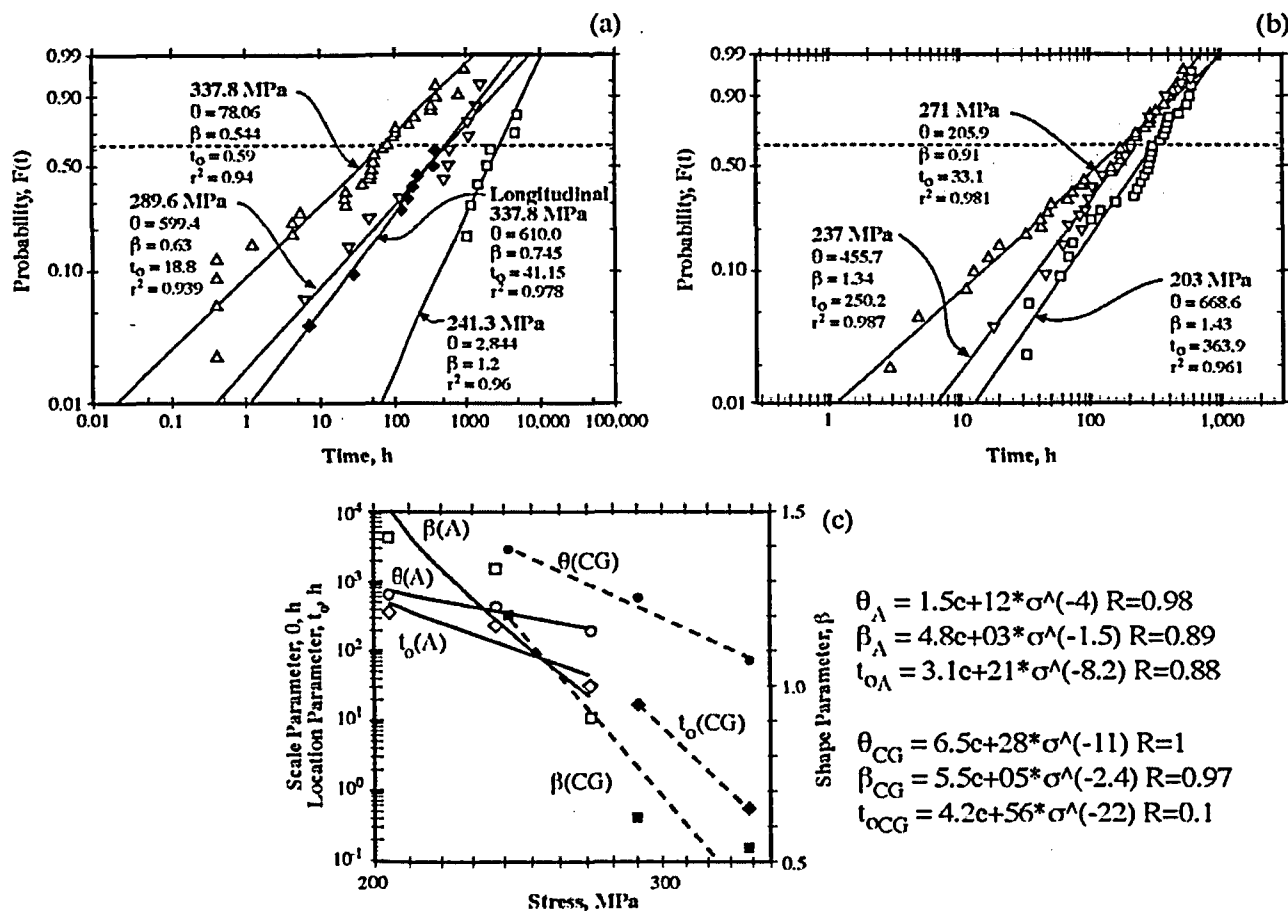
Chemistry, Location, and Depth of Deposits from Heated Crevice from PWR SG (Cattant, Sala)



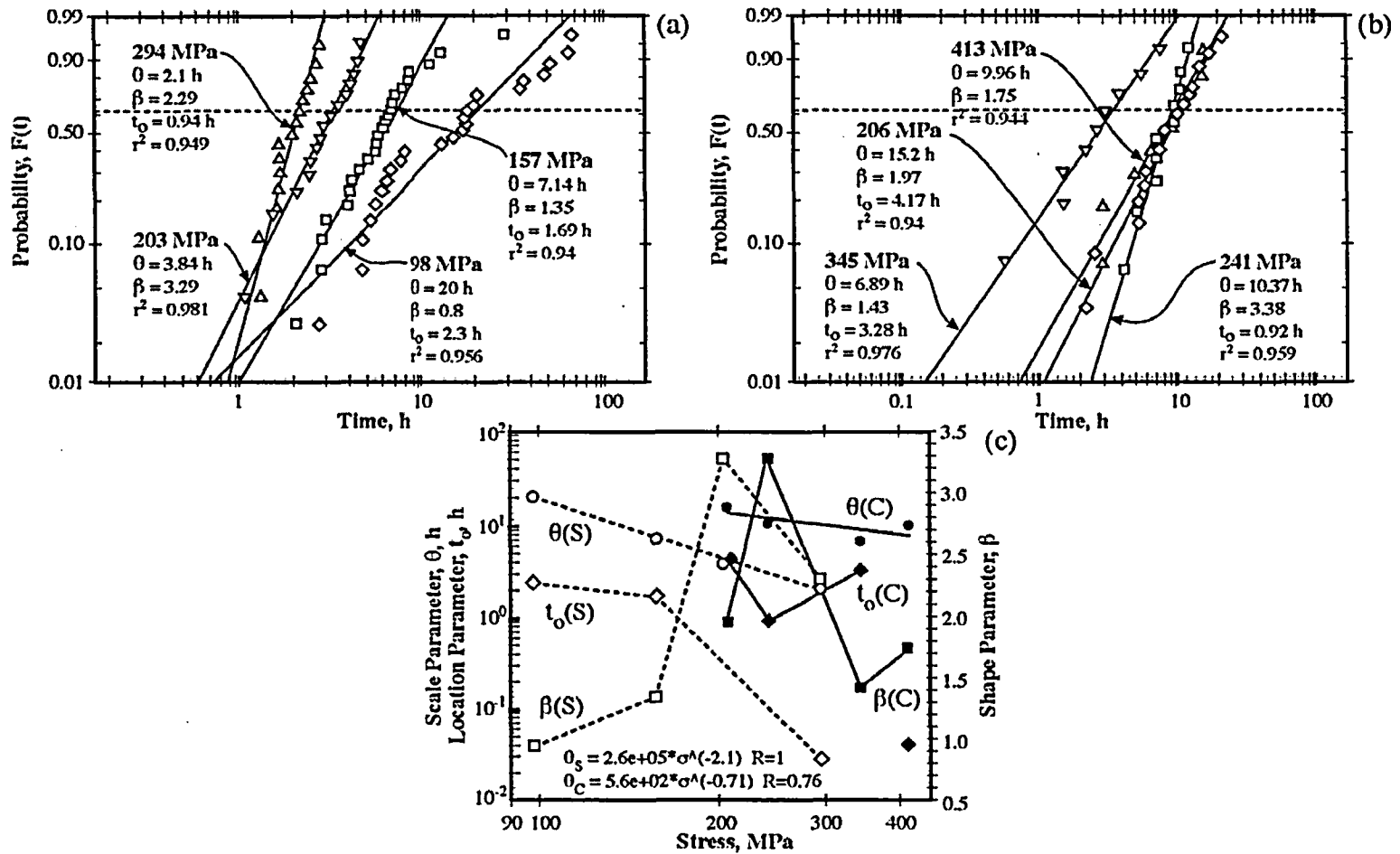
Probability vs. Time for LPSCC of Alloy 600 as a Function of Temperature
(Data from Webb, Jacko);
Dependencies of Statistical Parameters on $1/T$



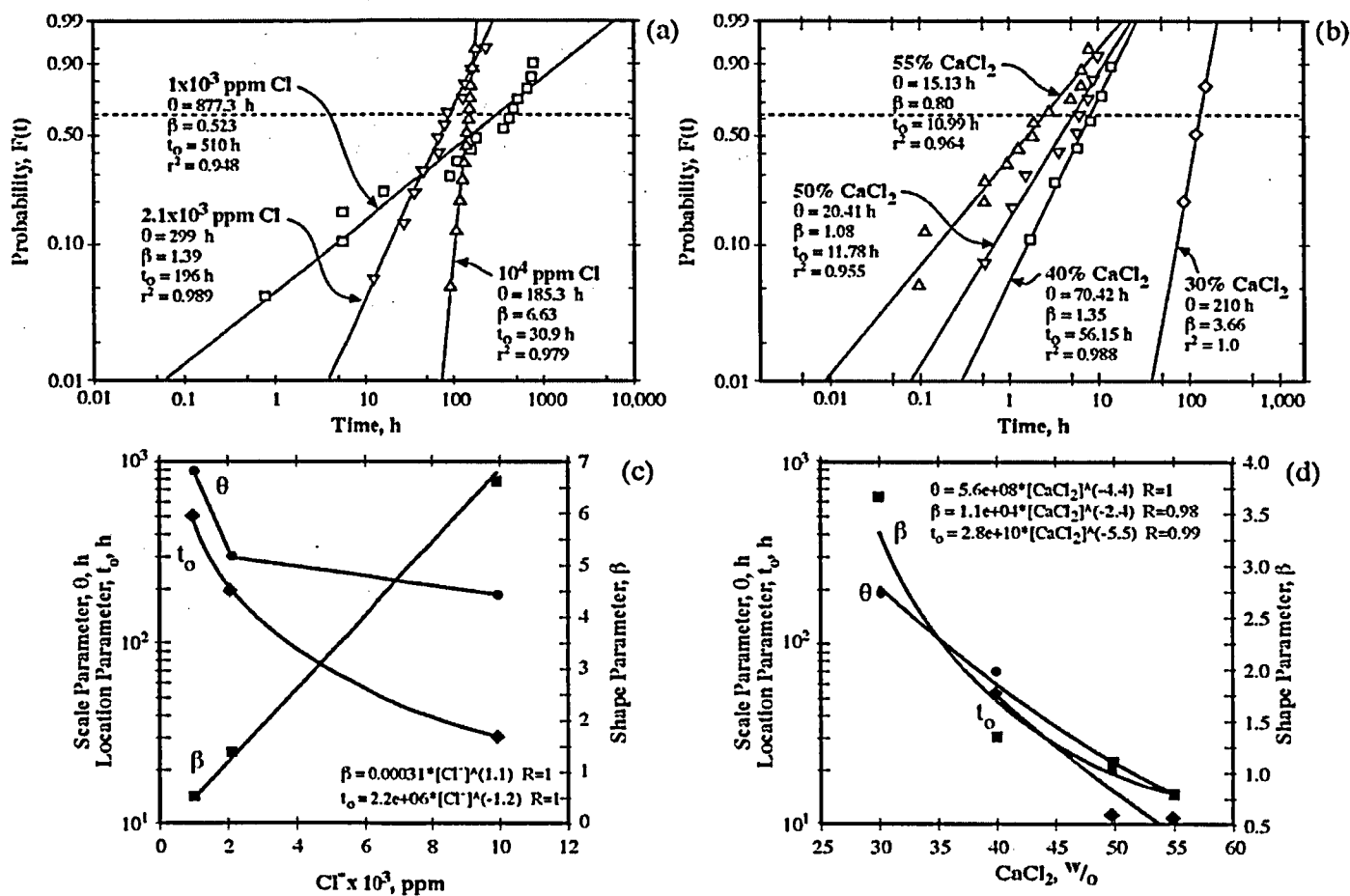
Probability vs. Time as a Function of Stress for Sensitized Type 304
Stainless Steel Exposed at 288°C in Pure Oxygenated Water
(Clark and Gordon, Akashi and Ohtomo);
Dependence of Statistical Parameters on Stress



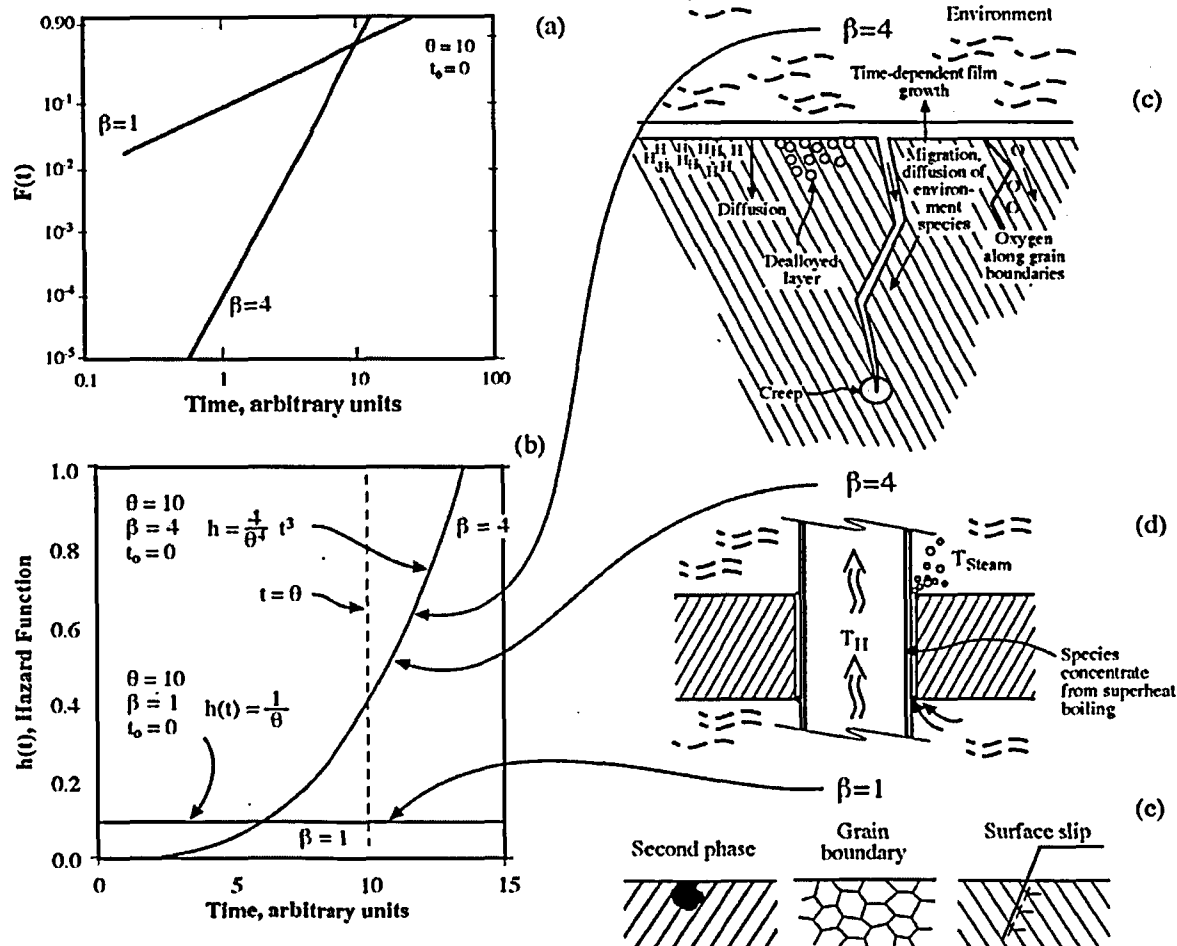
Probability vs. Time for Stainless Steel in Boiling MgCl_2 at 154°C
as a Function of Stress (Shibata and Takeyama, Cochran and Staehle);
Dependence of Statistical Parameters on Stress



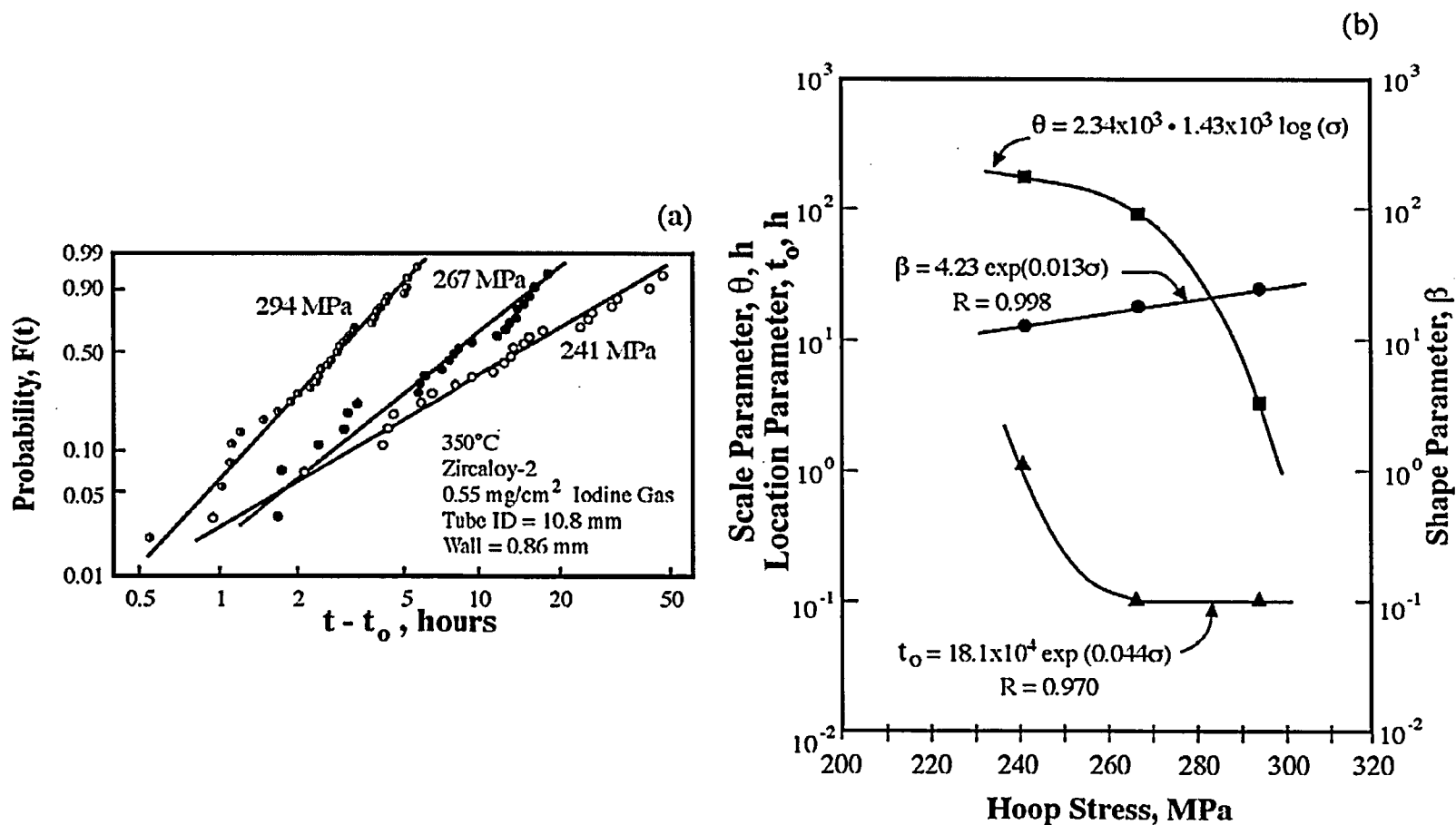
Probability vs. time for SCC of Ttype 304 Exposed to Dilute and Concentrated Chloride Solutions as a Function of Concentration
(Nakayama et al. 1.75 Sy at 80°C Crevice; Shibata et al. 200MPa at 100°C)
Dependence of Statistical Parameters on Concentration



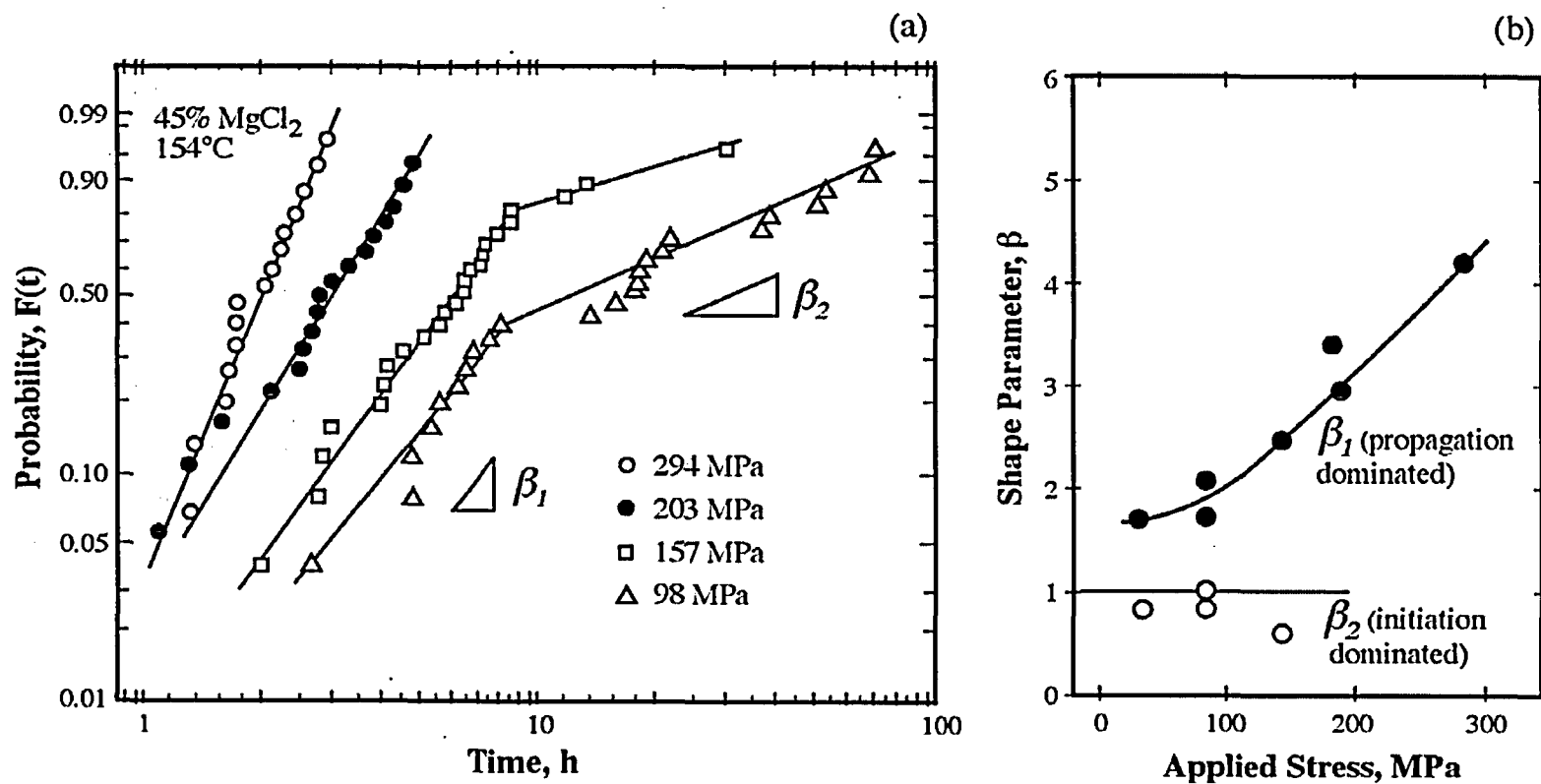
Effects of Physical Conditions on the Shape Parameter; Comparing Surface and Time Dependent Processes; Comparing with Cumulative Distribution and Hazard Function



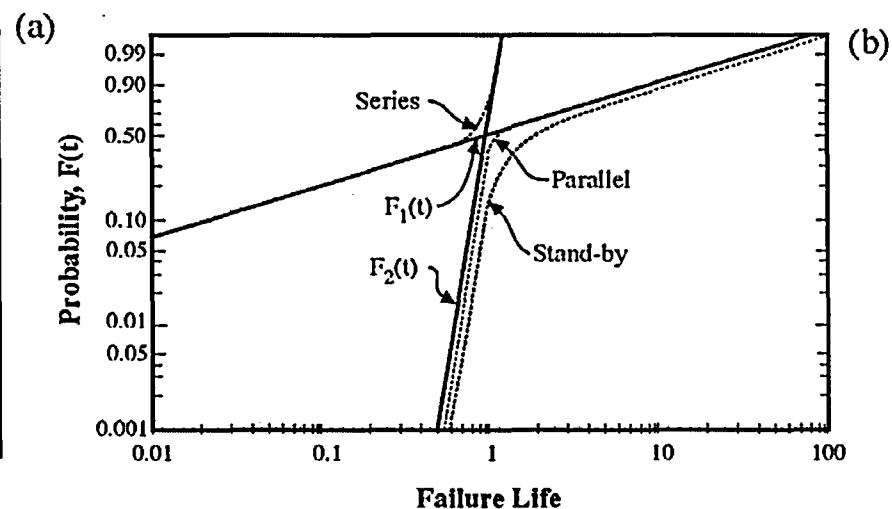
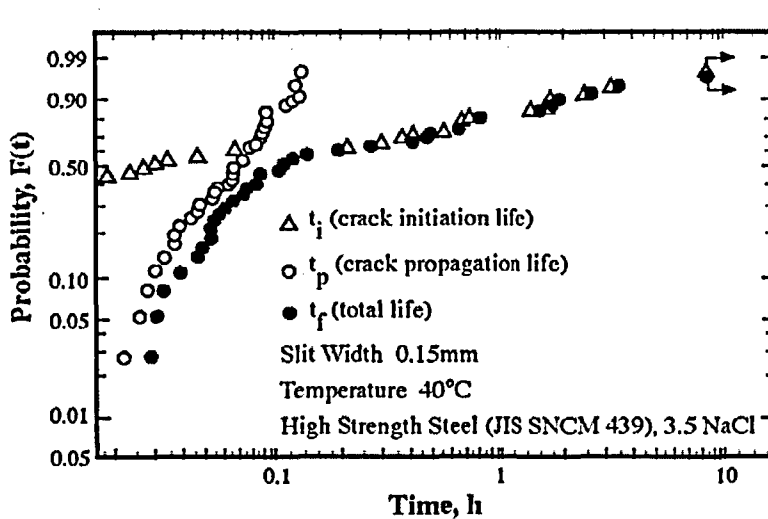
Probability of SCC vs. Time as a Function of Stress for Zircaloy 2
in Iodine Gas at 350°C; Statistical Parameters vs. Hoop Stress
(Shimada and Nagai)



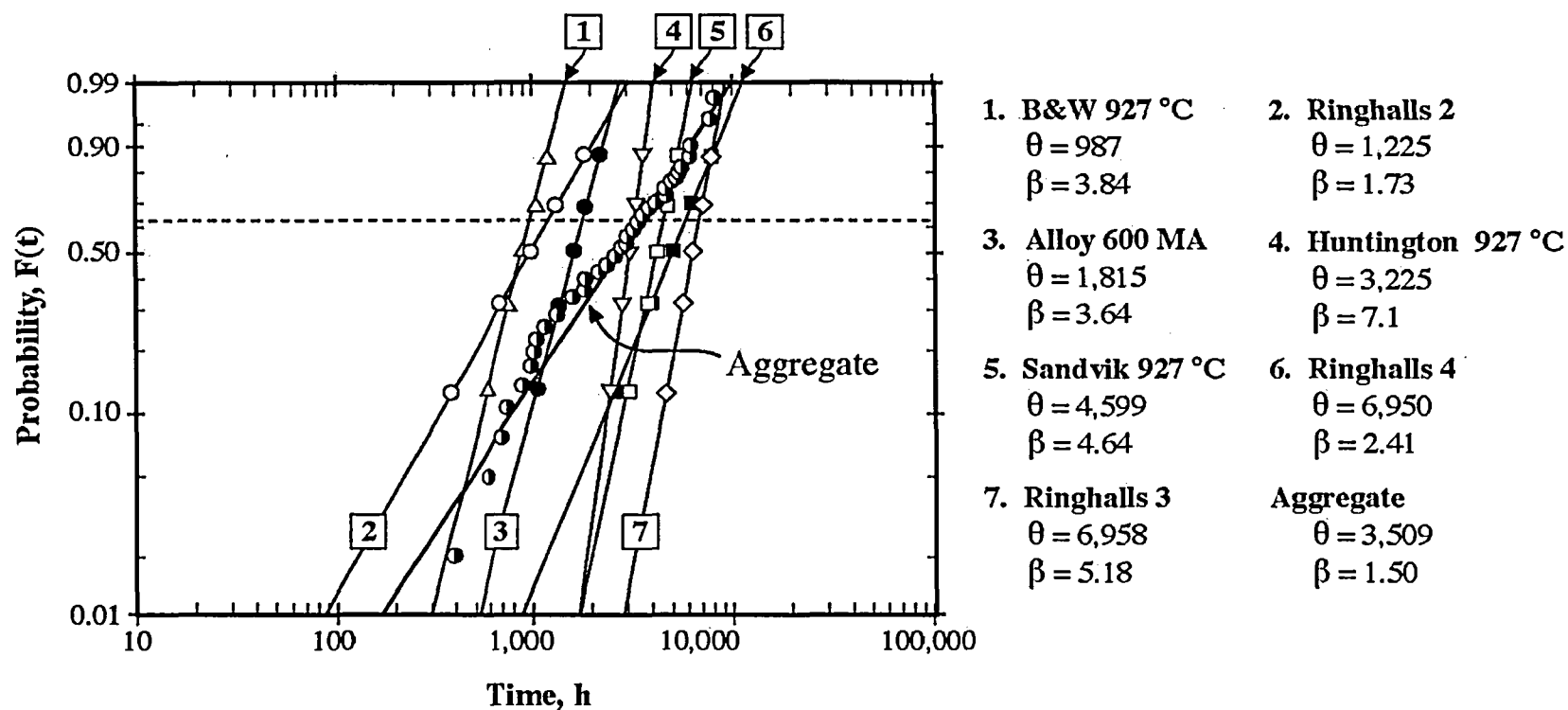
Probability vs. Time for Different Applied Stresses for
Type 304 Stainless Steel Exposed to MgCl_2 at 154°C ;
Shape Parameter vs. Applied Stress (Shibata and Takeyama)



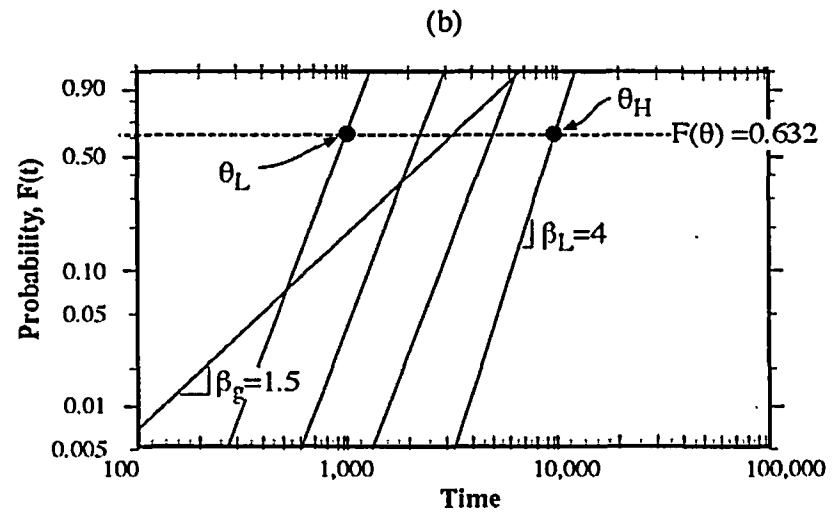
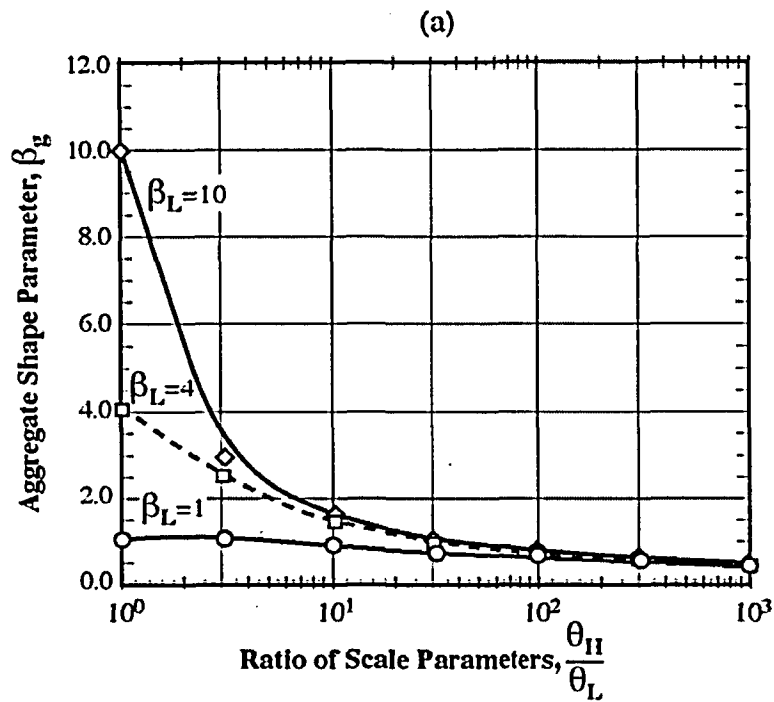
Probability vs. Time for Initiation and Propagation of SCC in a High Strength Steel in 3.5% NaCl at 40°C. (Ichikawa et al.)



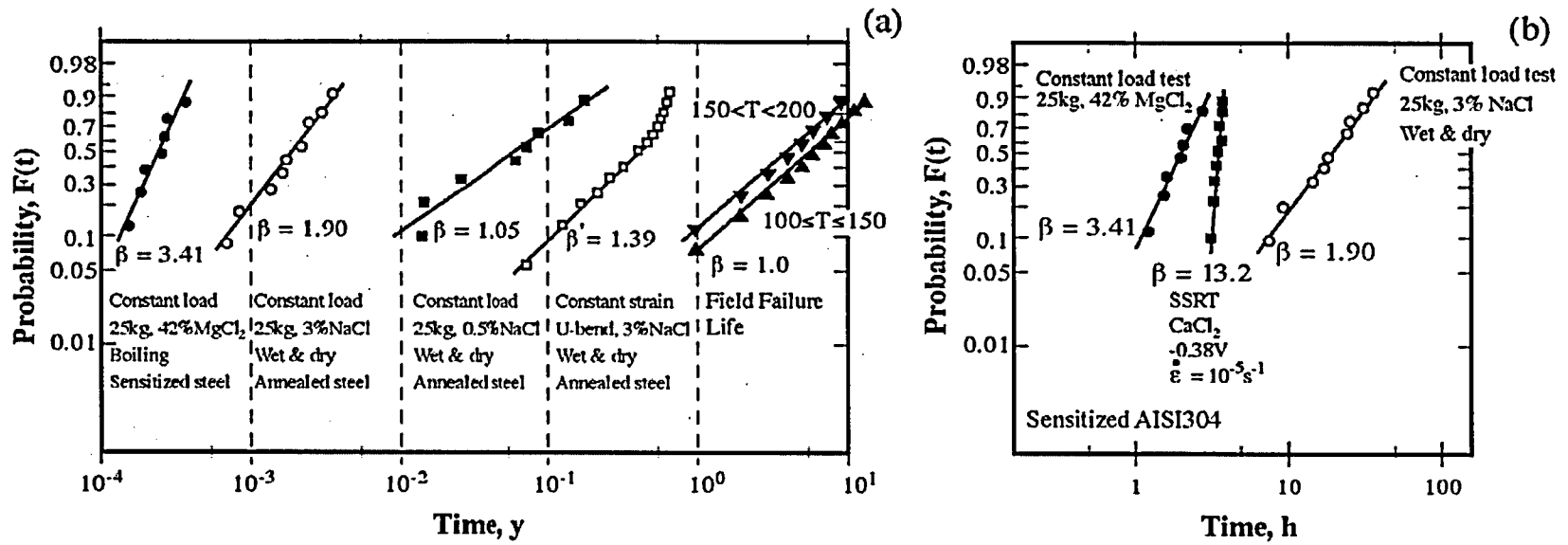
Probability vs. Time for the LPSCC of Alloy 600 in High Purity Water
with Hydrogen Additions Using RUB Specimens at 365°C from Different Heats.
(Estimated Data Points from Norring)
Aggregate of All Specimens



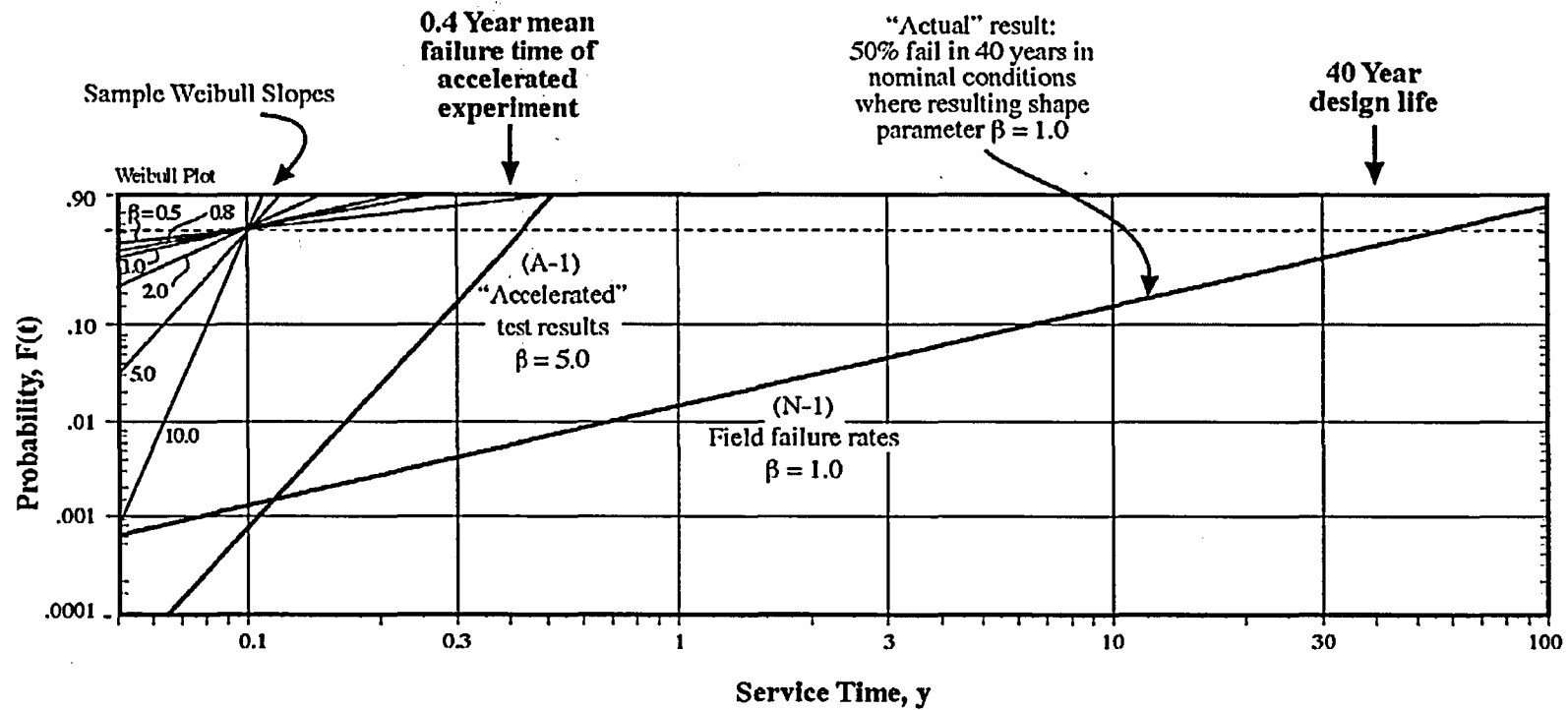
Dependence of Shape Parameter on the Ratio of Scale Parameters for Four Assumed Distributions and Constant Initial Shape Factor



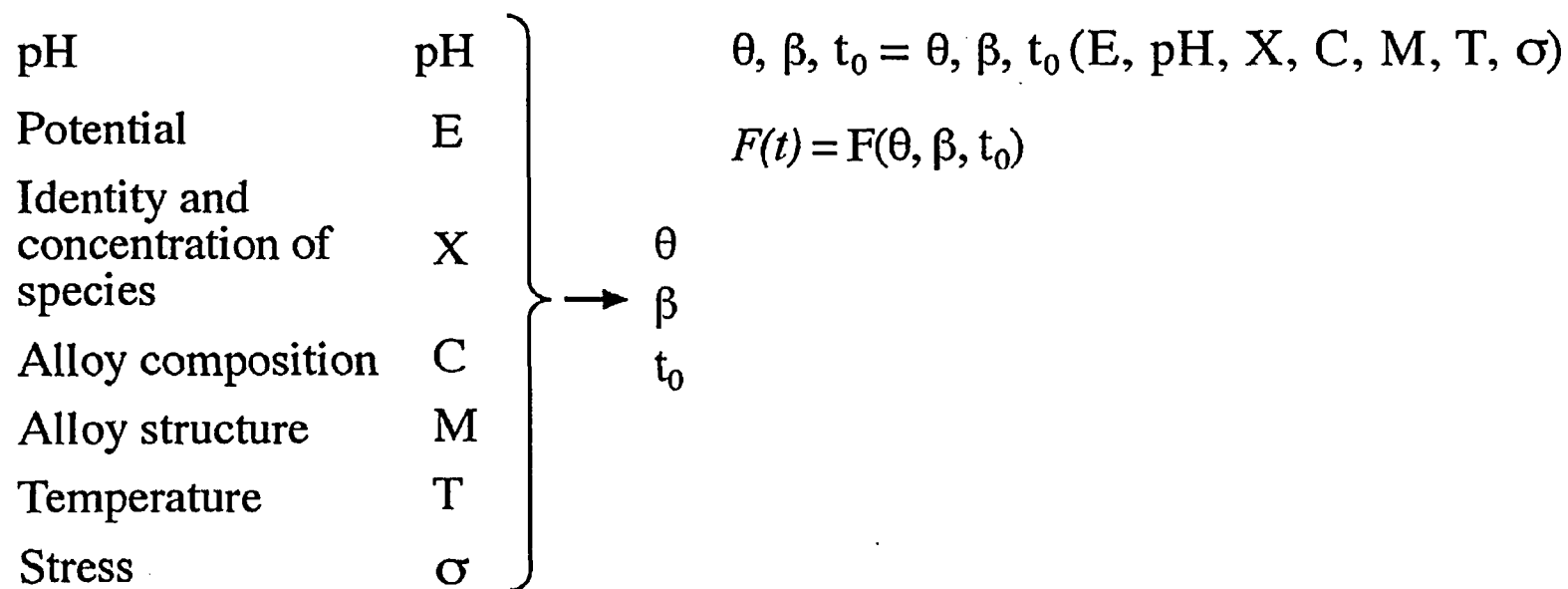
Probability vs. time for SCC of Type 304
Compared with Field Experience for Various Methods of Testing
(Sato et al.)

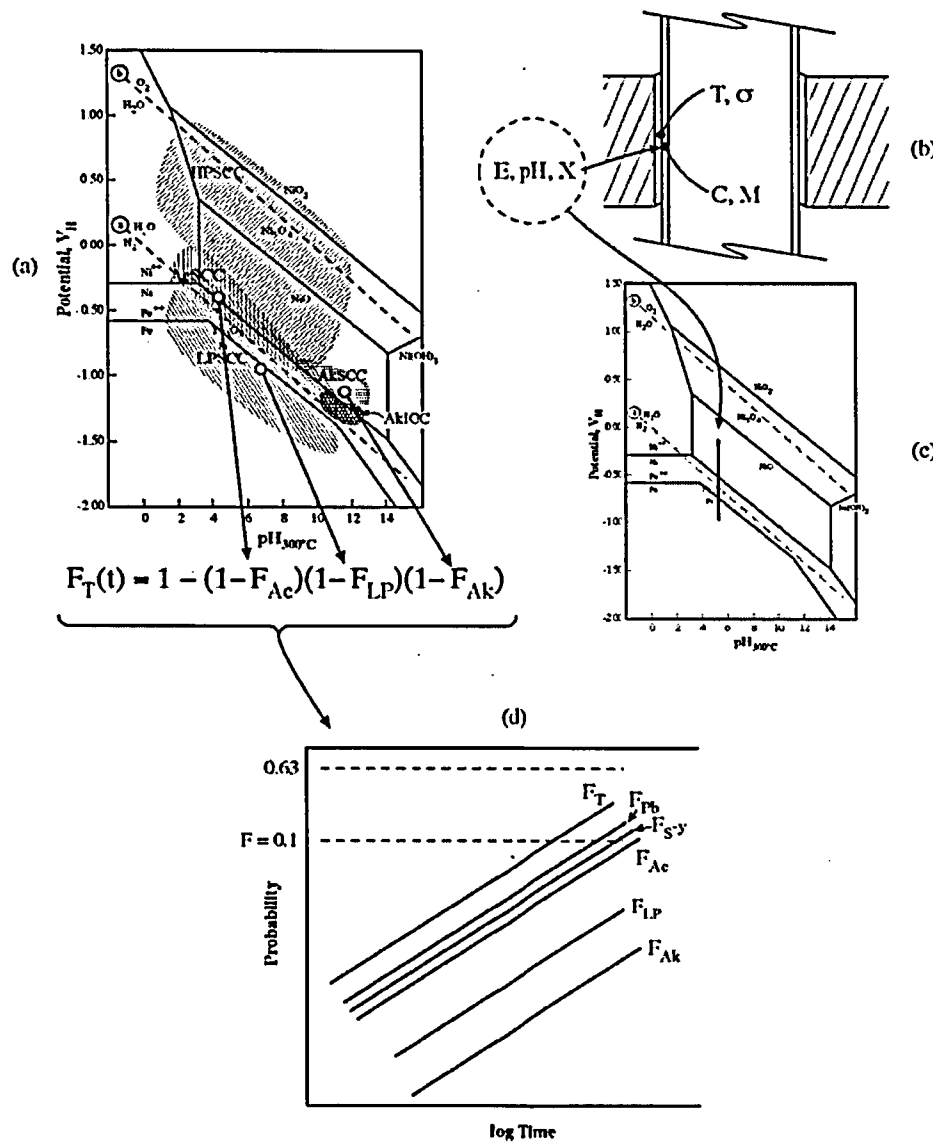


Probability vs. Service Time for Examples of Accelerated Test and Actual Conditions



Insert Dependencies on the Seven Primary Variables into Statistical Parameters





- Evaluate Each of the cdfs of the Submodes for the Dependencies on the Seven Primary Variables;
- Develop the Total Probability of Failure from Product of Reliabilities,
e.g. $R_T = R_{AKSCC} \times R_{LPSCC} \times R_{AcSCC} \times \dots$
- Evaluate at Selected Environment.

Conclusions

1. It is possible to predict the occurrence of the first failure by using past experience together with a statistical distribution for which the parameters are evaluated with primary variables.
2. This methods enables predicting the occurrence of first failures that do not occur at the same conditions as previous ones.
3. This method enables accounting for the multiple sets of submodes that may occur.
4. There are naturally difficulties of interactions of variables in this approach; however, a first approach is probably much more useful than nothing.



Elevated Temperature Grain Boundary Embrittlement and Ductility-Dip Cracking in Ni-base Weld Metals

John C. Lippold
The Ohio State University

Welding and Joining Metallurgy Group

Conference on Vessel Penetration Inspection, Cracking, and Repairs
September 29-October 2, 2003, Gaithersburg, MD



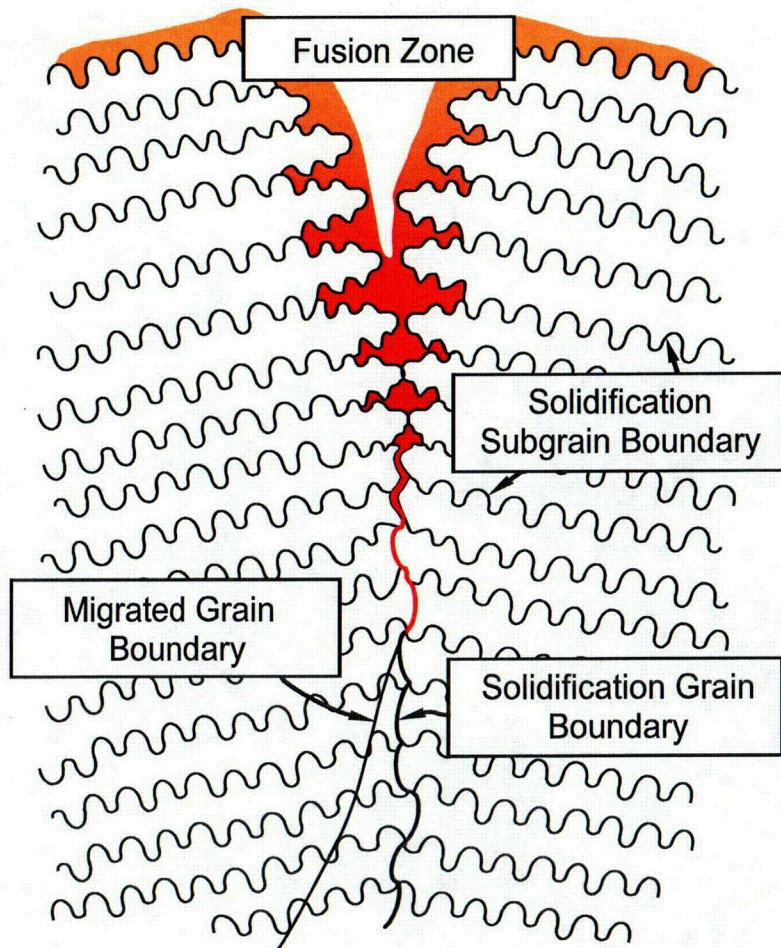
Weldability Issues with Austenitic Materials

Welding and Joining Metallurgy Group

Cracking Mechanism	Location	Factors that Promote
Solidification Cracking	Solidification Grain Boundary	Impurity segregation Continuous liquid films
Weld Metal Liquation Cracking	Solidification Grain Boundary Migrated Grain Boundary	Impurity segregation Large grain size High heat input
Ductility-Dip Cracking	Migrated Grain Boundary	Large grain size Grain boundary mobility
Reheat, or Strain-age, Cracking	Migrated Grain Boundary	Relaxation of residual stress Intragranular precipitation Impurity segregation
Copper-Contamination Cracking	Migrated Grain Boundary	Cu abraded on surface Temperature > 1093°C
Hydrogen-Assisted Cracking	Migrated Grain Boundary	Grain boundary precipitation Threshold H concentration

Weld Metal Boundaries

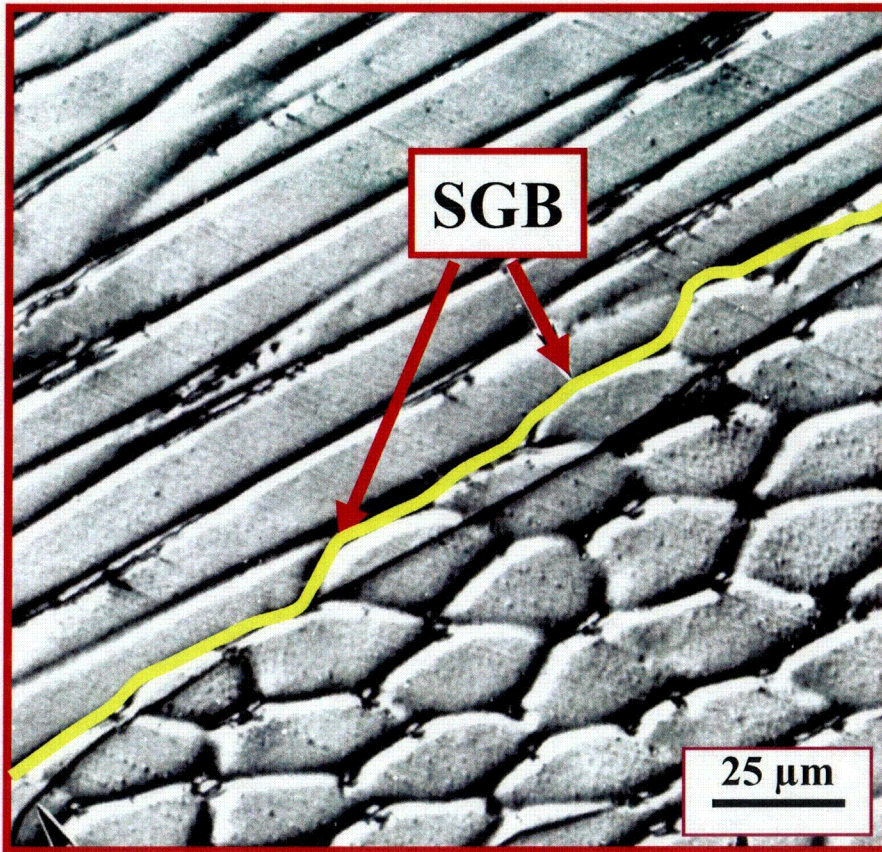
Welding and Joining Metallurgy Group



- Differentiated by
 - Composition
 - Structure
- Solidification subgrain boundaries (SSGBs)
 - Composition (Case 2)
 - Low angle misorientation
- Solidification grain boundaries (SGBs)
 - Composition (Case 3)
 - High or low angle misorientation
- Migrated grain boundaries (MGBs)
 - Local variation in composition
 - High angle misorientation

Solidification Grain Boundary

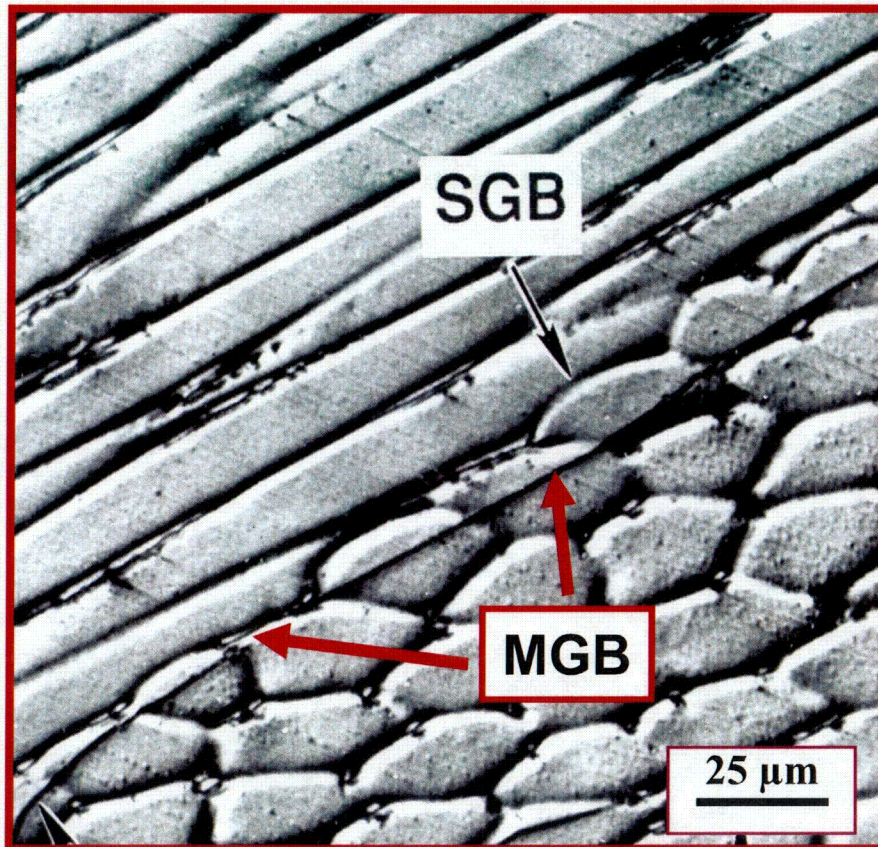
Welding and Joining Metallurgy Group



- Boundary between packets of subgrains
- Results from competitive growth
- Composition dictated by Case 3 solute redistribution
- Large misorientation across boundary at end of solidification - high angle boundary
- Most likely site for solidification cracking

Migrated Grain Boundary

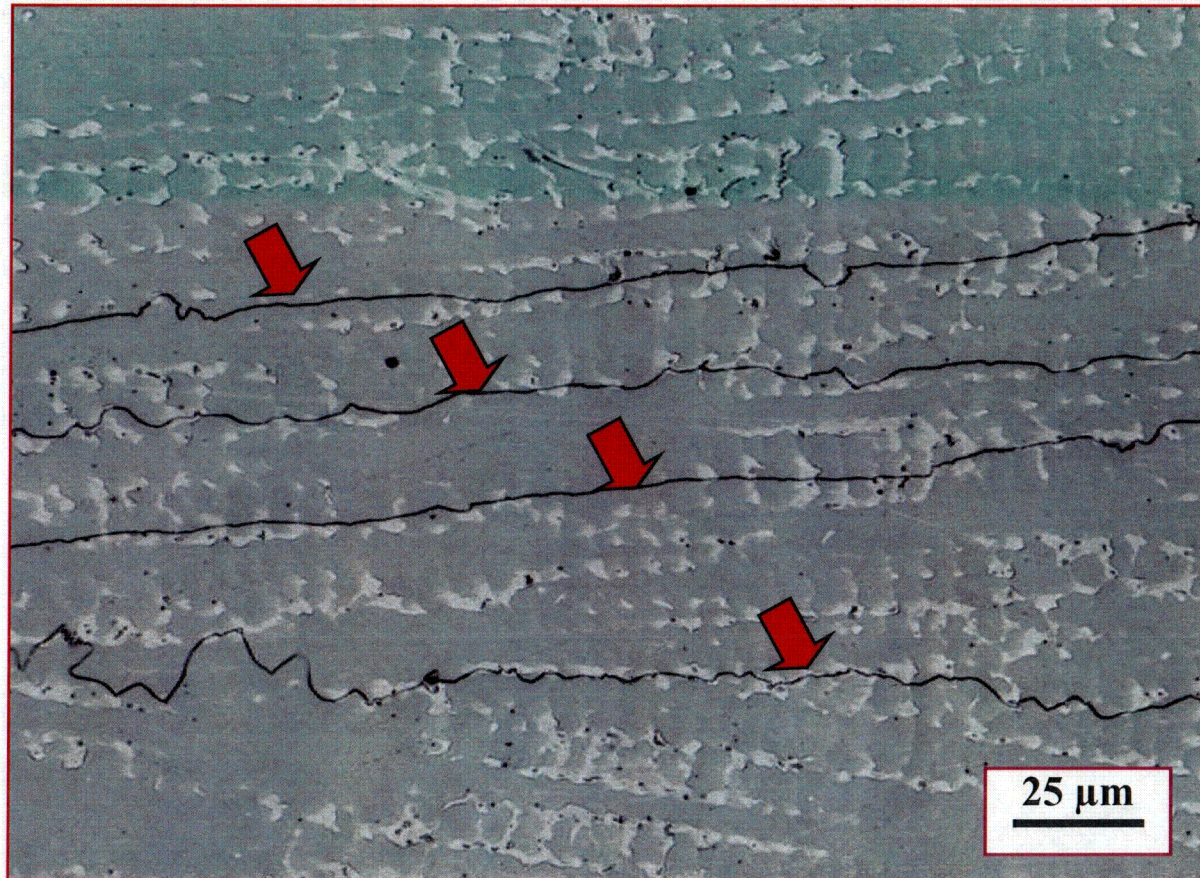
Welding and Joining Metallurgy Group



- Crystallographic component of SGB
- Migrates away from SGB in the solid state following solidification or during reheating
- Large misorientation across boundary - high angle boundary
- Composition varies locally
- Possible boundary “sweeping” and segregation
- Liquation and ductility dip cracking

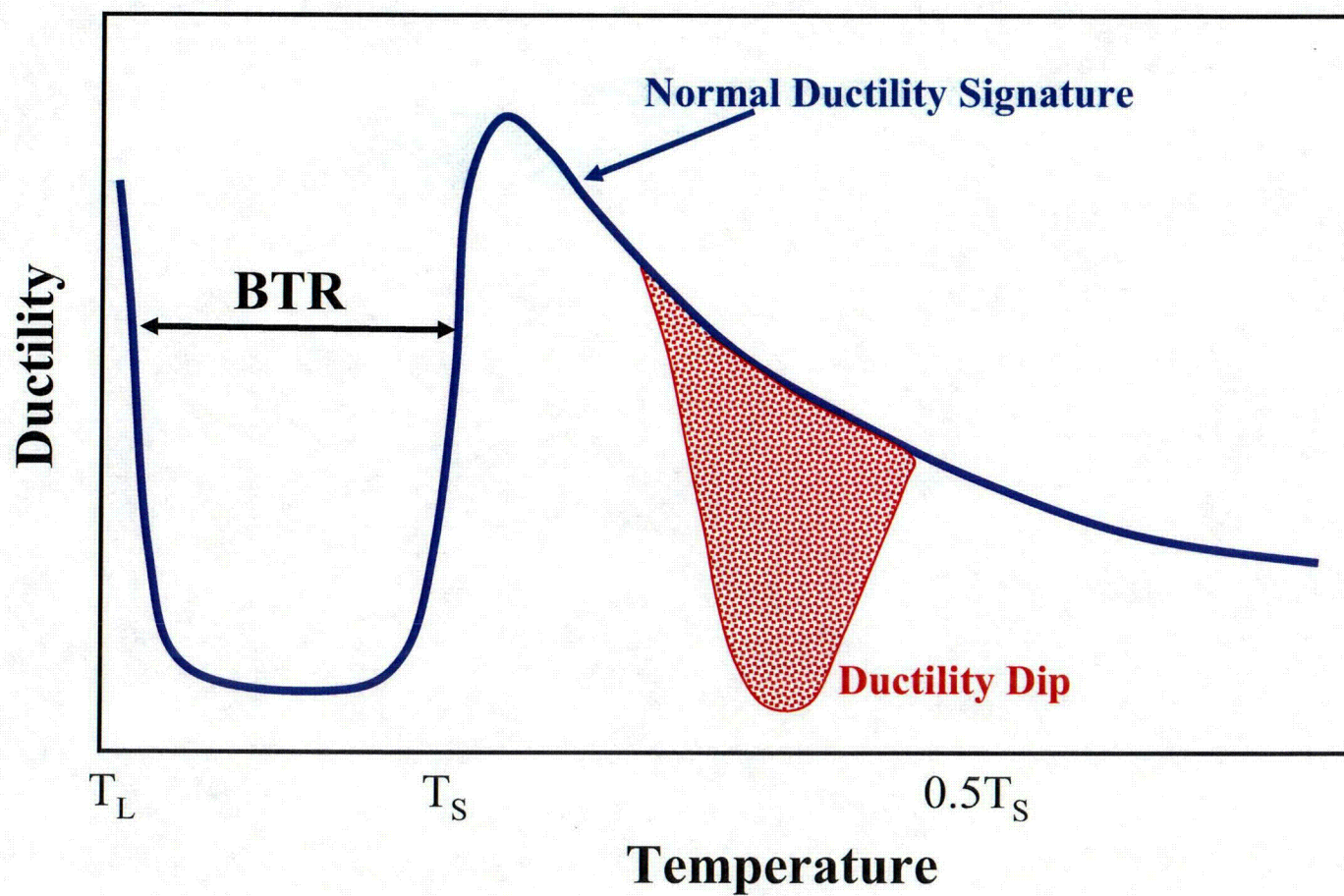
Migrated Grain Boundaries in Filler Metal 82

Welding and Joining Metallurgy Group



Ductility-dip Cracking

Welding and Joining Metallurgy Group





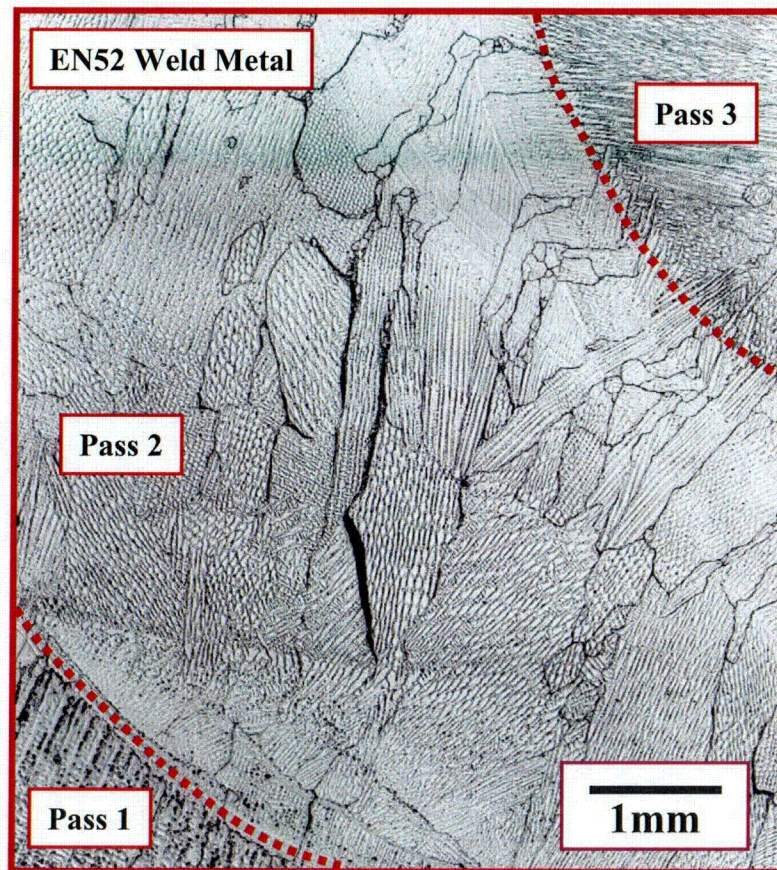
Weld Metal DDC Characteristics

Welding and Joining Metallurgy Group

- **Sharp drop in elevated temperature ductility**
- **Solid state cracking**
- **Austenitic (FCC) Alloys**
- **Large grain size**
- **High restraint levels**
- **Intergranular along migrated grain boundaries**

Ductility-dip cracking in Filler Metal 52 multipass weld deposit

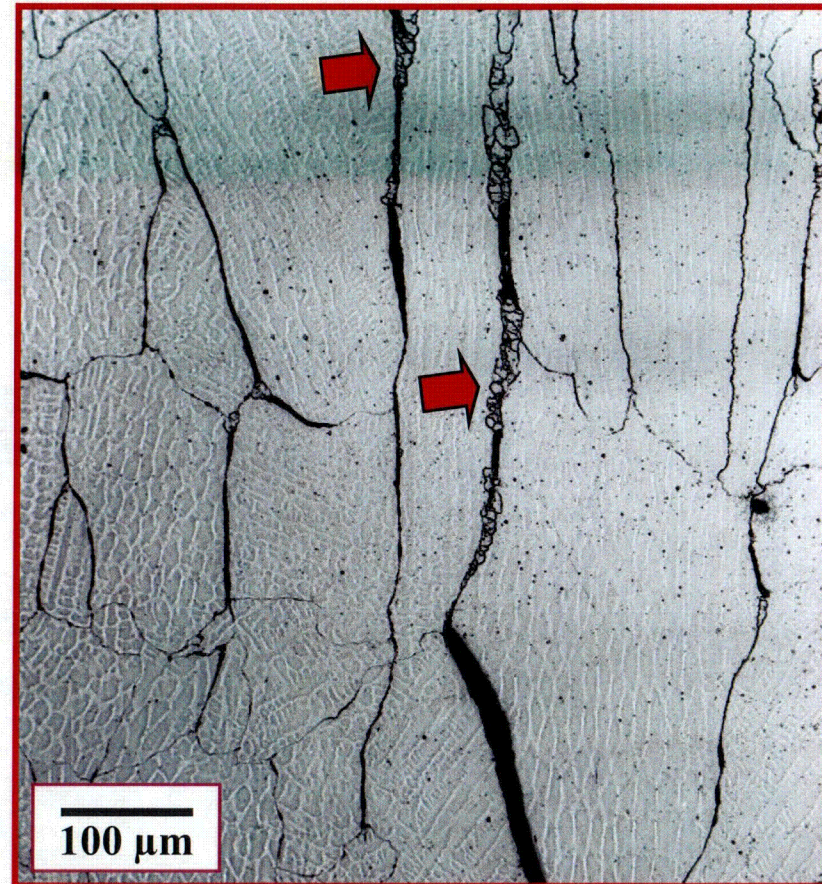
Welding and Joining Metallurgy Group



Ductility-dip cracking along migrated grain boundaries in Filler Metal 52 butter layer

Welding and Joining Metallurgy Group

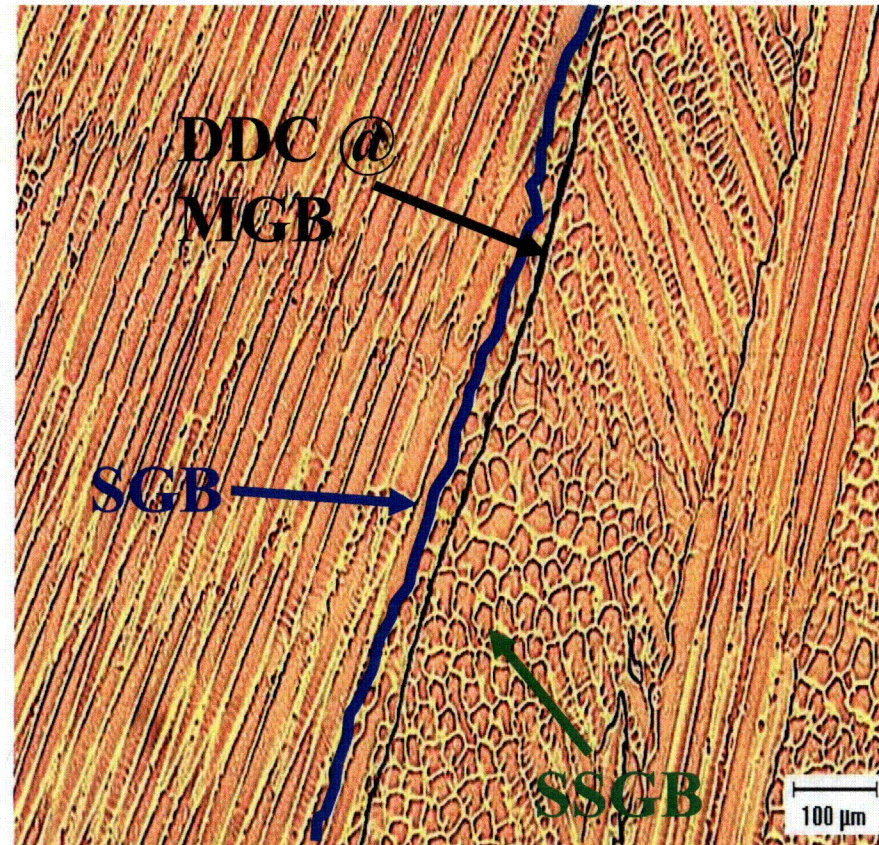
- Large grain size
- Ductility “exhaustion” at grain boundaries
- Recrystallization along grain boundaries due to high local strains (arrows)



Migrated grain boundaries in re-heated weld metals

Welding and Joining Metallurgy Group

- Crystallographic component of SGB
- High angle boundary
- Migrates on-cooling after solidification and during re-heating (multi-pass welds)
- Large grain size





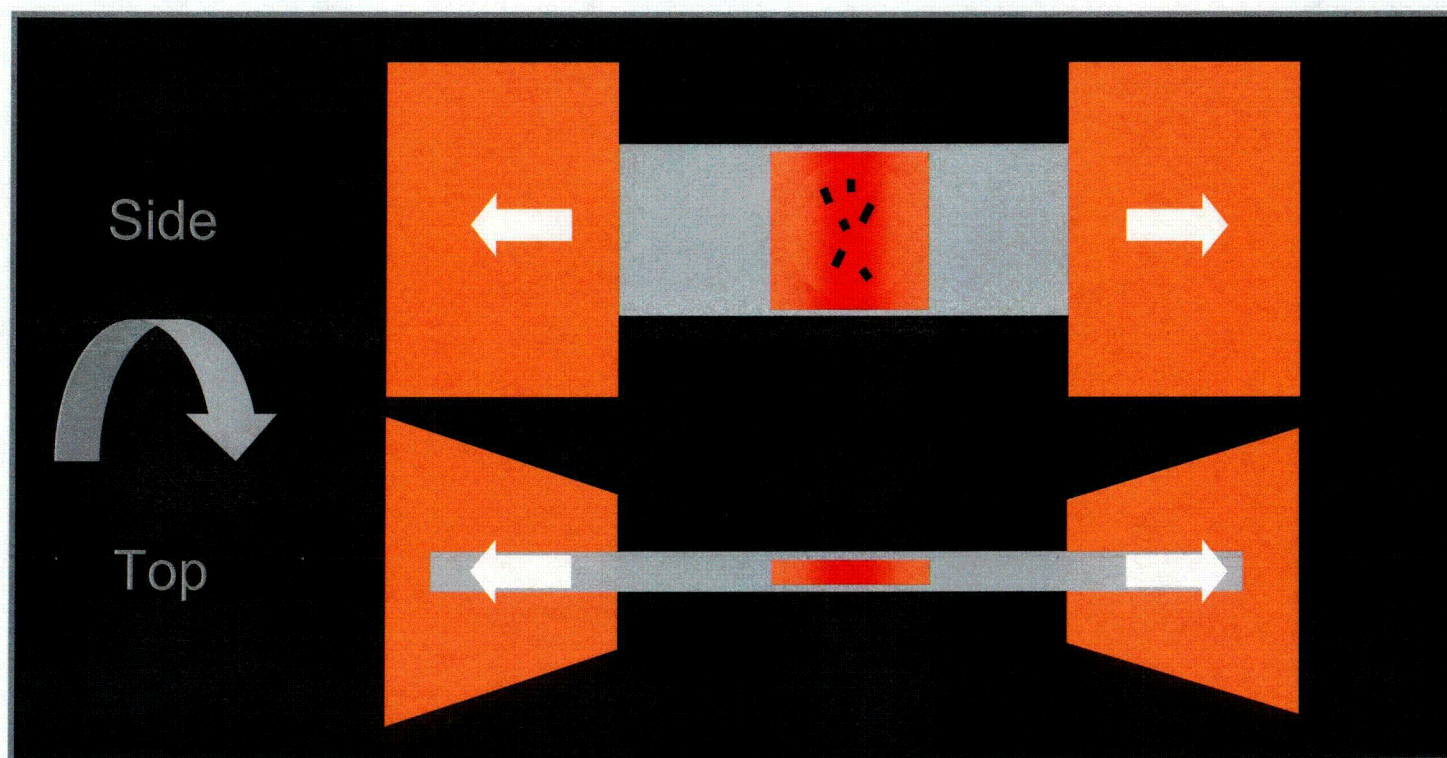
Factors Influencing DDC

Welding and Joining Metallurgy Group

- Strain concentration at Grain Boundaries (GB) and Triple Points
- GB orientation relative to the applied strain
- GB tortuosity
- Temperature
 - GB sliding inoperable at low Temperature
 - Recrystallization at high temperature
- Precipitates
- Impurities segregation (Sulfur)
- Hydrogen
 - H induced decohesion
 - H enhanced local plasticity

Strain-to-Fracture DDC Test

Welding and Joining Metallurgy Group





Testing filler metals - sample preparation

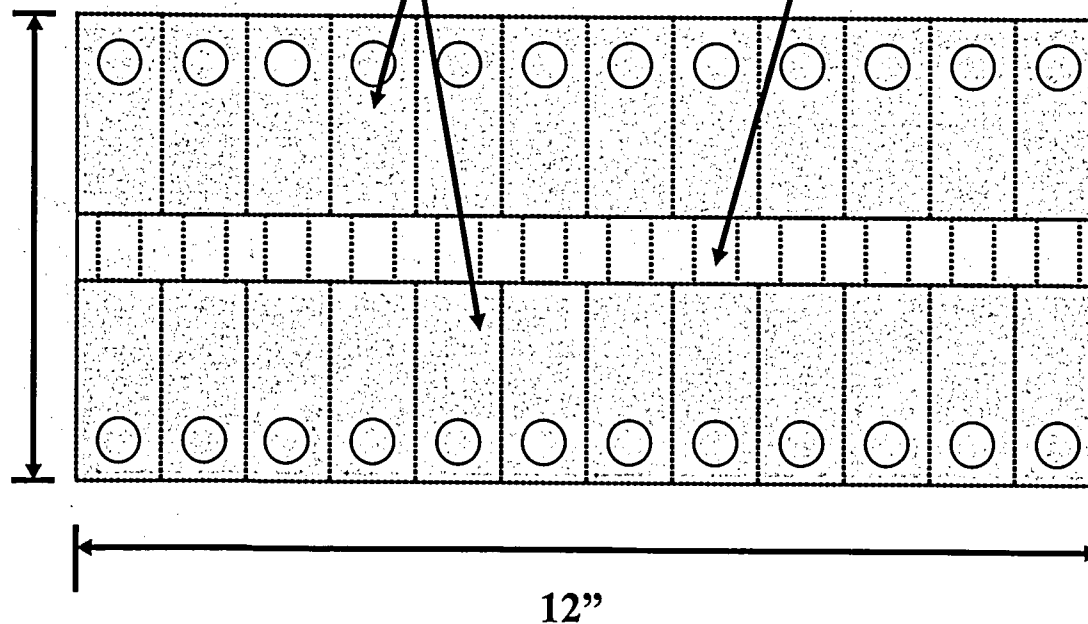
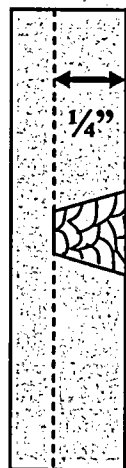
Welding and Joining Metallurgy Group

Side View

Top View

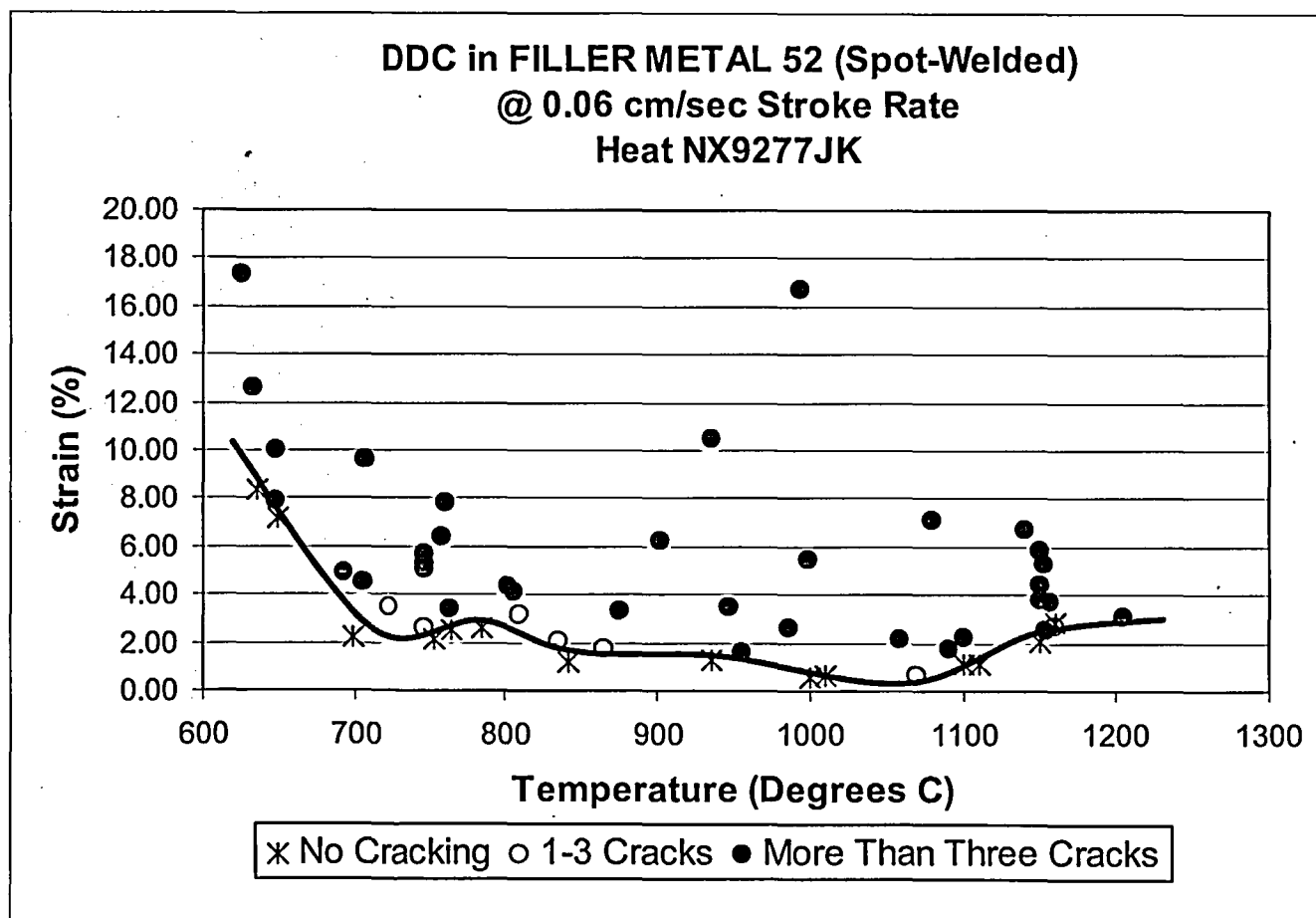
SA-36

Nickel-base Filler Metal



Filler Metal 52 STF Test Results

Welding and Joining Metallurgy Group

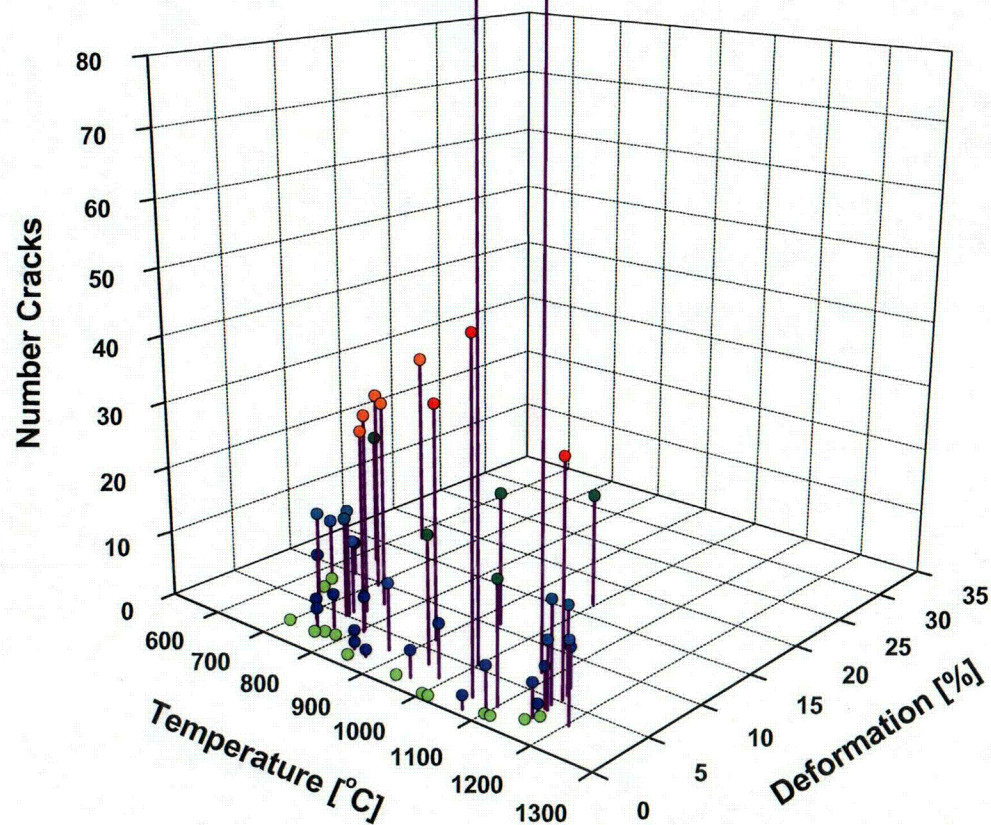




Filler Metal 52 STF Test Results

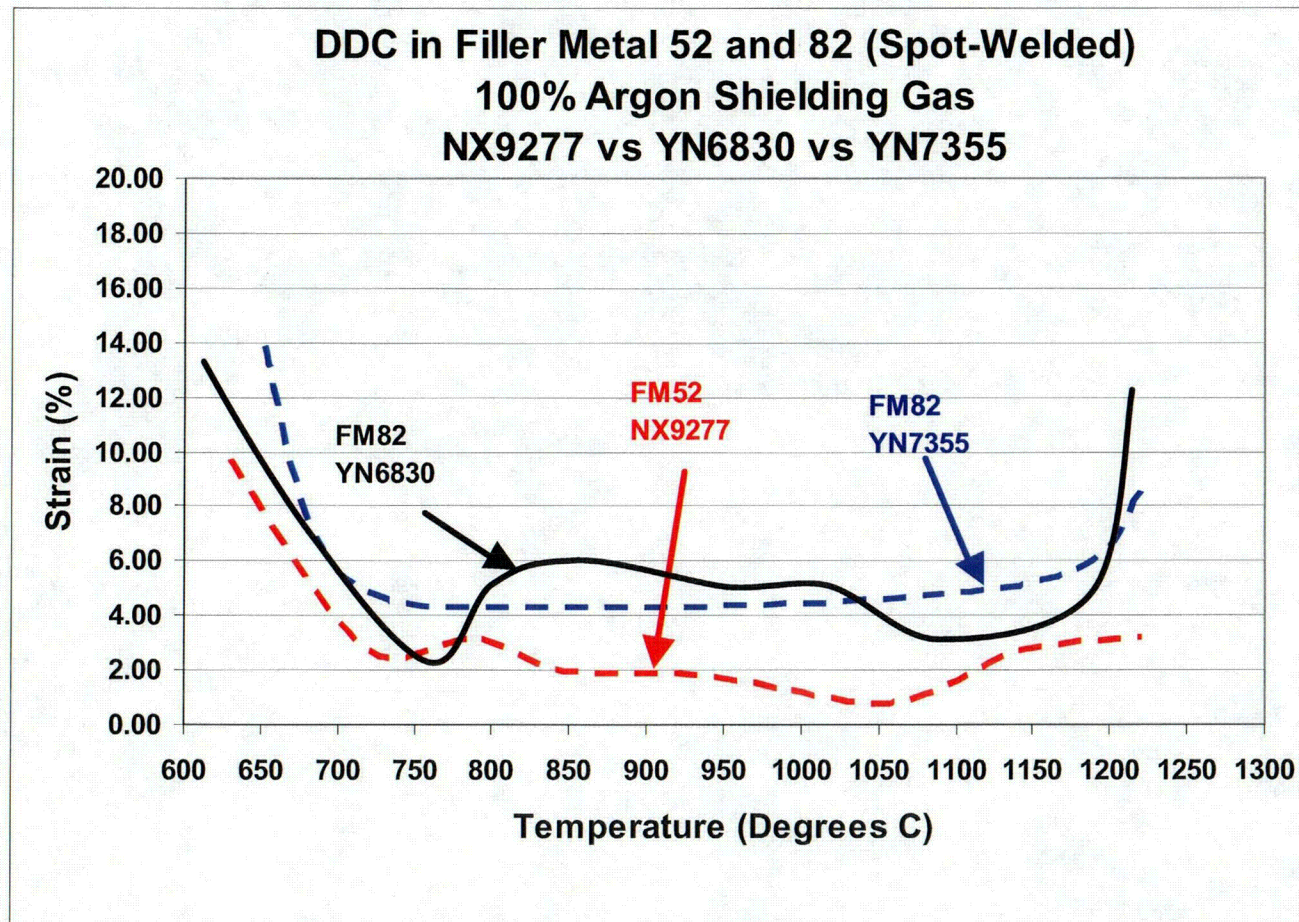
Welding and Joining Metallurgy Group

FM-52 Spot Welded



Filler Metal 52 vs. Filler Metal 82

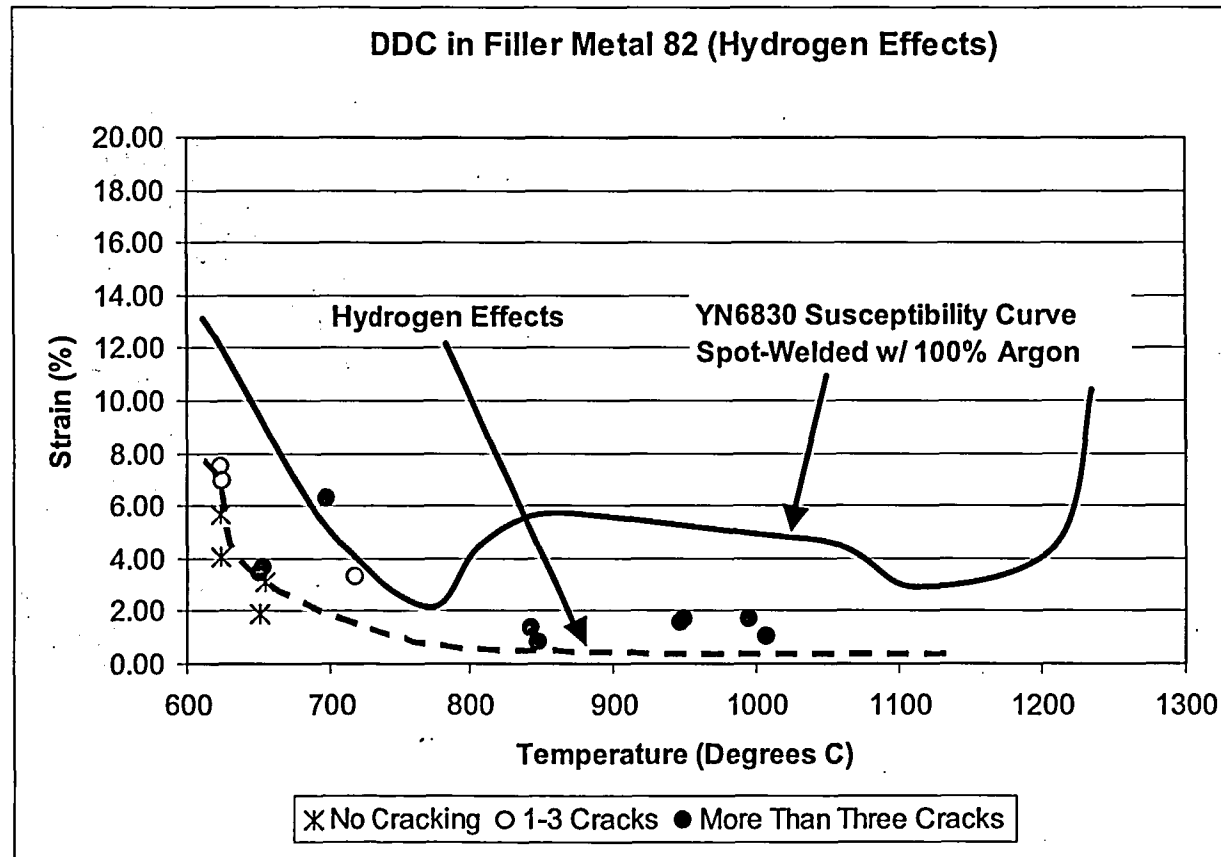
Welding and Joining Metallurgy Group





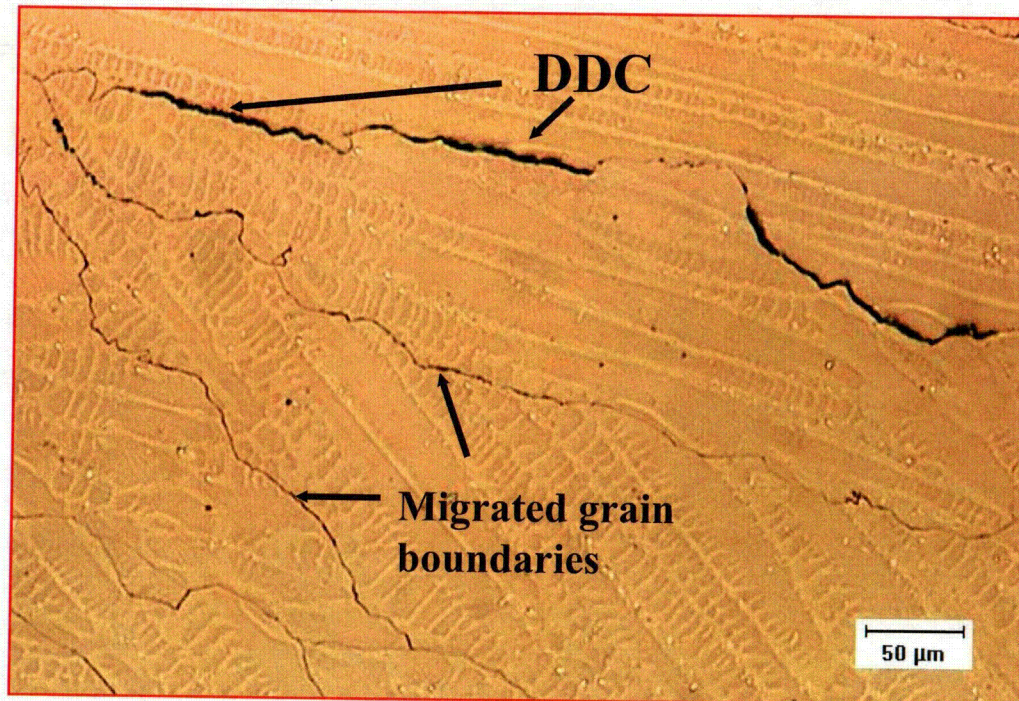
Filler Metal 82 – H₂ additions

Welding and Joining Metallurgy Group



Ductility-dip cracking

Welding and Joining Metallurgy Group



Characteristics

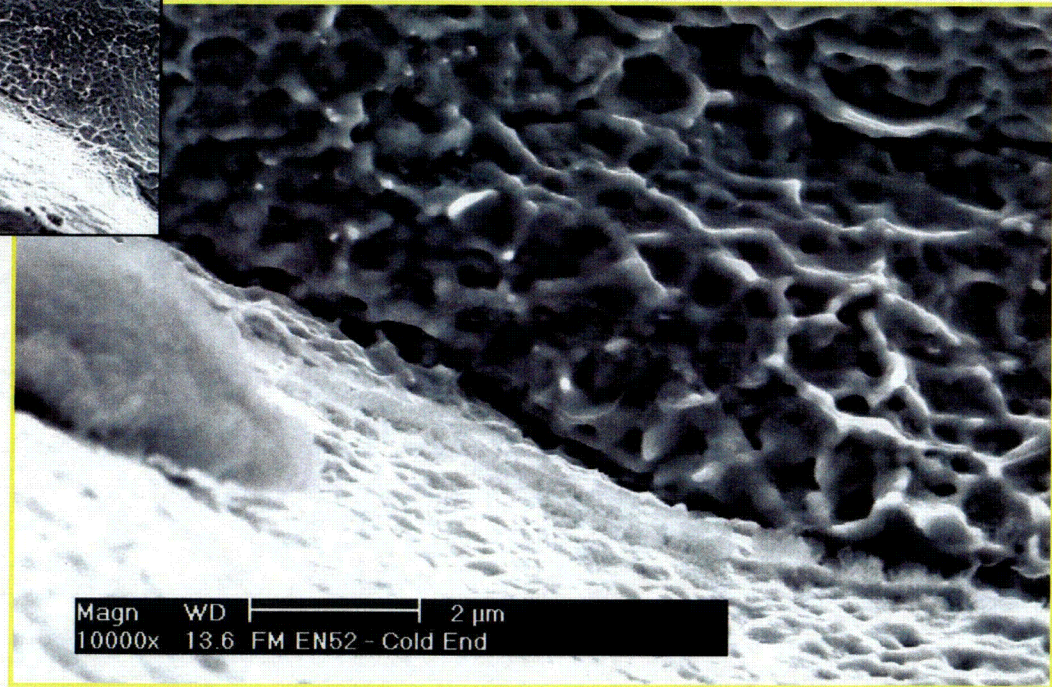
- Fully austenitic
- Large grain size
- Straight, smooth boundaries
- Low impurity content
- High restraint

DDC Fracture Surface in Filler Metal 52

Welding and Joining Metallurgy Group



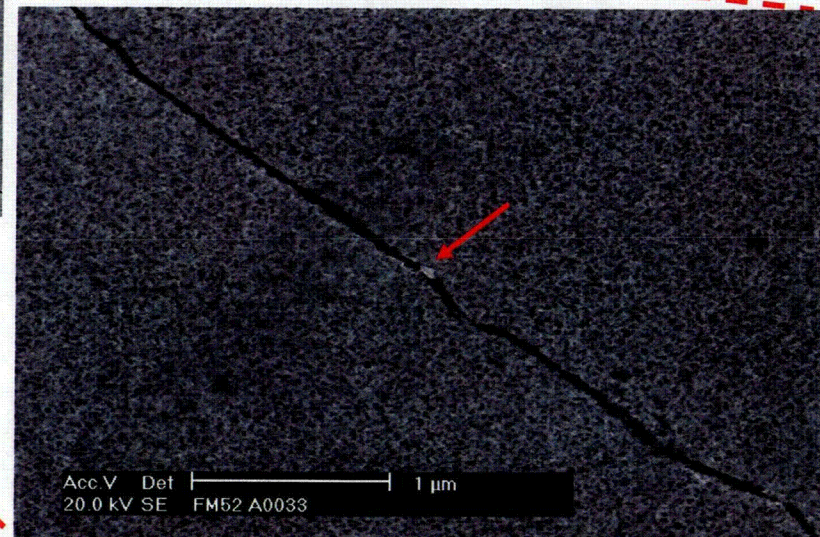
Ductile intergranular fracture along migrated grain boundaries



Grain boundary characteristics – Filler Metal 52

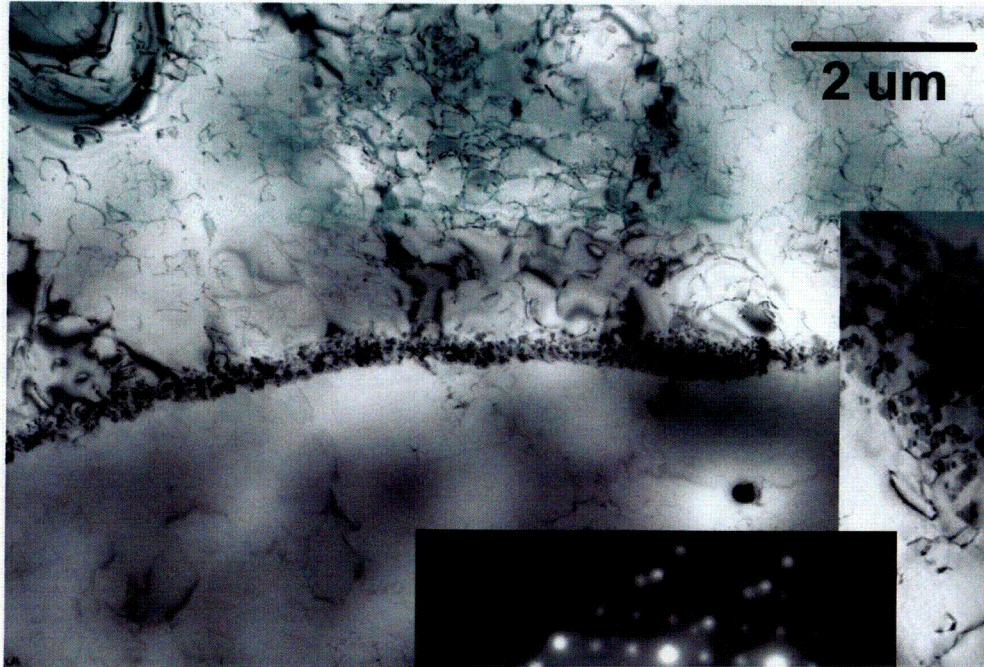
Welding and Joining Metallurgy Group

Long, straight, “clean” MGB in Filler Metal 52 at 986°C

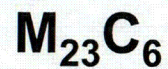


Intergranular Precipitation - FM 52

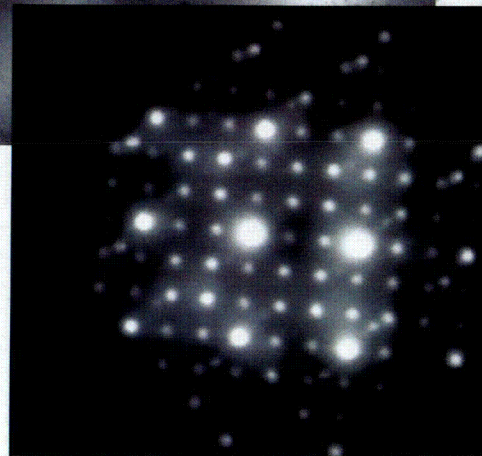
Welding and Joining Metallurgy Group



990 °C
Strain: 1.6%



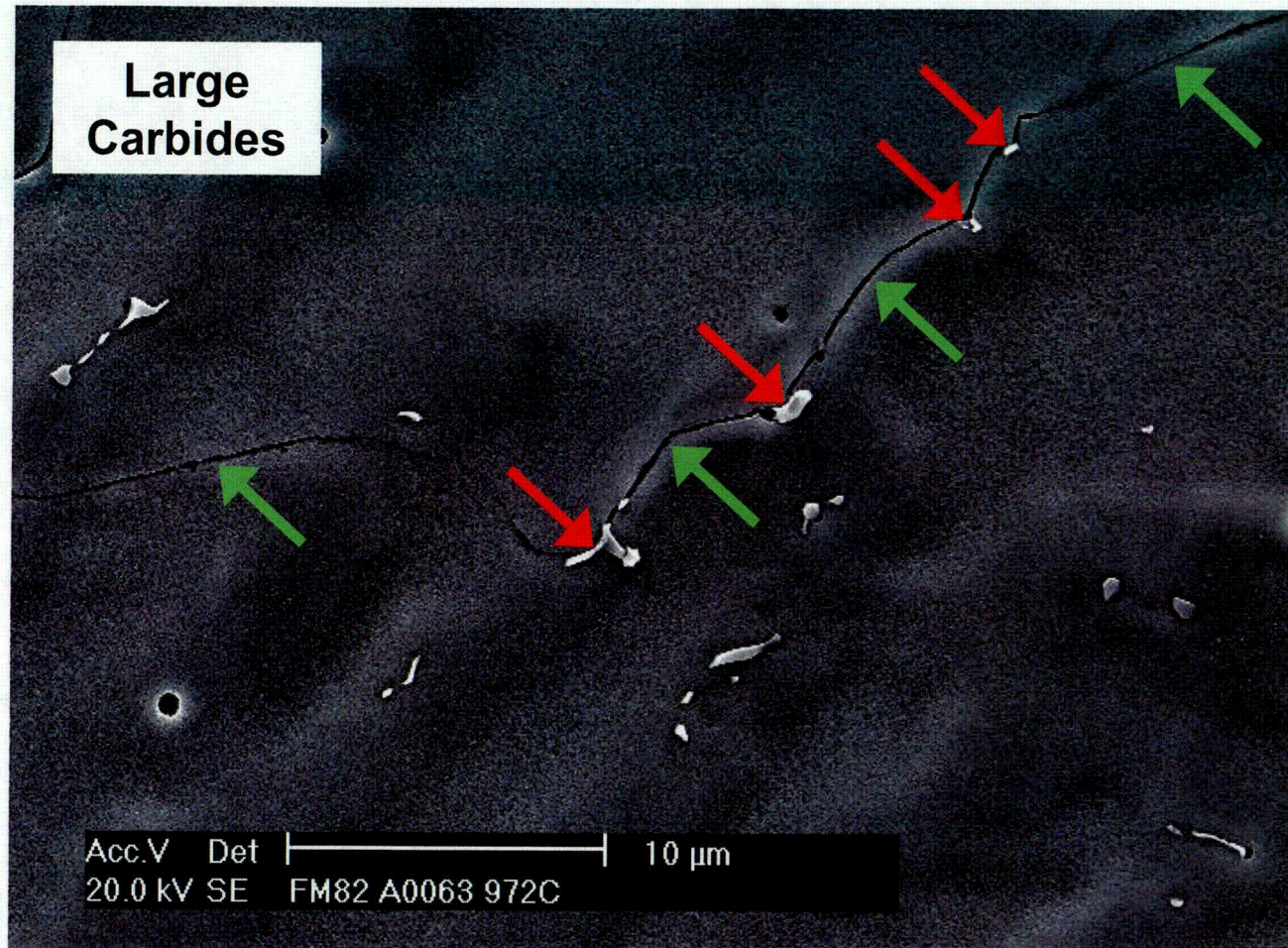
10 - 50 nm



Cube-on-Cube
Orientation Relationship

GB Pinning - Filler Metal 82

Welding and Joining Metallurgy Group



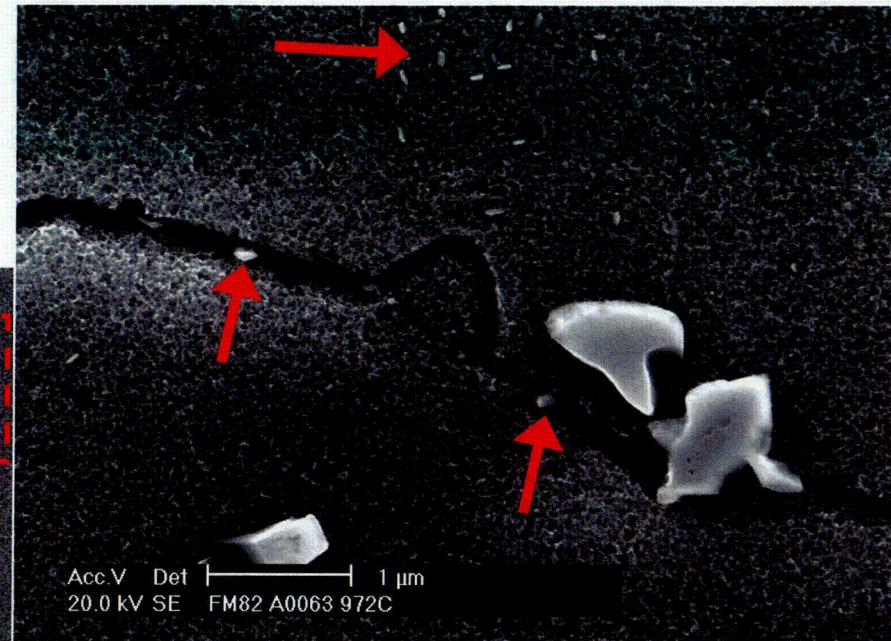
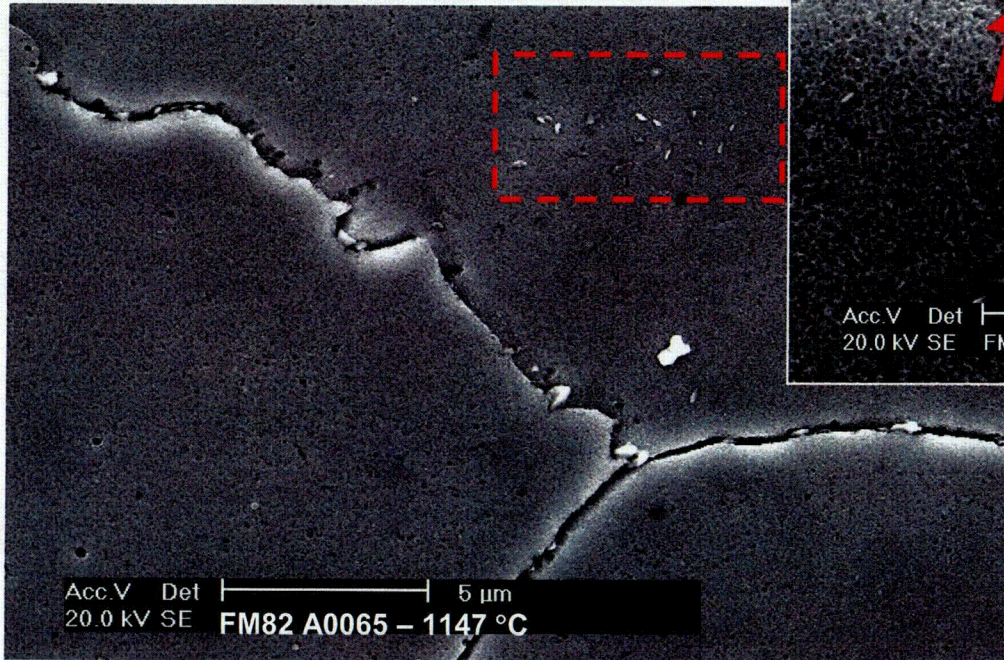
970 °C
Strain: 7.5%

Precipitates in Filler Metal 82

Welding and Joining Metallurgy Group

1150 °C
Strain: 11.3%

Heat – YN6830



970 °C
Strain: 7.5%

Heat – YN6830



Precipitates on Fracture Surface

Welding and Joining Metallurgy Group

597



FM-82
950 °C

Acc.V
5.00 kV

Det	SE
FM-82 A0281	

2 μm

C159

Medium Size (Nb,Ti)C Precipitates Filler Metal 82

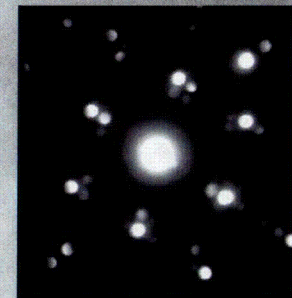
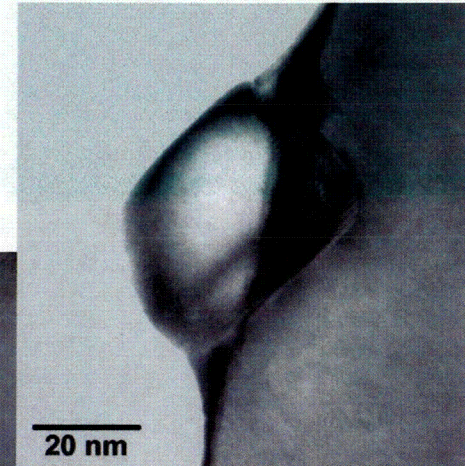
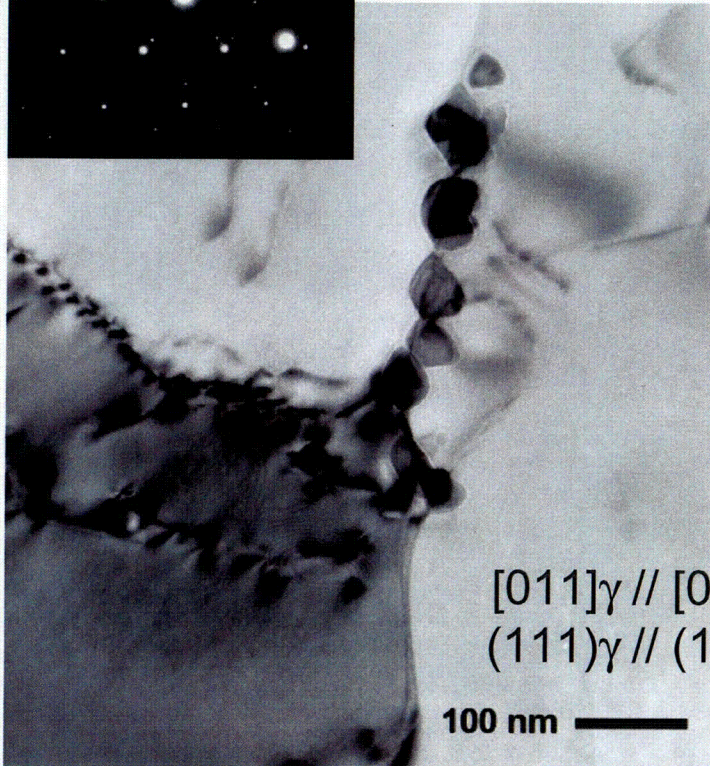
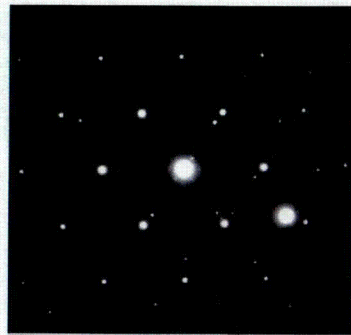
Welding and Joining Metallurgy Group

598

20 – 50 nm

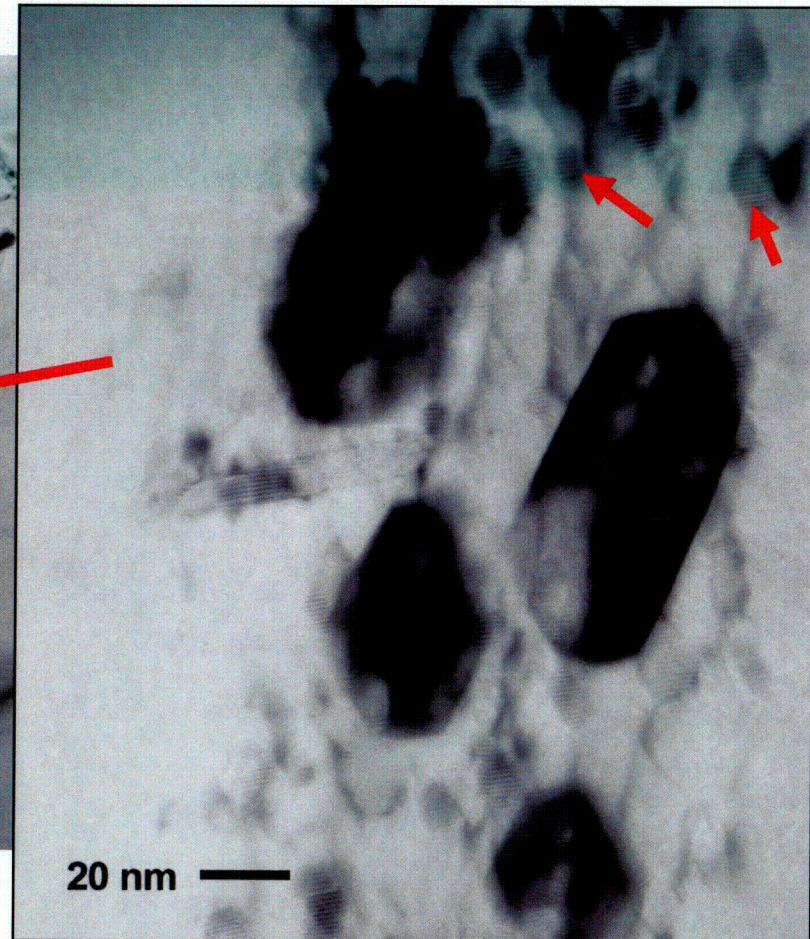
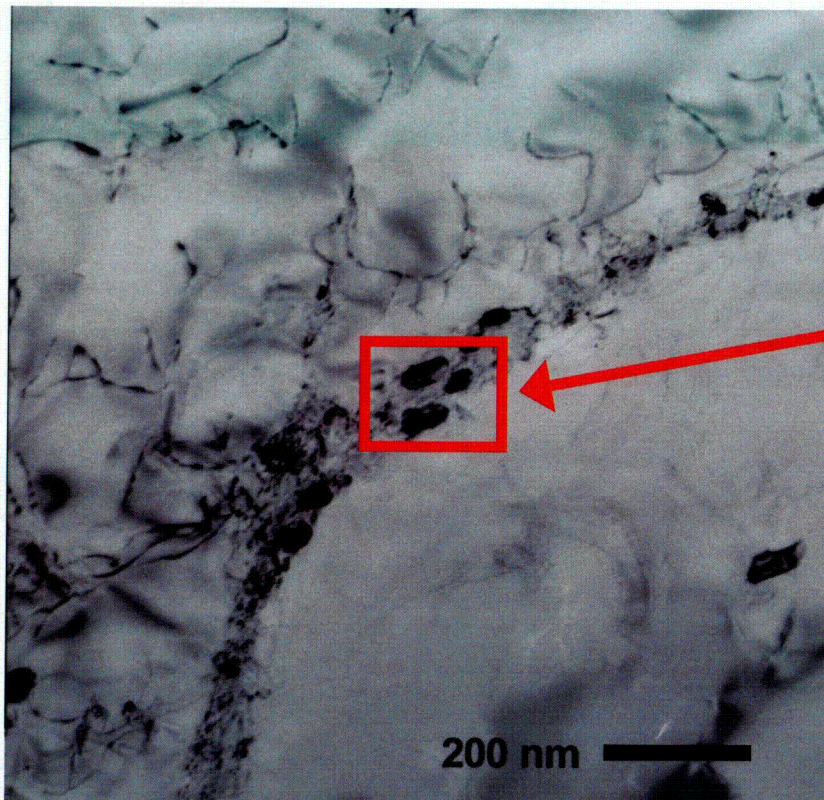
Aligned

Isolated



Small Precipitates - Filler Metal 82

Welding and Joining Metallurgy Group

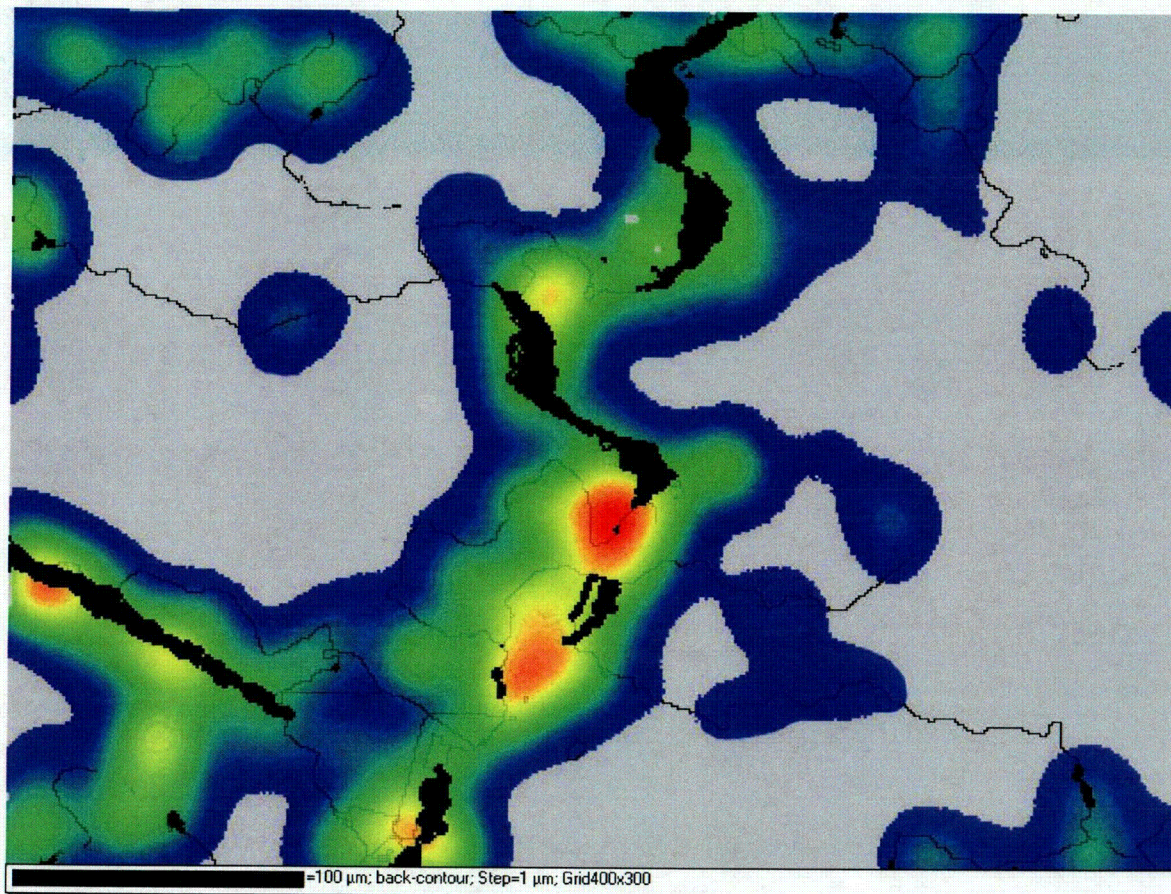


Small Precipitates: 10 nm



Strain Distribution

Welding and Joining Metallurgy Group



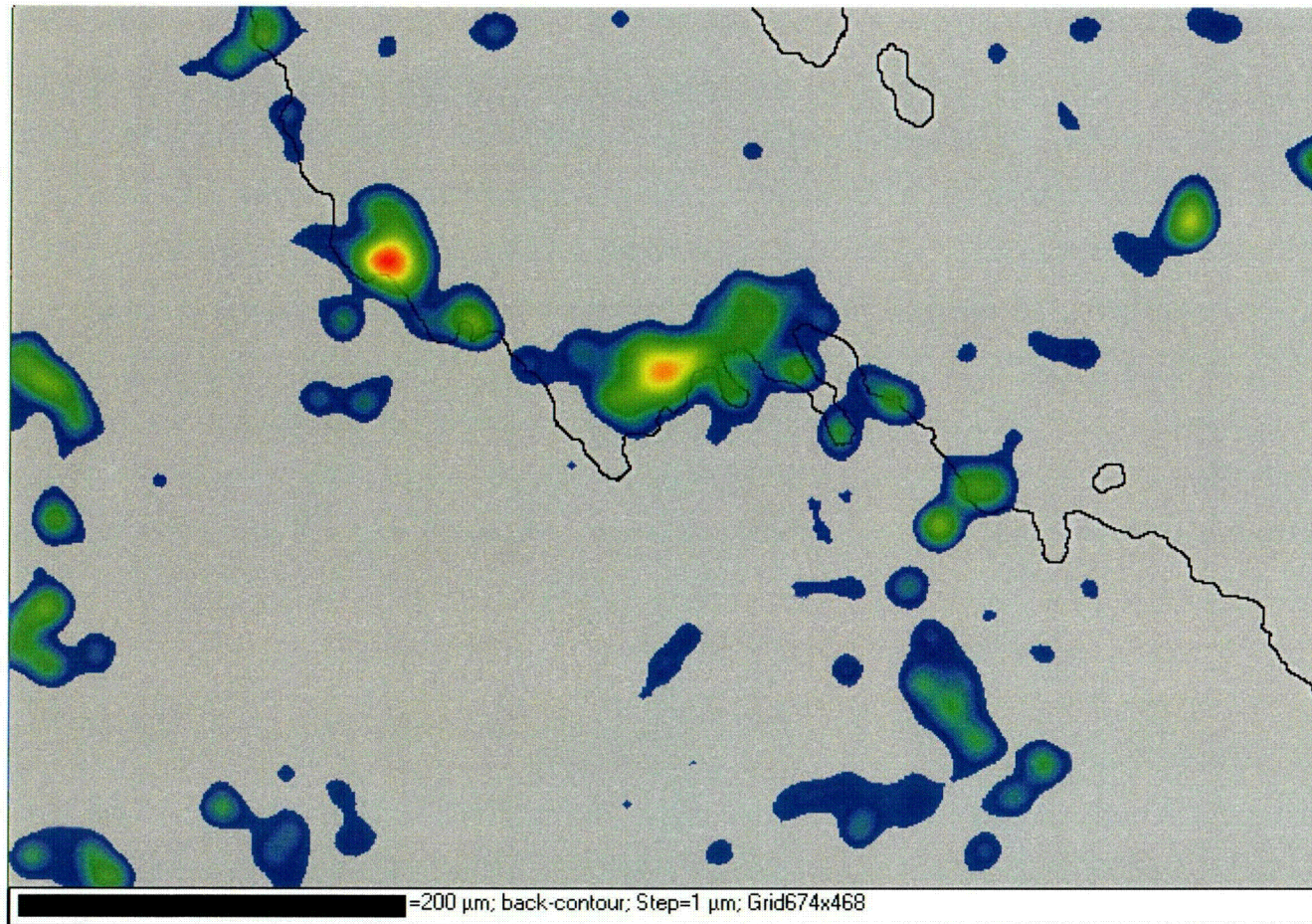
1147 °C
Strain: 11.3%

FM-82
Heat – YN6830



Strain Distribution

Welding and Joining Metallurgy Group



985 °C
Strain: 8.1%

FM-82
Heat – YN6830



Comparison

Welding and Joining Metallurgy Group

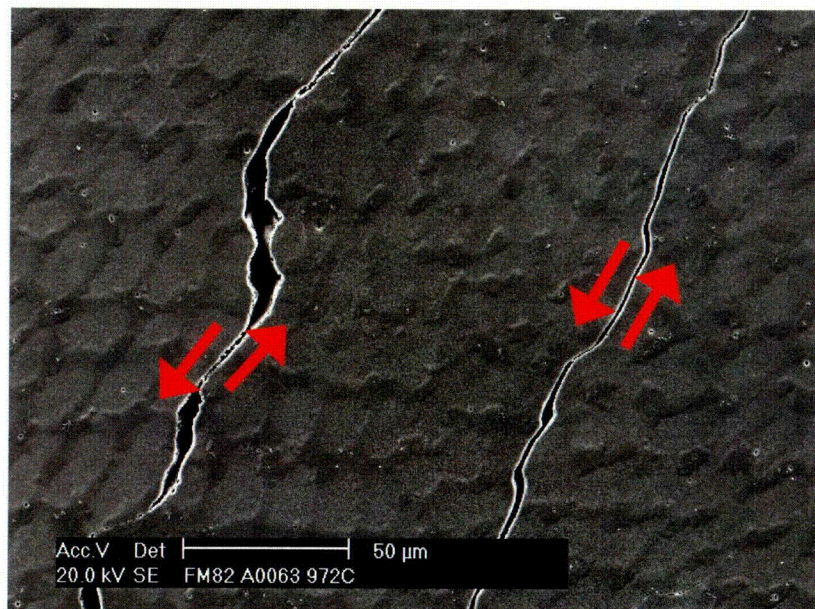
- **Filler Metal 52**
 - Long, straight grain boundaries (not tortuous)
 - Sporadic intergranular large carbides and nitrides
 - The nitrides are not enough to avoid grain growth
 - Consistent medium size $M_{23}C_6$ distribution
 - Small amount of intragranular precipitates

- **Filler Metal 82**
 - Very tortuous grain boundaries
 - Consistent inter- and intra-granular eutectic large (Nb,Ti)C distribution (1-3 μm)
 - Sporadic intergranular medium size and small (NbTi)C carbides
 - Small amount of intragranular carbides
 - No $M_{23}C_6$ observed

Insight Into the Mechanism

Welding and Joining Metallurgy Group

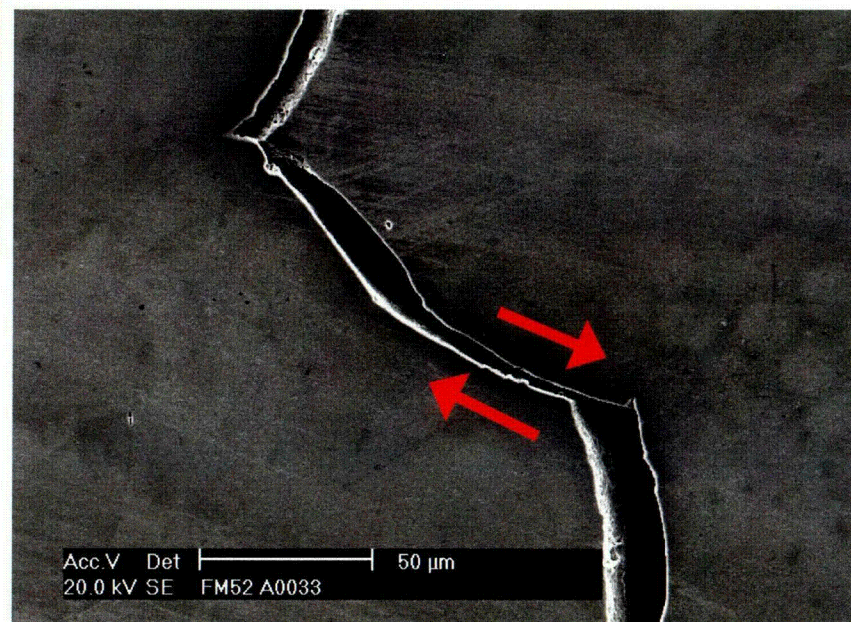
603



FM-82
972 °C

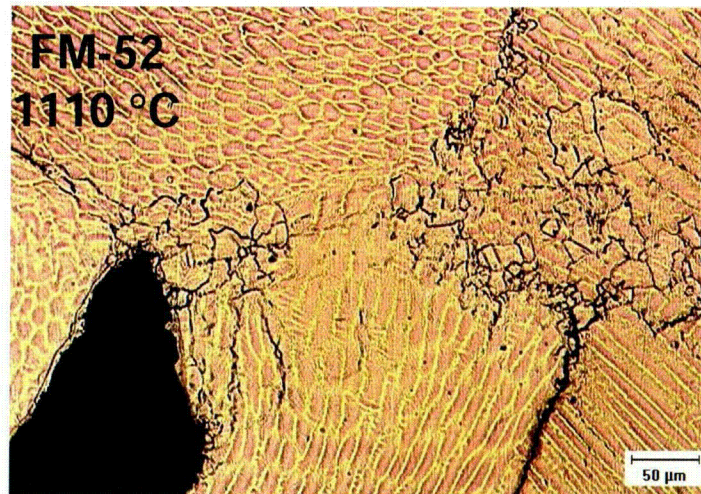
Grain Boundary Sliding

FM-52
986 °C

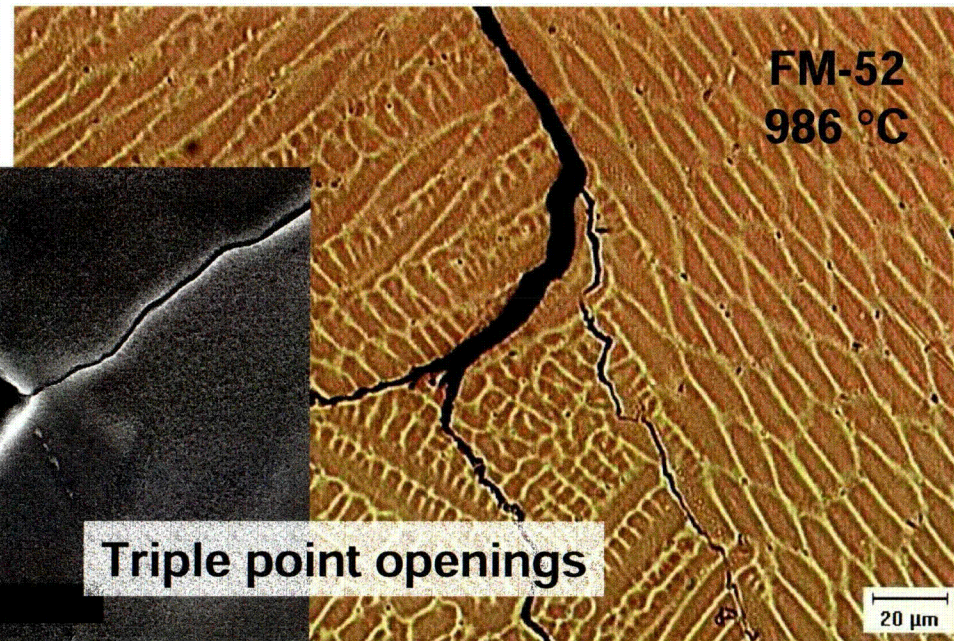


Insight Into the Mechanism

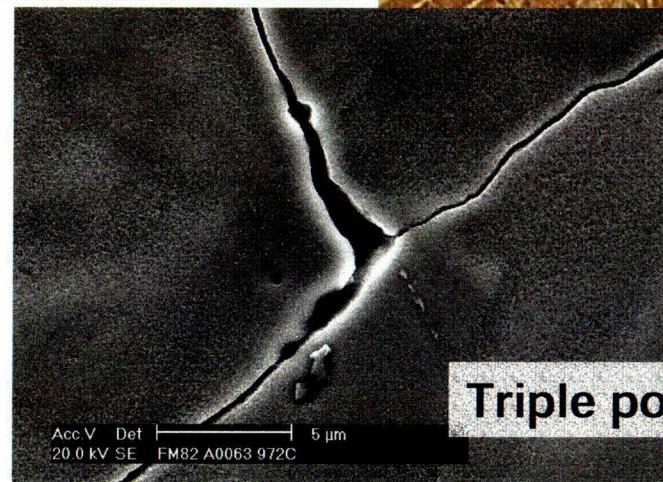
Welding and Joining Metallurgy Group



Dynamic recrystallization
at high temperatures



FM-82
972 °C



Triple point openings



DDC Mechanism Insight

Welding and Joining Metallurgy Group

- **Effect of grain boundary precipitates**
 - **“Locks” GB and/or “pins” GB migration**
 - **Increases GB tortuosity**
 - **Restricts grain growth**
 - **Reduces GB sliding**
 - **Reduces deformation accumulation at triple points**
 - **May be crack initiators (precipitate itself or interface)**
 - **Interaction with impurities**

- **Effect depends on**
 - **When and where the precipitate forms**
 - **Precipitate properties (MN - MC - $M_{23}C_6$)**
 - **Interface properties**
 - **Distribution**
 - **Size**



DDC Mechanism Insight

Welding and Joining Metallurgy Group

- **Grain boundary tortuosity**
 - Increases GB area versus straight grain boundaries
 - GB “locking” effect
 - Reduce deformation accumulation at triple points
 - Favors cracks arrest process

- **Hydrogen Effect**
 - Increases GB/Interface decohesion
 - Interaction with precipitates
 - Enhances GB sliding

Vessel Head Penetration Inspection, Cracking, and Repairs Conference

Impact of PWSCC and Current Leak Detection on Leak-Before-Break

D. Rudland⁽¹⁾, R. Wolterman⁽¹⁾, G. Wilkowski⁽¹⁾, and R. Tregoning⁽²⁾

(1) Engineering Mechanics Corporation of Columbus

(2) U.S. Nuclear Regulatory Commission, Office of Nuclear Reactor Research

Acknowledgements

- *Work supported by NRC-RES through subcontract from Battelle to Emc²*

R. Tregoning is NRC project manager

P. Scott is Battelle Project Manager

Emc²

LB-LOCA Redefinition Program

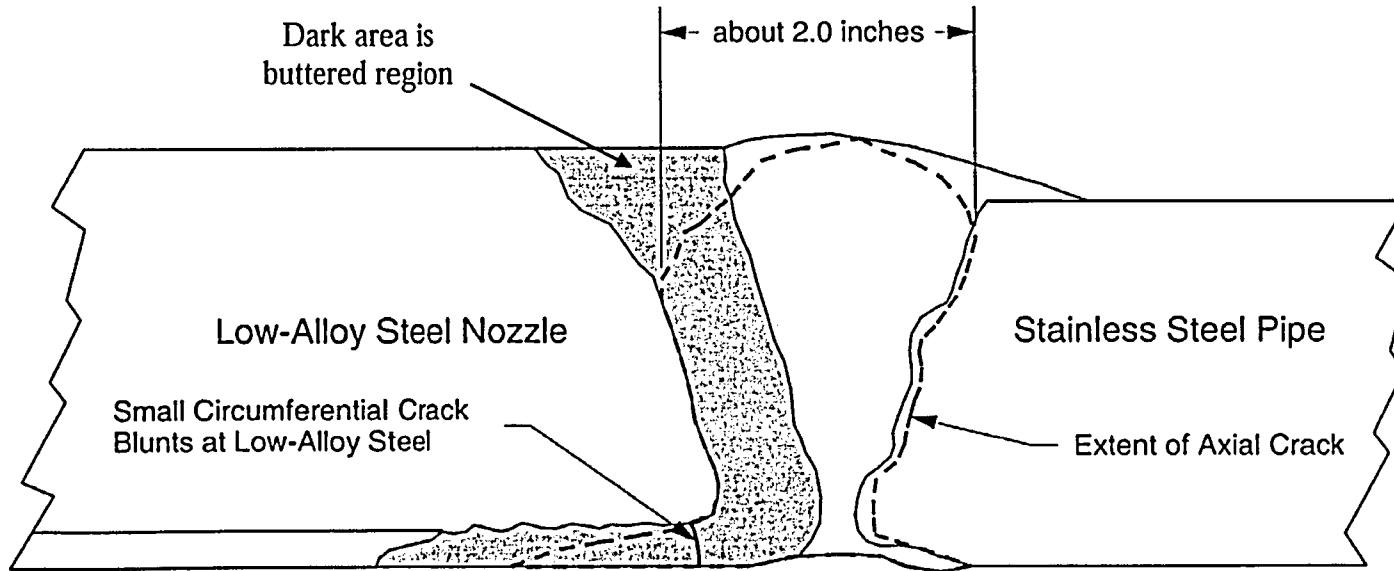
- *This effort small part of larger program*
- *On-going elicitation to assess failure probabilities*
- *Next generation of probabilistic pipe fracture code under development*
 - ◆ *Discussion with many people during this meeting to get updated subcritical crack initiation and growth models*
 - ◆ *Including many of the piping fracture analysis aspects from NRC's Degraded Piping Program, Short Cracks programs, IPIRG-1 and -2 programs*

Background

- *PWSCC in Ringhal and VC Summer hot legs, as well as more recent Belgium and Japanese PWSCC piping experiences raised concern about past LBB approvals for lines that at one time were thought to be free of any cracking mechanism.*
- *SRP 3.6.3 has a screening criterion to ensure that lines susceptible to potentially large cracks cannot be accepted for LBB relief of dynamic load effects of pipe whip supports and jet impingements shields.*
 - ◆ *"..requirement that corrosion resistance of piping be demonstrated....".*
- *Fortunately the PWSCC cracks to date have been primarily axial and a few small circumferential cracks; nevertheless, it was desirable to see if LBB could be satisfied if circumferential through-wall cracks occurred.*

Background

■ V.C. Summer PWSCCs in hot-leg



Background

- ***Inconel 82/182 bimetallic weld locations that might be susceptible to PWSCC***
 - ◆ ***RPV main coolant nozzles, core flood nozzles***
 - ◆ ***Pressurizer nozzle, spray nozzles, and surge lines***
 - ◆ ***Steam generator nozzles and RCP nozzles***
 - ◆ ***Many branch line connections***

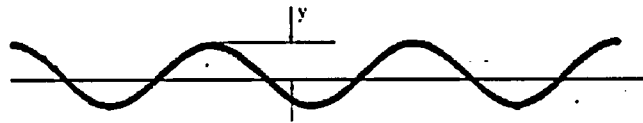
- ***Locations vary by NSSS supplier since main coolant piping could be stainless or clad carbon steels***

Revised LBB Analysis

- ***As part of the LB-LOCA redefinition program and the technical support for a new LBB Regulatory Guide, many past LBB submittals were reviewed***
- ***LBB analysis conducted in this effort using typical LBB loads and recalculating how the leakage size crack may change if it was a PWSCC crack, i.e., PWSCC cracks have a more tortuous flow path than fatigue cracks used in many past LBB submittals.***
 - ◆ ***Need to define PWSCC crack-morphology parameters (roughness, number of turns, actual flow path-to-thickness ratio) from cracks removed from service.***
 - ◆ ***Photomicrographs of several PWSCC service-removed cracks were available.***
- ***Recalculated leakage cracks for LBB cases and determined margins on leakage crack size versus critical crack size at N+SSE or other critical transient load (i.e., start-up/shut-down thermal loads for a surge line)***

Crack Morphology Parameters

- Surface roughness, number of turns, and actual flow path length are key crack morphology parameters.



$$R_q = \sqrt{\left(\frac{1}{L} \int_{x=0}^{x=L} y^2 dx \right)}$$

- Surface roughness and number of turns can depend on the magnitude of the crack-opening displacement (μ_G = global surface roughness, μ_L = local surface roughness).



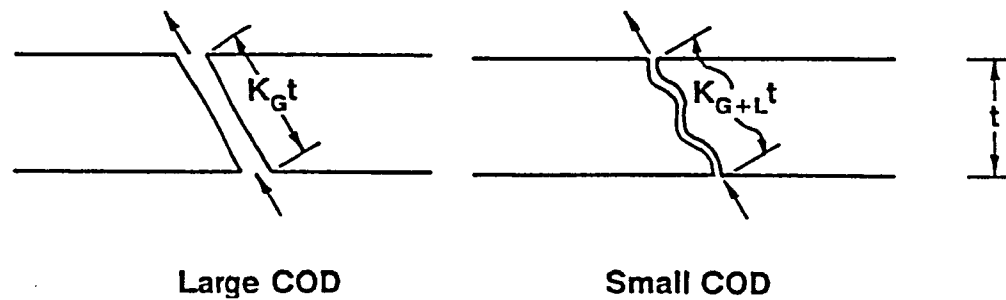
Large COD



Small COD

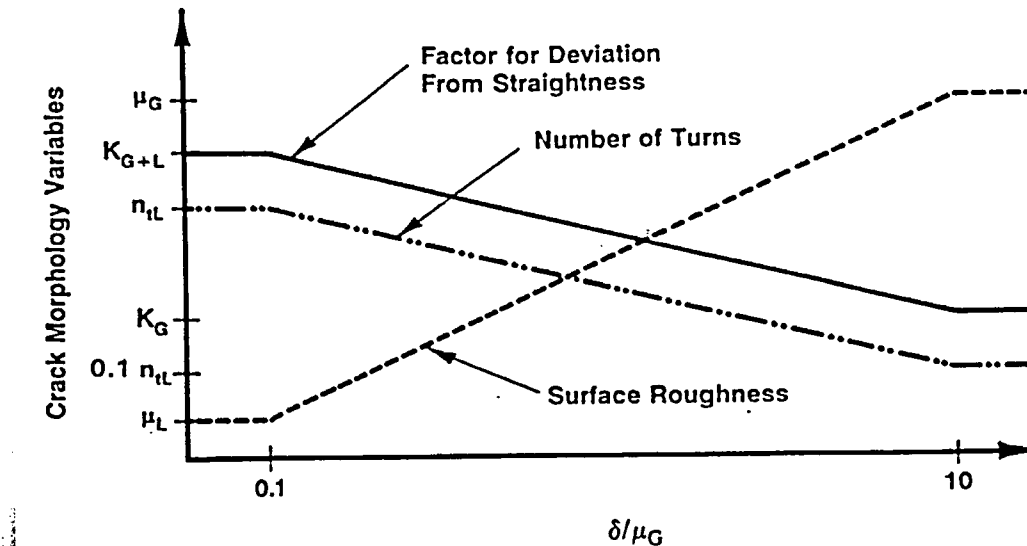
Crack Morphology Parameters

- Actual flow path length can depend on number of turns and will be greater than just the thickness of the pipe.



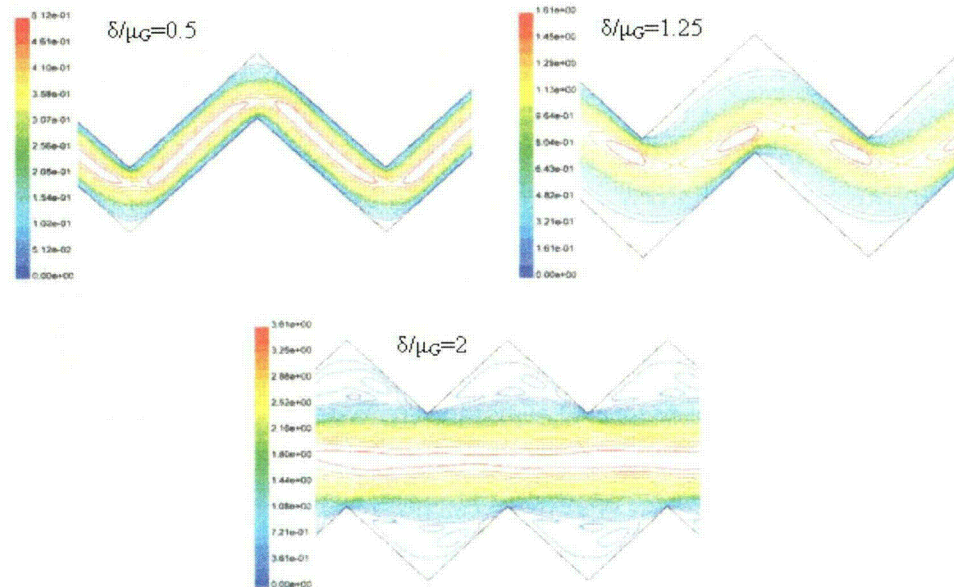
Crack Morphology Parameters

- **Interpolation procedure used to account for effect of COD on transition from:**
 - ♦ *very tight cracks (lower surface roughness, many turns, longer flow path length) to*
 - ♦ *large COD crack cases (higher roughness, fewer turns, and shorter effective flow length)*



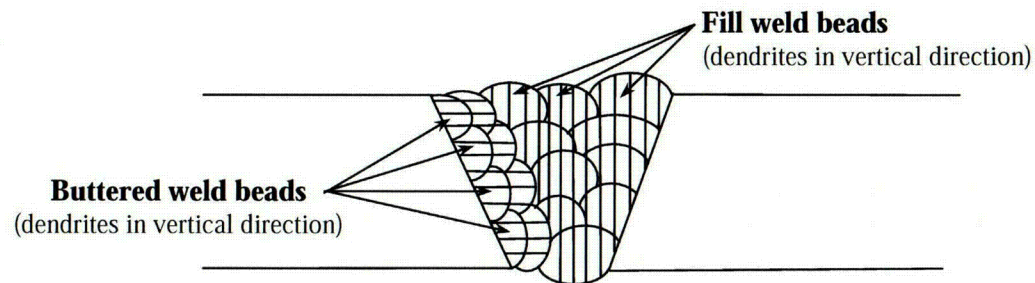
Crack Morphology Parameters

- *Interpolation procedure is approximate and could be improved with detailed CFM analysis*



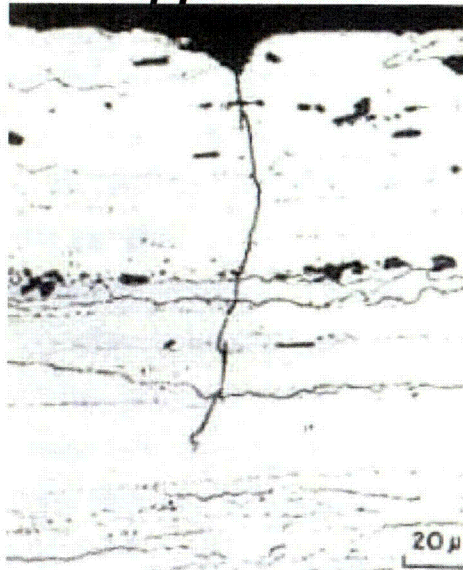
Unique aspects of PWSCC in bimetallic welds

- *Weld bead orientation may affect crack morphology parameters, i.e., cracks grow parallel to dendritic grains faster*

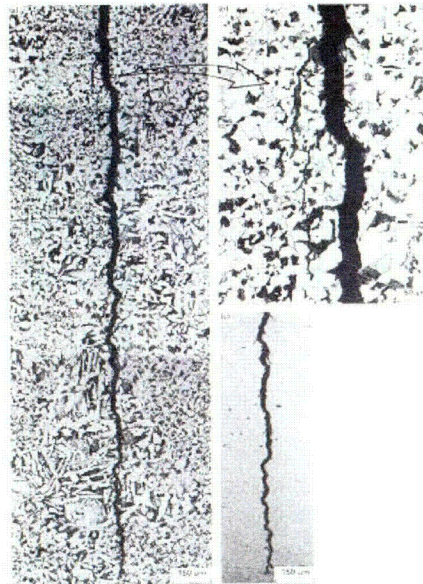


Statistical analysis of crack morphology for different types of cracks

- Evaluated service removed cracks in NUREG/CR-6004
"Probabilistic Pipe Fracture Evaluations for Leak-Rate-Detection Applications"



Air fatigue crack



Corrosion fatigue crack

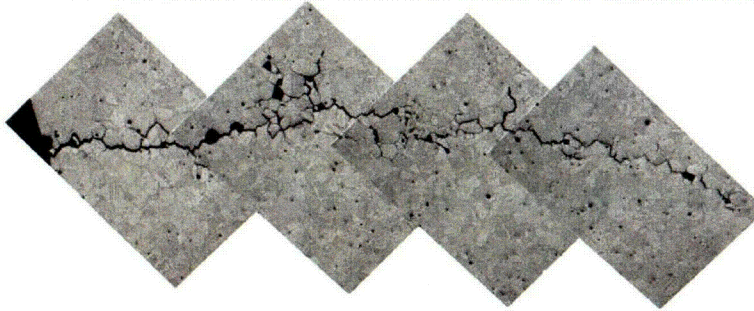


IGSCC crack

ϵ_{mc}^2

PWSCC cracks examined from metallographic sections

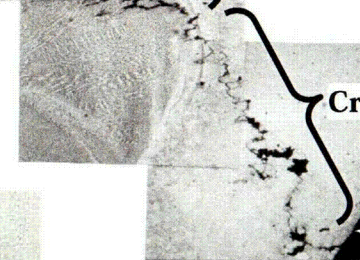
- ***Inconel 600 base metal (CRDM nozzle)***



- ***Inconel 600 base and weld metal (CRDM nozzle)***

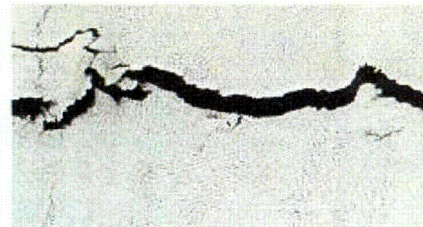


Crack in weld metal



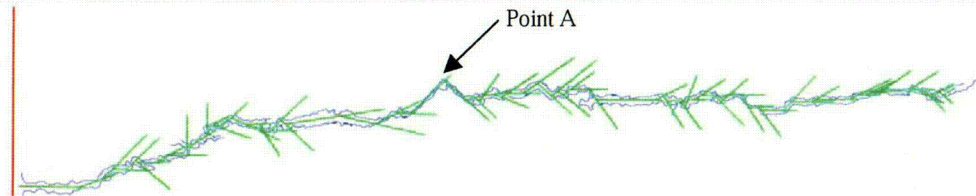
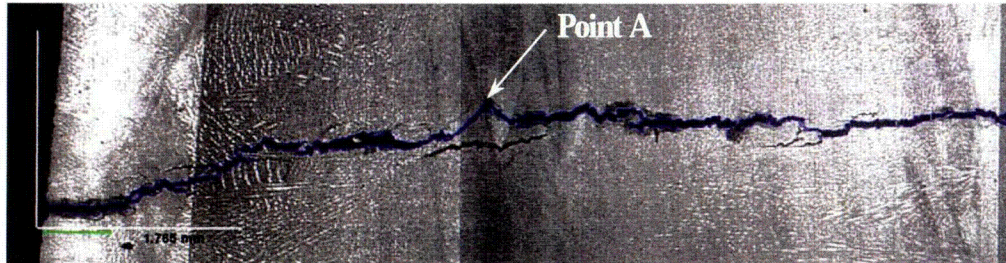
Crack in In600 base metal

- ***In 82/182 weld in pipe***

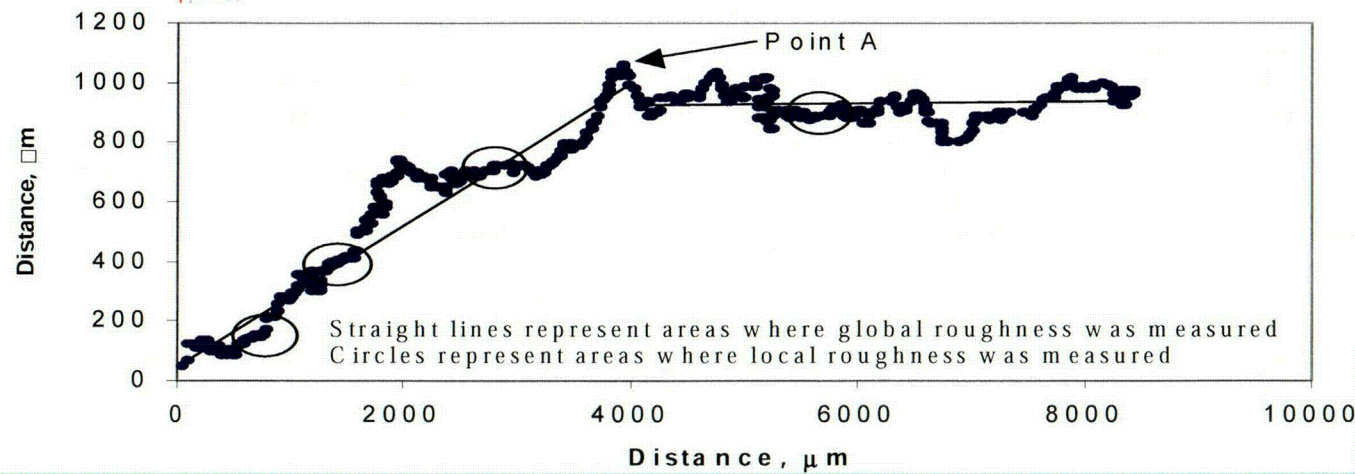


ϵmc^2

Example of determining crack morphology parameters



of turns



Roughness

ϵ_{mc}^2

:15

Comparison of Parameters for Various Cracking Mechanisms

■ PWSCC crack results

Location	μ_L (μm)	μ_G (μm)	n_{IL} (mm^{-1})	K_G	K_{G+L}
Hot-leg Inconel 82/182 weld Parallel to dendritic grain	7.5	52	3.95	1.022	1.132
	4.75	40	12.4	1.000	1.245
Hot-leg Inconel 82/182 weld Parallel to dendritic grain	21	125.5	5.42	1.015	1.278
	34.2	238	1.97	1.000	1.315
CRDM nozzle Inconel 82/182 weld Transverse to dendritic grains	10.2	282	8.3	1.500	2.487
CRDM tube Inconel 600 base metal	4.3	71	5.72	1.001	1.165
CRDM tube Inconel 600 base metal	22	166	9.56	1.170	1.614
CRDM tube Inconel 600 base metal	5.57	41	8.85	1.010	1.203

Mean and standard deviation of crack morphology parameters

Crack Morphology Variable	Corrosion Fatigue		IGSCC		PWSCC – Base		PWSCC – Weld ^(a)	
	Mean	Standard Dev	Mean	Standard Dev	Mean	Standard Dev	Mean	Standard Dev
$\mu_L, \mu\text{m}$	8.814	2.972	4.70	3.937	10.62	9.870	16.86	13.57
$\mu_G, \mu\text{m}$	40.51	17.65	80.0	39.01	92.67	65.26	113.9	90.97
n_L, mm^{-1}	6.730	8.070	28.2	18.90	8.043	2.043	5.940	4.540
K_G	1.017	0.0163	1.07	0.100	1.060	0.095	1.009	0.011
K_{G+L}	1.060	0.0300	1.33	0.170	1.327	0.249	1.243	0.079

(a) Crack growth *parallel* to long direction of dendritic grains.

Typical LBB Cases Analyzed

Case Number	Piping System	Bimetallic Weld-Location	OD, mm (inch)	Wall thickness, mm (inch)
1	Surge line	Surge line to pressurizer	356 (14.0)	35.7 (1.41)
2	Hot leg	Hot-leg safe end to reactor vessel nozzle	879 (34.6)	68.6 (2.70)
3	Hot leg	Hot-leg safe end to reactor vessel nozzle	878 (34.6)	68.3 (2.69)
4	Surge Line	Surge line to hot leg	406 (16.0)	40.4 (1.59)
5	Surge Line	Surge line to pressurizer	356 (14.0)	35.8 (1.41)
6	Surge Line	Surge line to pressurizer	305 (12.0)	33.3 (1.31)

Typical LBB Cases Analyzed

Case Number	Normal Operating Conditions				Faulted Conditions (N+SSE)			
	Pressure, MPa (psi)	Temp., C (F)	F _x w/press, MN (kips)	M _{en} , kN-m (in-kips)	Pressure, MPa (psi)	Temp., C (F)	F _x w/press, kN (kips)	M _{en} , kN-m (in-kips)
1	16.0 (2,327)	345 (653)	1.04 (234)	200 (1,770)	16.0 (2,327)	345 (653)	1,078 (242)	241.6 (2,138)
2	15.4 (2,235)	323 (614)	6.61 (1,490)	1720 (15,200)	15.4 (2,235)	323 (614)	7,126 (1,602)	1,861 (16,470)
3	15.4 (2,235)	323 (613)	6.19 (1,390)	3,680 (32,600)	15.4 (2,235)	322.8 (613)	7,864 (1,768)	4,397 (38,910)
4	14.8 (2,150)	316 (600)	1.29 (290)	209 (1,853)	14.8 (2,150)	316 (600)	NA	NA
5	14.8 (2,150)	316 (600)	0.98 (221)	243 (2,147)	14.8 (2,150)	316 (600)	NA	NA
6	15.5 (2,250)	345 (653)	0.689 (155)	220 (1,950)	15.5 (2,250)	345 (653)	NA	NA

Case Number	Average Properties						Minimum Properties					
	Yield	Ultimate	E	ϵ_0	α	n	Yield	Ultimate	E	ϵ_0	α	n
	MPa (ksi)	MPa (ksi)	GPa (msi)				MPa (ksi)	MPa (ksi)	GPa (msi)			
1 ^(a)	155 (22.4)	474 (68.7)	179.3 (26.0)	0.000863	6.50	3.80	130 (18.8)	454 (65.8)	179.3 (26.0)	0.000723	9.11	3.80
2 ^(b)	146 (21.1)	453 (65.7)	179.3 (26.0)	0.000812	8.10	3.35	142 (20.6)	434 (62.9)	175.8 (25.5)	0.000808	8.04	5.55
3 ^(a)	169 (24.5)	469 (68)	175.8 (25.5)	0.000961	3.75	4.82	163 (23.7)	427 (61.9)	175.8 (25.5)	0.000929	7.30	8.90
4 ^(c)	229 (33.2)	501 (72.7)	172.7 (25.05)	0.001325	12.1	2.83	NA	NA	NA	NA	NA	NA
5 ^(c)	229 (33.2)	501 (72.7)	172.7 (25.05)	0.001325	12.1	2.83	NA	NA	NA	NA	NA	NA
6 ^(b)	146 (21.1)	453 (65.7)	179.3 (26.0)	0.000812	8.10	3.35	142 (20.6)	434 (62.9)	175.8 (25.5)	0.000808	8.04	5.55

Emc²

LBB Results – Leakage flow lengths

■ ***PWSCC parallel to dendritic grain – main part of weld***

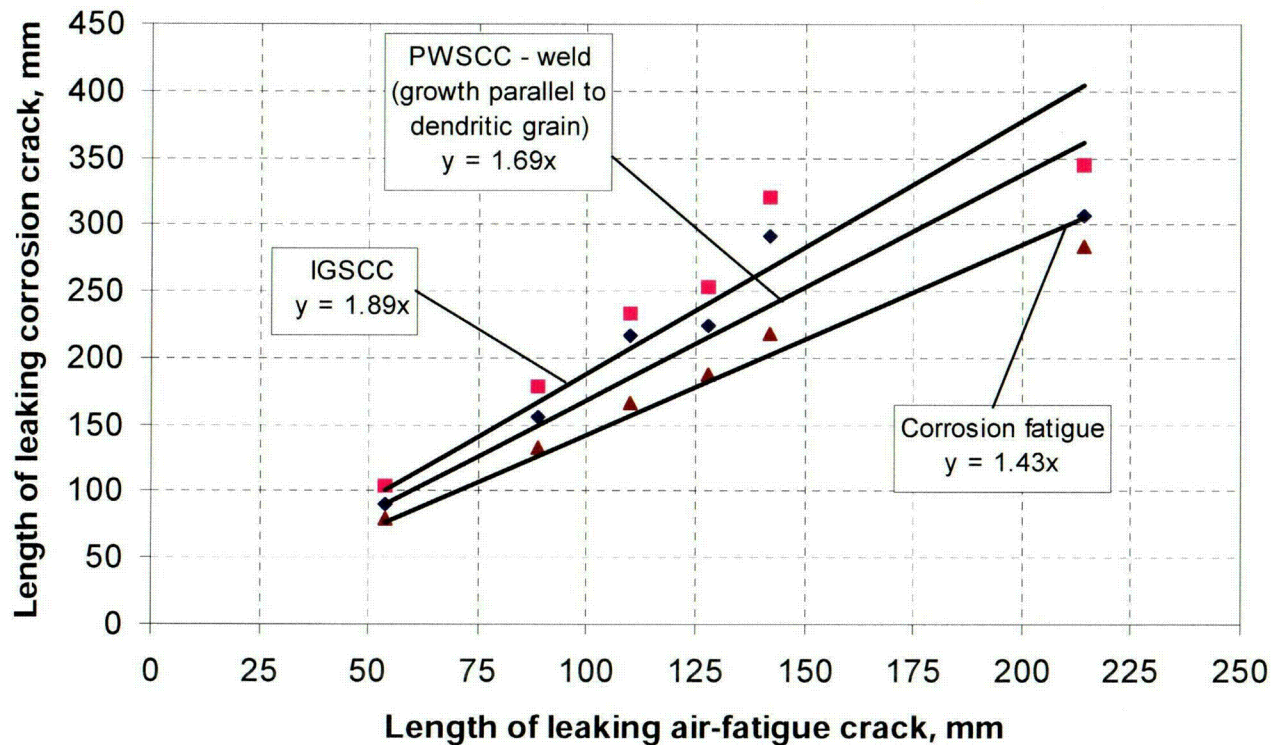
Case	Applicants'/ Published leakage size flaw, mm (inch)	Leakage crack size, mm (inch) (Using GE/EPRI with original h functions - COD dependence)			
		Air-fatigue crack (300- μ inch roughness no turns)	IGSCC	Corrosion- fatigue	PWSCC ^(a)
1 ^(b)	71 (2.80)	88.6 (3.49)	178 (6.99)	133 (5.25)	156 (6.13)
2 ^(c)	132 (5.20)	142 (5.61)	321 (12.6)	218 (8.52)	291 (11.4)
3 ^(c)	85 (3.35)	110 (4.35)	234 (9.23)	166 (6.54)	216 (8.50)
4 ^(c)	213 (8.40)	128 (5.03)	253 (9.98)	188 (7.39)	224 (8.81)
5 ^(c)	261 (10.26)	214 (8.44)	345 (13.59)	283 (11.13)	306 (12.03)
6 ^(c)	76 (3.00)	53.6 (2.11)	104 (4.11)	80.0 (3.15)	90.2 (3.55)

(a) Crack growing *parallel* to long direction of dendritic grains in Inconel 82/182 weld.

(b) 5 gpm leak rate – Factor of safety of 10 on 0.5 gpm leakage detection capability.

(c) 10 gpm leak rate – Factor of safety of 10 on 1 gpm leakage detection capability.

Comparison of length of leaking corrosion cracks with the length of air-fatigue cracks



LBB Results – Margins on crack size

■ ***PWSCC parallel to dendritic grain – main part of weld***

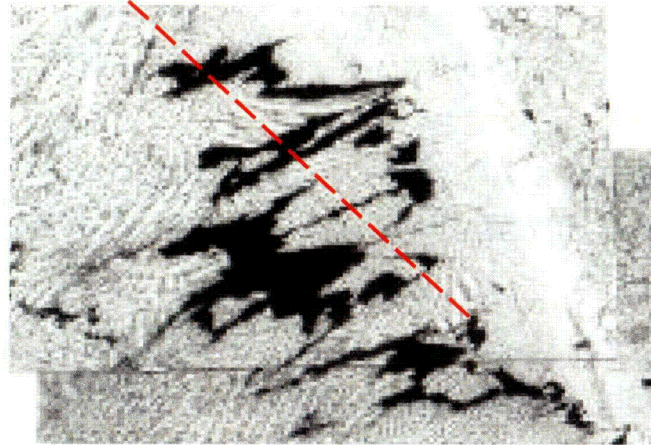
Case	Applicant/ Published critical flaw size, mm (inch)	Margin on leakage crack size				
		Applicants'/ Published margin	Calculations from this report			
			Air-fatigue crack (300- μ inch roughness no turns)	IGSCC	Corrosion -fatigue	PWSCC ^(a)
1	427 (16.8)	6.0	4.82	2.40	3.21	2.74
2	NA ^(b)	>2	5.51	2.45	3.63	2.70
3	190 (7.5)	2.24	1.72	0.81	1.15	0.88
4	396 (15.6)	1.86	3.10	1.56	2.11	1.77
5	462 (18.2)	1.77	2.16	1.34	1.64	1.51
6	163 (6.4)	2.13	3.03	1.56	2.03	1.80

(a) Crack growing *parallel* to long direction of dendritic grains.

(b) Applicant's critical flaw size was not available. Critical flaw size was calculated using NRCPIPE Version 3.0. For this case, the critical flaw size was calculated as 785 mm (30.9 inch).

PWSCC growth across the long direction of the dendritic grains – buttered region

Crack growth and shortest path leakage direction



ϵmc^2

:23

LBB Results – Leakage flaw lengths

- *PWSCC perpendicular to dendritic grain – buttered region crack*

Case	Applicants'/ Published Leakage Size Flaw, mm (inch)	Leakage crack size, mm (inch) (Using GE/EPRI with original h functions & SQUIRT with COD dependence)	
		Air-fatigue crack (300-μinch roughness with no turns)	PWSCC ^(a) (with crack growing <i>perpendicular</i> to long direction of dendritic grains)
1 ^(b)	71 (2.80)	88.7(3.49)	187 (7.35)
2 ^(c)	132 (5.20)	142 (5.61)	356 (14.02)
3 ^(c)	85 (3.35)	110 (4.35)	287 (11.28)
4 ^(c)	213 (8.40)	128 (5.03)	271 (10.68)
5 ^(c)	261 (10.26)	214 (8.44)	353 (13.89)
6 ^(c)	76 (3.00)	53.6 (2.11)	120 (4.72)

(a) Crack morphology parameters are derived from only one photomicrograph, Figure 19 of Reference 12.

(b) 5 gpm leak rate – Factor of safety of 10 on 0.5 gpm leakage detection capability.

(c) 10 gpm leak rate – Factor of safety of 10 on 1 gpm leakage detection capability.

LBB Results – Margins on crack size

■ ***PWSCC perpendicular to dendritic grain – buttered region crack***

Case	Applicants'/ Published Critical Flaw Size, mm (inch)	Margin on leakage crack size		
		Applicants'/ Published margin	Margins from analysis in this report	
			Air fatigue crack (300-μinch roughness with no turns)	PWSCC ^(b) (with crack growing <i>perpendicular</i> to long direction of dendritic grains)
1	427 (16.8)	6.0	4.82	2.28
2	NA ^(a)	>2	5.51	2.21
3	190 (7.5)	2.24	1.72	0.66
4	396 (15.6)	1.86	3.10	1.46
5	462 (18.2)	1.77	2.16	1.31
6	163 (6.4)	2.13	3.03	1.35

(a) Applicant's critical flaw size was not available. Critical flaw size was calculated using NRCPIPE Version 3.0. For this case, the critical flaw size was calculated as 785 mm (30.9 inch).

(b) Crack morphology parameters are derived from only one photomicrograph, Figure 19 of Reference 15.

Conclusions

- *PSWCC cracks have a more tortuous flow path than air fatigue cracks that were frequently used in past LBB submittals*
- *PWSCC crack morphology parameters determined from a few limited service cracks*
- *PWSCC crack morphology slightly less severe than IGSCC if crack grow parallel to dendritic grains, but could be worse if going perpendicular to dendritic grain – buttered region*

Conclusions

- *An updated LBB analysis was conducted using typical LBB submittals*
 - ◆ *J-R curves for In82/182 in progress*

- *PWSCC cracks have leakage crack lengths that are longer than air fatigue cracks (used in many LBB submittals) at the same leakrate*
 - ◆ *~70% longer if PWSCC is parallel to dendritic grain – main weldment*
 - ◆ *~110% longer if PWSCC is perpendicular to dendritic grain – buttered region*

Conclusions

- *Average margin on LBB crack length decreased from 3.39 for air-fatigue crack to*
 - ◆ *1.9 for the PWSCC crack growing parallel to the long direction of the dendritic grains*
 - ◆ *1.55 for the PWSCC crack growing transverse to the long direction of the dendritic grains*
- *LBB difficult to satisfy for PWSCC crack cases using draft SRP 3.6.3 procedures*
- *PWSCCs could result in long circumferential surface cracks, which could make breaks more likely to occur than by using the simple circumferential through-wall crack analysis*
 - ◆ *LBB screening criteria not satisfied*

NRC FORM 335 (9-2004) NRCMD 3.7		U.S. NUCLEAR REGULATORY COMMISSION		1. REPORT NUMBER (Assigned by NRC, Add Vol., Supp., Rev., and Addendum Numbers, if any.) NUREG/CP-0191	
BIBLIOGRAPHIC DATA SHEET (See instructions on the reverse)					
2. TITLE AND SUBTITLE Proceedings of the Vessel Penetration Conference on Inspection, Crack Growth and Repair; Volume 1: Manuscripts Proceedings of the Vessel Penetration Conference on Inspection, Crack Growth and Repair; Volume 2: Presentations				3. DATE REPORT PUBLISHED	
				MONTH September	YEAR 2005
5. AUTHOR(S) Compiled and edited by T. S. Mintz and W. H. Cullen, Jr.				4. FIN OR GRANT NUMBER 	
				6. TYPE OF REPORT Conference Proceedings	
8. PERFORMING ORGANIZATION - NAME AND ADDRESS (If NRC, provide Division, Office or Region, U.S. Nuclear Regulatory Commission, and mailing address; if contractor, provide name and mailing address.) Division of Engineering Technology Office of Nuclear Regulatory Research U. S. Nuclear Regulatory Commission Washington, DC 20555-0001				7. PERIOD COVERED (Inclusive Dates)	
9. SPONSORING ORGANIZATION - NAME AND ADDRESS (If NRC, type "Same as above"; if contractor, provide NRC Division, Office or Region, U.S. Nuclear Regulatory Commission, and mailing address.) Same as above					
10. SUPPLEMENTARY NOTES Conference held September 29 - October 2, 2003 in Gaithersburg, Maryland, USA					
11. ABSTRACT (200 words or less) These two volumes of proceedings contain the visual projections (in Volume I), and the contributed manuscripts (in Volume II) from the Conference on Vessel Head Penetration, Crack Growth and Repair, held at the Gaithersburg Marriott at Washingtonian Center on September 29 - October 2, 2003. The conference was co-sponsored by the U. S. Nuclear Regulatory Commission and Argonne National Laboratory. Over two hundred attendees were provided with 45 presentations, divided into five sessions: (I) Inspection Techniques, Results, and Future Developments, (II) Continued Plant Operation, (III) Structural Analysis and Fracture Mechanics Issues, (IV) Crack Growth Rate Studies for the Disposition of Flaws, and (V) Mitigation of Nickel-Base Alloy Degradation and Foreign Experience. The conference opened with a plenary session including presentations giving the overview from the NRC Office of Regulatory Research, and an overview of nickel-base alloy cracking issues worldwide. The conference closed with a panel session consisting of industry representatives and NRC management discussing the prognosis for future issues in this area of concern.					
12. KEY WORDS/DESCRIPTORS (List words or phrases that will assist researchers in locating the report.) Stress corrosion cracking Non-destructive inspection Ultrasonic inspection Eddy Current inspection Alloy 600 Alloy 182 Alloy 690 Alloy 152				13. AVAILABILITY STATEMENT unlimited	
				14. SECURITY CLASSIFICATION (This Page) unclassified	
				(This Report) unclassified	
				15. NUMBER OF PAGES	
				16. PRICE	

NUREG/CP-0191
Vol. 2, Part 1

**PROCEEDINGS OF THE CONFERENCE ON VESSEL PENETRATION INSPECTION,
CRACK GROWTH AND REPAIR**

SEPTEMBER 2005